OPEN ACCESS
IOP Publishing
Journal of Physics A: Mathematical and Theoretical
J. Phys. A: Math. Theor. **55** (2022) 443002 (55pp)
https://doi.org/10.1088/1751-8121/ac8254

Topical Review

Chapter 1: Modern fundamentals of amplitudes

Andreas Brandhuber[1], Jan Plefka[2] and Gabriele Travaglini[1,*]

[1] Centre for Theoretical Physics, Department of Physics and Astronomy, Queen Mary University of London, London E1 4NS, United Kingdom
[2] Institut für Physik und IRIS Adlershof, Humboldt-Universität zu Berlin, Zum Großen Windkanal 2, D-12489 Berlin, Germany

E-mail: a.brandhuber@qmul.ac.uk, jan.plefka@hu-berlin.de and g.travaglini@qmul.ac.uk

Received 13 April 2022, revised 24 June 2022
Accepted for publication 19 July 2022
Published 30 November 2022

Abstract

This chapter introduces the foundational concepts and techniques for scattering amplitudes. It is meant to be accessible to readers with only a basic understanding of quantum field theory. Topics covered include: the four-dimensional spinor-helicity formalism and the colour decomposition of Yang–Mills scattering amplitudes; the study of soft and collinear limits of Yang–Mills and gravity amplitudes; the BCFW recursion relation and generalised unitarity, also in the superamplitudes formalism of $\mathcal{N} = 4$ supersymmetric Yang–Mills; an overview of standard and hidden symmetries of the S-matrix of $\mathcal{N} = 4$ supersymmetric Yang–Mills, such as the conformal, dual conformal and Yangian symmetries; and a brief excursus on form factors of protected and non-protected operators in Yang–Mills theory. Several examples and explicit calculations are also provided.

Keywords: scattering amplitudes, quantum field theory, gravity

(Some figures may appear in colour only in the online journal)

*Author to whom any correspondence should be addressed.

Original content from this work may be used under the terms of the Creative Commons Attribution 4.0 licence. Any further distribution of this work must maintain attribution to the author(s) and the title of the work, journal citation and DOI.

Contents

1. Introduction

The most remarkable property of scattering amplitudes is their unexpected simplicity. Consider for example the scattering of $2 \to n$ gluons at tree level. Textbooks usually discuss the case $n = 2$, which requires the computation of four Feynman diagrams. They often fail to mention that, as n grows, life is not so simple, as table 1 shows:

If the result of a calculation as n increases were to grow in complexity in the way the table above suggests, there would be no surprise. This is not the case. Indeed, there are families of amplitudes for which all-multiplicity expressions are available. The most famous one is the infinite sequence of maximally helicity violating gluon amplitudes, or MHV in short, where all gluons have the same helicity except two, say i and j (in a convention where the momenta of the n particles are all outgoing). For any n, these amplitudes are expressed by the spectacularly beautiful Parke–Taylor formula [2, 3]

$$A_n^{\rm MHV}(1^+,\dots,i^-,\dots j^-,\dots,n^+) = ig^{n-2}\frac{\langle ij\rangle^4}{\langle 12\rangle\langle 23\rangle\dots\langle n1\rangle}. \tag{1}$$

One does not need to understand the meaning of the symbols in (1) (which will be explained later) to appreciate that Feynman diagrams fail to account for its simplicity, which is effectively independent of the number of gluons. In a landmark paper [4], Witten related the simplicity of (1) to the fact that when transformed to Penrose's twistor space [5, 6], MHV amplitudes have support on the simplest curve in twistor space—a (complex) line. This result led to remarkable closed formulae for the tree-level S-matrix of $\mathcal{N} = 4$ super Yang–Mills (SYM) [7–9], and a novel diagrammatic approach that uses MHV amplitudes as effective vertices [10].

Table 1. The number of Feynman diagrams that contribute to $2 \to n$ gluon scattering at tree level [1]. This number grows factorially with n.

n	2	3	4	5	6	7	8	9
# of diagrams	4	25	220	2, 485	34, 300	559, 405	10, 525, 900	224, 449, 225

Two tasks are then ahead. The first is to provide a framework, or choose coordinates, that makes this simplicity manifest; this is similar to picking polar coordinates to describe circular motion. The second is to devise methods and find symmetries which can explain this simplicity, at the same time providing new, powerful ways to calculate amplitudes while avoiding Feynman diagrams. This chapter provides the beginning of an answer to both tasks.

The most economic language to describe the scattering of massless particles is the spinor-helicity formalism, which we introduce in section 2. It provides a parameterisation of the momenta and polarisations of massless particles in terms of a set of variables which automatically satisfy the on-shell condition $p^2 = 0$ for lightlike momenta. Section 3 introduces colour decomposition, which leads to the concept of colour-ordered, or partial amplitudes in Yang–Mills theory—quantities which depend only on kinematic data but not on colour, which will be one of the main subjects of the rest of this article. With the aim of deriving amplitudes without ever looking at a Lagrangian, we discuss in section 4 the possible forms of the smallest scattering amplitudes of particle of spin s, showing that they can be derived from symmetry principles alone. Starting from these building blocks, in section 5 we introduce the BCFW recursion relation, one of the most efficient methods to derive the tree-level S-matrix of Yang–Mills theory and gravity. In section 6 we pause and consider the basic symmetry of scattering amplitudes—the Poincaré group (translations plus Lorentz)—and the conformal group, which is an invariance of tree-level Yang–Mills amplitudes. Amplitudes are singular in soft and collinear limits, with a universal behaviour which is often very useful to constrain their form. The corresponding factorisation theorems are derived at tree level in Yang–Mills and gravity theories in section 7, using a combination of MHV diagrams and recursion relations. Section 8 introduces supersymmetry and superamplitudes—objects with package together amplitudes with a fixed total helicity, and are invariant under supersymmetry transformations. Here we focus on maximally supersymmetric Yang–Mills theory, and formulate supersymmetric BCFW recursion relations, also deriving MHV superamplitudes as an example. It has often been said that the scattering amplitudes in $\mathcal{N} = 4$ SYM are the 'hydrogen atom' of four-dimensional relativistic scattering (see e.g. [11]). This is due to the fact that they are very constrained: superamplitudes in $\mathcal{N} = 4$ SYM enjoy the superconformal symmetry of the Lagrangian of the theory, as well as certain hidden symmetries of its S-matrix: the dual superconformal and Yangian symmetries. We review these in section 9, again focusing on the MHV superamplitude as a simple example. In section 10 we introduce the modern unitarity-based approach to compute loop amplitudes in theories with and without supersymmetry. In particular we review the computation of MHV (super)amplitudes both from two-particle and quadruple cuts, and of the all-plus four-point amplitude at one loop in pure Yang–Mills. Finally, section 11 serves as a taster of recent applications of on-shell techniques devised for amplitudes to form factors. These are slightly off-shell quantities, falling in between amplitudes (fully on shell) and correlation functions (fully off shell). In appendix A we outline our conventions and the Lorentz transformation properties of the spinor variables introduced in section 2.

2. Spinor-helicity formalism

2.1. Massless particles and their helicity

Elementary particles carry an internal angular momentum known as spin $\vec{S}$. The projection of the particle's spin on the direction of motion is known as its *helicity* $h := \frac{\vec{p}\cdot\vec{S}}{|\vec{p}|}$, where $\vec{p}$ denotes the particle three-momentum. If the particle is massless, the helicity is a Lorentz-invariant quantity[3]. Moreover, for massless particles of spin s the helicity can only take the extremal values $h = \pm s$. Scattering states of massless particles are therefore labeled by the on-shell momentum and helicity: $|p, h\rangle$. Let us now take a look at the cases of spin $s = 1/2$, 1 and 2.

$s = 1/2$. The momentum-space Dirac equation for positive- and negative-energy solutions, $u(p)$ and $v(p)$, reads

$$(\not{p} - m)u(p) = 0, \qquad (\not{p} + m)v(p) = 0. \tag{2}$$

Clearly, they coincide in the massless case $\not{p}u = 0 = \not{p}v$. States of definite helicity are obtained via the projectors $\frac{1}{2}(1 \pm \gamma_5)$,

$$u_\pm = \frac{1}{2}(1 \pm \gamma_5)u(p), \qquad v_\mp = \frac{1}{2}(1 \pm \gamma_5)v(p), \tag{3}$$

and in the massless case one can identify $u_\pm(p) = v_\mp(p)$. Hence spin $1/2$ states are labeled by $|p, \pm 1/2\rangle$.

$s = 1$. Gauge fields carry helicities $h = \pm 1$ described by polarisation vectors $\epsilon_\mu^{(\pm)}(p)$ that obey the transversality condition

$$p \cdot \epsilon^{(\pm)}(p) = 0, \tag{4}$$

as well as the relations

$$\epsilon^{(\pm)}(p) \cdot \epsilon^{(\pm)}(p) = 0, \qquad \epsilon^{(+)}(p) \cdot \epsilon^{(-)}(p) = -1, \qquad (\epsilon_\mu^{(\pm)}(p))^* = (\epsilon_\mu^{(\mp)}(p)). \tag{5}$$

The corresponding on-shell states are labeled as $|p, \pm 1\rangle$.

$s = 2$. Gravitons come in two helicities $h = \pm 2$. Their symmetric polarisation tensors $\epsilon_{\mu\nu}^{(\pm\pm)}(p)$ obey $p^\mu \epsilon_{\mu\nu}^{(\pm\pm)}(p) = 0$, and can be chosen to be traceless: $\epsilon^{(\pm\pm)\,\mu}{}_\mu = 0$. They can be represented as *direct products* of gauge field polarisation vectors:

$$\epsilon_{\mu\nu}^{(++)}(p) = \epsilon_\mu^{(+)}(p)\epsilon_\nu^{(+)}(p), \qquad \epsilon_{\mu\nu}^{(--)}(p) = \epsilon_\mu^{(-)}(p)\epsilon_\nu^{(-)}(p). \tag{6}$$

This representation automatically entails the above on-shell properties.

2.2. Momenta and polarisations of massless particles

The key property of the spinor-helicity formalism is to provide a representation of momenta and polarisations using one set of variables that automatically obey the on-shell constraint $p^2 = 0$ as well as the conditions on the polarisations, e.g. $\not{p}u_\pm = 0$ for spin-$1/2$ particles, or (4) for gluons. These variables ultimately lead to simpler final expression for the

[3] This can be understood as follows: for a massive particle a Lorentz boost can be used to go to a frame in which the helicity is flipped, however no boost can 'overtake' a massless particle, which moves at the speed of light.

amplitudes of fermions, gluons, photons and gravitons. The starting point is to rewrite p^μ as a Weyl bi-spinor:

$$p^\mu \to p^{\dot\alpha\alpha} = \bar\sigma_\mu^{\dot\alpha\alpha}\, p^\mu = \begin{pmatrix} p^0 - p^3 & -p^1 + ip^2 \\ -p^1 - ip^2 & p^0 + p^3 \end{pmatrix}, \tag{7}$$

where $\bar\sigma_\mu^{\dot\alpha\alpha} = (\mathbb{1}, -\vec\sigma)$ and $\vec\sigma$ are the Pauli matrices. This relation implements the isomorphism between the Lorentz group $SO(3,1)$ and $SL(2,\mathbb{C})$, as discussed in appendix A. The crucial observation is now that the on-shell condition for a massless particle $p^2 = 0$ is equivalent to $\det p = 0$, and the rank of the matrix $p^{\dot\alpha\alpha}$ is thus equal to one. Hence, the four-momentum can be written as

$$p^{\dot\alpha\alpha} = \tilde\lambda^{\dot\alpha}\,\lambda^\alpha. \tag{8}$$

This is one of the most important formulae in this article. λ^α and $\tilde\lambda^{\dot\alpha}$ are commuting Weyl spinors, known as *helicity spinors* [12–14] (see [15–23] for a precursor formalism). For complexified momenta, λ and $\tilde\lambda$ are independent variables, and importantly (8) is invariant under a *little-group* transformation

$$\lambda \to z\lambda, \qquad \tilde\lambda \to z^{-1}\tilde\lambda, \qquad z \in \mathbb{C}^*. \tag{9}$$

On the other hand in real Minkowski space the four-momentum is real, which translates into the condition $(\lambda^\alpha)^* = \pm\tilde\lambda^{\dot\alpha}$, where the sign is the same as that of the energy p^0. That also reduces the little group to a $U(1)$ (since $|z| = 1$ in this case), as expected for massless particles [24, 25]. For real momenta, an explicit realisation of the spinors is

$$\lambda^\alpha = \frac{1}{\sqrt{p^0 - p^3}}\begin{pmatrix} p^0 - p^3 \\ -p^1 - ip^2 \end{pmatrix}, \qquad \tilde\lambda^{\dot\alpha} = \frac{1}{\sqrt{p^0 - p^3}}\begin{pmatrix} p^0 - p^3 \\ -p^1 + ip^2 \end{pmatrix}. \tag{10}$$

Since $|p^0| \geqslant |p^3|$, the quantity $\sqrt{p^0 + p^3}$ is real (imaginary) for positive (negative) p^0.

Spinor indices are raised or lowered with the Levi-Civita tensor:

$$\lambda_\alpha := \epsilon_{\alpha\beta}\,\lambda^\beta, \qquad \tilde\lambda_{\dot\alpha} := \epsilon_{\dot\alpha\dot\beta}\,\tilde\lambda^{\dot\beta}, \tag{11}$$

which allows us to form two basic Lorentz-invariant quantities

$$\langle ij\rangle := \lambda_i^\alpha \lambda_{j\alpha}, \qquad [ij] := \tilde\lambda_{i\dot\alpha}\tilde\lambda_j^{\dot\alpha}, \tag{12}$$

introducing the NW-SE (SW-NE) contractions for the undotted and dotted Weyl indices and the handy bracket notation (see appendix A for a discussion of the Lorentz transformation properties of spinors). Here i and j denote the particles' labels. We can then write the product of two momenta p_i and p_j as

$$\epsilon_{\alpha\beta}\epsilon_{\dot\alpha\dot\beta}\, p_i^{\dot\alpha\alpha}\, p_j^{\dot\beta\beta} = \epsilon_{\alpha\beta}\epsilon_{\dot\alpha\dot\beta}\,\bar\sigma_\mu^{\dot\alpha\alpha}\,\bar\sigma_\nu^{\dot\beta\beta}\, p_i^\mu\, p_j^\nu = 2\, p_i \cdot p_j, \tag{13}$$

where $\epsilon_{\alpha\beta}\epsilon_{\dot\alpha\dot\beta}\,\bar\sigma_\mu^{\dot\alpha\alpha}\,\bar\sigma_\nu^{\dot\beta\beta} = \mathrm{Tr}(\bar\sigma_\mu\sigma_\nu) = 2\eta_{\mu\nu}$, and we have defined $\sigma_{\mu\,\alpha\dot\alpha} := \epsilon_{\alpha\beta}\epsilon_{\dot\alpha\dot\beta}\bar\sigma_\mu^{\dot\beta\beta} = (\mathbb{1}, \vec\sigma)$. Mandelstam invariants also have a very simple representation in spinor variables:

$$s_{ij} = (p_i + p_j)^2 = 2\, p_i \cdot p_j = \langle ij\rangle[ji]. \tag{14}$$

We have seen that spinor-helicity variables are useful to describe the momenta of massless on-shell particles as the mass-shell condition is automatically met, but what is their relation to the

helicity of the on-shell states? One quickly sees that they solve the massless Dirac equation and can be identified with the helicity states $u_\pm(p)$ and $v_\pm(p)$. Indeed, using the chiral representation of the Dirac matrices γ^μ, one has

$$\not{p} = p_\mu \gamma^\mu = \begin{pmatrix} 0 & p_{\alpha\dot\alpha} \\ p^{\dot\beta\beta} & 0 \end{pmatrix} = \begin{pmatrix} 0 & \lambda_\alpha \tilde\lambda_{\dot\alpha} \\ \tilde\lambda^{\dot\beta}\lambda^\beta & 0 \end{pmatrix}. \tag{15}$$

Now writing

$$u_+(p) = v_-(p) = \begin{pmatrix} \lambda_\alpha \\ 0 \end{pmatrix} := |p\rangle, \qquad u_-(p) = v_+(p) = \begin{pmatrix} 0 \\ \tilde\lambda^{\dot\alpha} \end{pmatrix} := |p], \tag{16}$$

using the convenient bra-ket notation $|\bullet\rangle$ and $|\bullet]$, we see that the massless Dirac equation $\not{p}|p\rangle = \not{p}|p] = 0$ is satisfied since $\langle\lambda\,\lambda\rangle = [\tilde\lambda\,\tilde\lambda] = 0$. Hence, the helicity states of massless spin-$1/2$ fermions are captured by λ and $\tilde\lambda$. For negative momenta, we will define

$$|-p\rangle := i\,|p\rangle, \qquad |-p] := i\,|p]. \tag{17}$$

Moving on to massless spin-1 states, we can re-express the polarisation vectors $\epsilon^{(\pm)}_\mu(p)$ as bi-spinors via $\epsilon^{(\pm)}_{\alpha\dot\alpha} = \sigma^\mu_{\alpha\dot\alpha}\epsilon^{(\pm)}_\mu$, with

$$\epsilon^{(-)}_{\alpha\dot\alpha} = \sqrt{2}\frac{\lambda_\alpha\tilde\xi_{\dot\alpha}}{[\lambda\xi]}, \qquad \epsilon^{(+)}_{\alpha\dot\alpha} = \sqrt{2}\frac{\xi_\alpha\tilde\lambda_{\dot\alpha}}{\langle\xi\lambda\rangle}. \tag{18}$$

Here ξ and $\tilde\xi$ are arbitrary reference spinors that will drop out of any final expression for a scattering amplitude. The only condition is that they are not parallel to λ and $\tilde\lambda$, e.g. $\xi \neq c\lambda$. In fact the freedom in choosing a reference spinor in the polarisation bi-spinors can be attributed to gauge transformations, since

$$\epsilon^{(+)}_{\alpha\dot\alpha}(\xi+\delta\xi) = \epsilon^{(+)}_{\alpha\dot\alpha}(\xi) + p_{\alpha\dot\alpha}\sqrt{2}\frac{\langle\lambda\,\delta\xi\rangle}{\langle\lambda\,\xi\rangle^2}. \tag{19}$$

We also note the completeness relation $\sum_{h=\pm}(\epsilon^{(h)})_\mu(\epsilon^{(h)})^*_\nu = -\eta_{\mu\nu} + \frac{p_\mu q_\nu + p_\nu q_\mu}{p\cdot q}$, where $q_{\alpha\dot\alpha} = \xi_\alpha\tilde\xi_{\dot\alpha}$. Graviton polarisations then follow from (6) as products of the $\epsilon^{(\pm)}_{\alpha\dot\alpha}$.

2.3. Massive particles

We can also introduce on-shell variables for *massive* momenta [26]. In this case the on-shell condition $\det p = p^2 = m^2$ implies that $p_{\alpha\dot\alpha}$ has rank two and can be expressed in terms of a pair of spinor variables λ^I and $\tilde\lambda_I$ with $I = 1, 2$. The bi-spinor representation of a four-dimensional massive momentum then becomes

$$p_\mu\sigma^\mu_{\alpha\dot\alpha} := p_{\alpha\dot\alpha} = \lambda^I_\alpha\tilde\lambda_{\dot\alpha\,I}. \tag{20}$$

Also note that the on-shell condition becomes

$$\det\, p \;=\; \det\,\lambda \times \det\,\tilde\lambda = m^2. \tag{21}$$

For real momenta, (20) is invariant under $SU(2)$ transformations L acting on the I indices: $\lambda^I \to \lambda^J L_J{}^I$, $\tilde\lambda_I \to (L^{-1})_I{}^J\tilde\lambda_J$, which are naturally identified with the little group transformations of massive particles [24, 25].

2.4. Useful formulae

We close this section with two useful formulae for our helicity spinors. The first is the Schouten identity $\langle\lambda_1\,\lambda_2\rangle\,\lambda_3^\alpha + \langle\lambda_2\,\lambda_3\rangle\,\lambda_1^\alpha + \langle\lambda_3\,\lambda_1\rangle\,\lambda_2^\alpha = 0$, or, contracting with an arbitrary spinor λ_a,

$$\langle 12\rangle\,\langle 3a\rangle + \langle 23\rangle\,\langle 1a\rangle + \langle 31\rangle\,\langle 2a\rangle = 0, \tag{22}$$

and similarly for the conjugate spinors. It reflects the fact that there is no completely anti-symmetric three-tensor $\Omega^{\alpha\dot\beta\gamma}$. A second identity descends from momentum conservation $\sum_{i=1}^n \lambda_i^\alpha\,\tilde\lambda_i^{\dot\alpha} = 0$, from which it follows that $\sum_{i=1}^n \langle a\,i\rangle\,[i\,b] = 0$, for arbitrary λ_a and $\tilde\lambda_b$. Finally we quote the two useful relations

$$\left.\begin{matrix}\langle ab\rangle[bc]\langle cd\rangle[da]\\ [ab]\langle bc\rangle[cd]\langle da\rangle\end{matrix}\right\} = \mathrm{Tr}\left(\frac{1\mp\gamma^5}{2}\,\not a\,\not b\,\not c\,\not d\right)$$
$$= 2[(a\cdot b)(c\cdot d) - (a\cdot c)(b\cdot d) + (a\cdot d)(b\cdot c) \mp i\epsilon(abcd)], \tag{23}$$

where $\epsilon(abcd) := \epsilon_{\mu\nu\rho\sigma}a^\mu b^\nu c^\rho d^\sigma$.

3. Colour decomposition

We now turn our attention to gauge field theories. Having introduced helicity spinors as efficient variables to describe the kinematics, we now introduce a formalism that allows to disentangle the colour degrees of freedom from the kinematic ones. There are two such formalisms for an efficient colour management: the trace-based and the structure constant based (or DDM) formalism. In $SU(N_c)$ gauge theories coupled to matter, one mostly encounters two representations of the gauge group:

- Adjoint representation: gluons A_μ^a and their superpartners (gluinos and scalars) carry adjoint indices $a - 1,\ldots,N_c^2 - 1$.
- Fundamental & anti-fundamental representation: quarks and anti-quarks carry (anti)-fundamental indices $i = 1,\ldots,N_c$ and $\bar\imath = 1,\ldots,N_c$.

The $SU(N_c)$ algebra is represented by fundamental generators $(T^a)_i{}^{\bar\jmath}$ which are $N_c \times N_c$ hermitian, traceless matrices. In our conventions the structure constants take the form

$$f^{abc} = -\frac{i}{\sqrt{2}}\,\mathrm{Tr}(T^a[T^b,T^c]), \tag{24}$$

or $[T^a,T^b] = i\sqrt{2}f^{abc}T^c$, with $\mathrm{Tr}(T^aT^b) = \delta^{ab}$. Moreover, the $SU(N_c)$ Fierz-type identity

$$(T^a)_{i_1}^{\bar\jmath_1}\,(T^a)_{i_2}^{\bar\jmath_2} = \delta_{i_1}^{\bar\jmath_2}\,\delta_{i_2}^{\bar\jmath_1} - \frac{1}{N_c}\delta_{i_1}^{\bar\jmath_1}\,\delta_{i_2}^{\bar\jmath_2}, \tag{25}$$

is important for the colour decomposition of amplitudes and can be understood as a completeness relation for a basis of Hermitian matrices spanned by $\{\mathbb{1}, T^a\}$.

3.1. Trace basis

The colour dependence of a given Feynman graph arises from its vertices. The three-gluon vertex carries one structure constant f^{abc}, the four-gluon interaction a product of two f^{abc}, while the gluon-quark–anti-quark interaction comes with a generator $(T^a)_i{}^{\bar\jmath}$. In order to work out the colour dependence of a given Feynman diagram, imagine replacing all structure constants

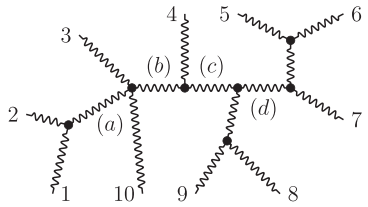

$$(a) : (p_1 + p_2)^2 \to 0\,, \qquad (b) : (p_{10} + p_1 + p_2 + p_3)^2 \to 0$$
$$(c) : (p_5 + p_6 + p_7 + p_8 + p_9)^2 \to 0\,, \qquad (d) : (p_5 + p_6 + p_7)^2 \to 0$$

Figure 1. Possible poles in a colour-ordered Feynman diagram.

appearing in it by the trace formula (24). This transforms the expression to products of T^a generators with contracted and open indices. Open fundamental indices correspond to quark lines in the diagram, open adjoint indices to the external gluon states. Contracted adjoint indices can be used to merge traces and products of generators by repeatedly applying the Fierz-type identity (25):

$$(A\,T^a\,B)^{\bar{j}}_i\,(C\,T^a\,D)^{\bar{l}}_k = (A\,D)^{\bar{l}}_i\,(C\,B)^{\bar{j}}_k - \frac{1}{N_c}(A\,B)^{\bar{j}}_i\,(C\,D)^{\bar{l}}_k. \tag{26}$$

In the end we will arrive at an expression of traces and strings of T^a's with only open indices corresponding to external states of the form

$$\mathrm{Tr}(T^{a_1}\dots T^{a_n})\dots\mathrm{Tr}(T^{b_1}\dots T^{b_m})\,(T^{c_1}\dots T^{c_p})^{\bar{j}_1}_{i_1}\dots(T^{d_1}\dots T^{d_p})^{\bar{j}_s}_{i_s}. \tag{27}$$

For pure gluon amplitudes, things are even simpler: in pure Yang–Mills theory the interaction vertices of $SU(N_c)$ and $U(N_c)$ gauge groups are identical, as $f^{0bc} = 0$ by virtue of (24) where $T^0 = \frac{\mathbb{1}}{\sqrt{N_c}}$ is the $U(1)$ generator (this leads to the photon decoupling theorem discussed in section 3.4). Hence, the $\frac{1}{N_c}$ part of (25) is not active here. In conclusion, tree-level gluon amplitudes reduce to a *single*-trace structure and can be brought into the *colour*-decomposed form

$$\mathcal{A}^{\mathrm{tree}}_n(\{a_i, h_i, p_i\}) = \sum_{\sigma\in S_n/\mathbb{Z}_n} \mathrm{Tr}(T^{a_{\sigma_1}}\,T^{a_{\sigma_2}}\dots T^{a_{\sigma_n}})\,A^{\mathrm{tree}}_n(\sigma_1,\sigma_2,\dots,\sigma_n). \tag{28}$$

Here h_i denote the helicities and a_i the adjoint colour indices of the external states, and we use the notation $\sigma = \{p_\sigma, h_\sigma\}$. Moreover, $S_n/\mathbb{Z}_n$ is the set of all non-cyclic permutations of n elements, which is equivalent to S_{n-1}. The A_n are called *partial* or *colour-ordered* amplitudes and carry all kinematic information that is now separated from the colour degrees of freedom. Partial amplitudes A_n are simpler than the full amplitudes $\mathcal{A}_n$ as they are individually gauge invariant and exhibit poles only in channels of cyclically adjacent momenta $(p_i + p_{i+1} + \dots + p_{i+s})^2 \to 0$, see figure 1.

For tree-level gluon-quark–anti-quark amplitudes with a single quark line one has

$$\mathcal{A}^{\mathrm{tree}}_{n,q\bar{q}}(\{a_i, h_i, p_i\}|\{i, q_1^{h_{q_1}}, \bar{j}, q_2^{h_{q_2}}\}) = \sum_{\sigma\in S_{n-2}} (T^{a_{\sigma_1}}\dots T^{a_{\sigma_{n-2}}})^{\bar{j}}_i\,A^{\mathrm{tree}}_{n,q\bar{q}}(\sigma_1,\dots,\sigma_{n-2}|q_1^{h_{q_1}}, q_2^{h_{q_2}}). \tag{29}$$

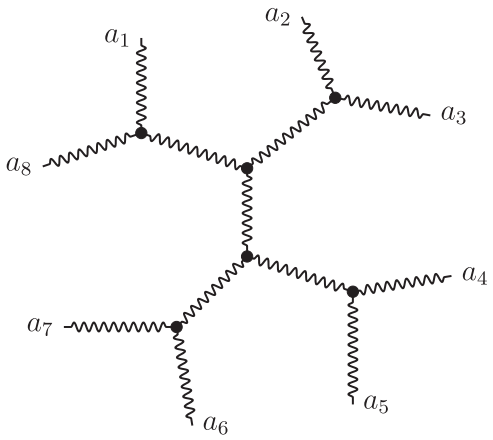

Figure 2. Typical colour tree in a structure constant based (DDM) colour expansion.

Increasing the number of quark lines yields a more involved structure as more strings and $\frac{1}{N_c}$ factors appear, see [1, 27, 28] for details.

At loop level, pure gluon amplitudes contain also multi-trace contributions arising from the merging performed using (25). For example, at one loop one has

$$\begin{aligned}\mathcal{A}_n^{1-\text{loop}}(\{a_i,h_i,p_i\}) &= N_c \sum_{\sigma\in S_n/\mathbb{Z}_n} \text{Tr}(T^{a_{\sigma_1}} T^{a_{\sigma_2}} \dots T^{a_{\sigma_n}}) A_{n;1}^{(1)}(\sigma_1,\dots,\sigma_n) \\ &+ \sum_{i=2}^{[n/2]+1} \sum_{\sigma\in S_n/\mathbb{Z}_n} \text{Tr}(T^{a_{\sigma_1}} \dots T^{a_{\sigma_{i-1}}})\ \text{Tr}(T^{a_{\sigma_i}} \dots T^{a_{\sigma_n}}) A_{n;i}^{(1)}(\sigma_1,\dots,\sigma_n),\end{aligned} \tag{30}$$

where the $A_{n;1}^{(1)}$ are called the primitive (colour-ordered) amplitudes, and the $A_{n;c>1}^{(1)}$ are the higher primitive amplitudes. The latter can be expressed as linear combinations of the primitive ones [29]. In the large-N_c limit the single-trace contributions are enhanced. In colour-summed cross sections, which are of interest in applications, the contribution of the higher primitive amplitudes is suppressed by $\frac{1}{N_c^2}$.

3.2. DDM basis

An alternative basis for the colour decomposition of pure-gluon (or purely adjoint particles) amplitudes makes use of the structure constants f^{abc} and is due to Del Duca, Dixon and Maltoni (DDM) [30]. Consider the colour dependence of an n-gluon tree amplitude. This can be represented as a sum over tri-valent graphs with vertices linear in f^{abc}, see figure 2. In this process we artificially 'blow' up a four-valent gluon vertex to sums of products of tri-valent vertices by multiplying it by $1 = q^2/q^2$ where $\frac{i}{q^2}$ is the propagator of the 'blown up' leg. One then uses the Jacobi identity

$$f^{abe}\, f^{cde} = f^{dae}\, f^{bce} - f^{dbe}\, f^{ace} \tag{31}$$

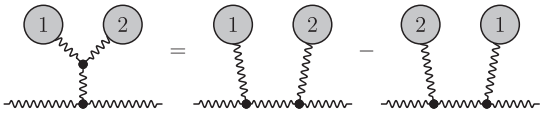

successively in order to shrink branched trees to branchless ones resulting in a 'half-ladder' expression. In this way we can completely reduce a coloured amplitude to a half-ladder basis in colour space:

$$\mathcal{A}_n^{\text{tree}}(\{a_i, h_i, p_i\}) = \sum_{\sigma \in S_{n-2}} f^{a_1 a_{\sigma_2} e_1} f^{e_1 a_{\sigma_3} e_2} f^{e_2 a_{\sigma_4} e_3} \dots f^{e_{n-3} a_{\sigma_{n-1}} a_n} A_n^{\text{tree}}(1, \sigma_2, \dots, \sigma_{n-1}, n), \tag{32}$$

where we now sum over permutations σ of the $n-2$ elements $\{2, 3, \dots, n-1\}$. The half-ladder colour basis fixes two (arbitrary) legs, here 1 and n:

$f^{a_1 a_{\sigma_2} e_1} f^{e_1 a_{\sigma_3} e_2} f^{e_2 a_{\sigma_4} e_3} \dots f^{e_{n-3} a_{\sigma_{n-1}} a_n} =$

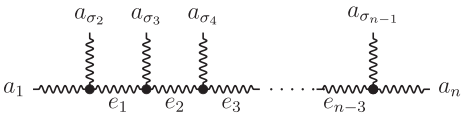

therefore the DDM basis consists of $(n-2)!$ independent partial amplitudes. This is to be contrasted with the $(n-1)!$ partial amplitudes in the trace basis. Hence, there must exist non-trivial identities between partial amplitudes allowing one to reduce the basis accordingly. These are known as Kleiss–Kuijf relations [31] and take the form

$$A_n^{\text{tree}}(1, \{\alpha\}, n, \{\beta\}) = (-1)^{n_\beta} \sum_{\sigma \in \alpha \sqcup\!\sqcup \beta^{\text{T}}} A_n^{\text{tree}}(1, \sigma, n), \tag{33}$$

where n_β denotes the number of elements in the set β and β^{T} is the set β with reversed ordering. The shuffle or ordered permutation $\alpha \sqcup\!\sqcup \beta^{\text{T}}$ means to merge α and β^{T} while preserving the individual orderings of α and β^{T}. The Kleiss–Kuijf relations can be proven by rewriting the DDM basis in terms of the trace basis discussed above.

It turns out that there exists yet another non-trivial identity between partial amplitudes allowing one to further reduce the basis of primitive amplitudes to $(n-3)!$ independent elements. This is due to the Bern–Carrasco–Johansson relation [32, 33], discussed in chapter 2 of this review [34]. It takes the schematic form

$$A_n^{\text{tree}}(\sigma_1, \dots, \sigma_n) = \sum_{\rho \in S_{n-3}} K_\rho^{(\sigma)} A_n^{\text{tree}}(1, 2, \rho_3, \dots, \rho_{n-1}, n), \tag{34}$$

with kinematic-dependent coefficients $K_\rho^{(\sigma)}$. Finally, we note that there is also a generalisation of the DDM basis to include fundamental matter [35, 36].

3.3. Colour-ordered Feynman rules

One can establish colour-ordered Feynman rules that generate the partial (colour-ordered) amplitudes by stripping off the colour factors from the usual Feynman rules. This is particularly easy for the gluon and quark propagators,

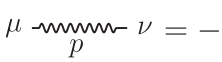

$$= -\frac{i}{p^2 + i\varepsilon}\eta_{\mu\nu}\,, \qquad \mu \longrightarrow \nu = \frac{i\not{p}}{p^2 + i\varepsilon}\eta_{\mu\nu}\,, \tag{35}$$

while for the vertices one finds

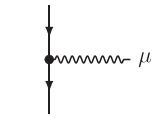

$$= -\frac{i}{\sqrt{2}} g\, \gamma^{\mu}\,,$$

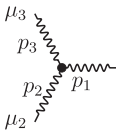

$$= \frac{i}{\sqrt{2}} g \Big[(p_1 - p_2)^{\mu_3} \eta^{\mu_1\mu_2} + (p_2 - p_3)^{\mu_1} \eta^{\mu_2\mu_3} + (p_3 - p_1)^{\mu_2} \eta^{\mu_3\mu_1} \Big]\,,$$

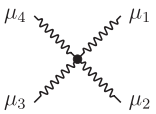

$$= \frac{i}{2} g^2 \Big[2\eta_{\mu_1\mu_3}\eta_{\mu_2\mu_4} - \eta_{\mu_1\mu_2}\eta_{\mu_3\mu_4} - \eta_{\mu_2\mu_3}\eta_{\mu_4\mu_1} \Big]\,. \tag{36}$$

3.4. General properties of colour-ordered amplitudes

Colour-ordered amplitudes are gauge invariant and obey general properties which reduce considerably the number of independent structures:

1. Cyclicity:

$$A(1, 2, \ldots, n) = A(2, \ldots, n, 1), \tag{37}$$

which follows from consistency with the definition (28) and cyclicity of the trace.

2. Parity:

$$[A(1, 2, \ldots, n)]^* = A(\bar{1}, \bar{2}, \ldots, \bar{n}). \tag{38}$$

Here $\bar{i}$ denotes the inversion of the helicity of particle i.

3. Charge conjugation:

$$A(1_q, 2_{\bar{q}}, 3, \ldots, n) = -A(1_{\bar{q}}, 2_q, 3, \ldots, n), \tag{39}$$

that is, flipping the helicity of a quark line changes the sign of the amplitude. This descends from the colour-ordered quark–quark–anti-quark vertex above.

4. Reflection:

$$A(1, 2, \ldots, n) = (-1)^n A(n, n-1, \ldots, 1). \tag{40}$$

It follows from the anti-symmetry of the colour-ordered gluon vertices under reflection of all legs. It also holds in the presence of quark lines but only at tree level.

5. Photon decoupling, or dual Ward identity:

$$\sum_{\sigma \in \mathbb{Z}_{n-1}} A(\sigma_1, \ldots, \sigma_{n-1}, n) = 0, \tag{41}$$

where $\sigma = \{\sigma_1, \ldots, \sigma_{n-1}\}$ are cyclic permutations of $\{1, 2, \ldots, n-1\}$. It follows from (28) and the fact that a gluon amplitude with a single photon vanishes since $f^{0bc} = 0$.

4. Three-point amplitudes

4.1. From symmetries

Scattering amplitudes are covariant under little group transformations of massless momenta (9). This is encoded in the following relation [4]:

$$-\frac{1}{2}\left(\lambda_i^\alpha \frac{\partial}{\partial\lambda_i^\alpha} - \tilde{\lambda}_i^{\dot\alpha}\frac{\partial}{\partial\tilde{\lambda}_i^{\dot\alpha}}\right)A \;=\; h_i\, A, \tag{42}$$

where h_i is the helicity of particle i. It is an immediate consequence of how the wavefunction of a particle of helicity h_i scales under (9). Combined with Lorentz invariance, (42) can be used to determine the functional form of three-point amplitudes of particles of any spin, without ever looking at a Lagrangian, as we now show.

We begin by noting that momentum conservation $p_1 + p_2 + p_3 = 0$ implies $p_i \cdot p_j = 0$ for $i, j = 1, 2, 3$. In real Minkowski space this means that $\langle ij\rangle = 0$ and $[ij] = 0$ for all particles: simply there is no scattering! Life is less constrained in complexified Minkowski space, where the spinors λ and $\tilde{\lambda}$ become independent, and two solutions are possible:

$$\langle i\, j\rangle = 0 \quad \text{and} \quad [i\, j] \neq 0, \quad \text{or} \quad \langle i\, j\rangle \neq 0 \quad \text{and} \quad [i\, j] = 0, \quad \forall\; i, j. \tag{43}$$

Looking for instance at the helicity assignment $1^{-s}, 2^{-s}, 3^{+s}$, one can immediately see, using (42), that the answer must have the form

$$A(1^{-s}, 2^{-s}, 3^{+s}) \sim [A(1^-, 2^-, 3^+)]^s, \tag{44}$$

where for the amplitude with $s = 1$ two options arise: $A(1^-, 2^-, 3^+) \sim \langle 12\rangle^3/(\langle 23\rangle\langle 31\rangle)$ or $A(1^-, 2^-, 3^+) \sim [23][31]/[12]^3$. It turns out that nature has chosen the first one, and we will set

$$A(1^-, 2^-, 3^+) \;=\; ig\,\frac{\langle 1\,2\rangle^3}{\langle 2\,3\rangle\langle 3\,1\rangle}, \tag{45}$$

where g is the Yang–Mills coupling constant[4]. There are several reasons to see why this is the correct choice. First, an n-point amplitude has dimension $4 - n$. With the choice of (45), the coupling constant g is dimensionless, as the Yang–Mills coupling should be, while the other option requires a dimensionful coupling. This would also imply that the corresponding interaction in the Lagrangian is non-local.

The amplitude in (45) is the first in the MHV family (1). We now quote the $\overline{\text{MHV}}$ three-point amplitude, which is obtained from (45) by replacing $\langle ab\rangle \to -[ab]$[5]:

$$A(1^+, 2^+, 3^-) \;=\; -ig\,\frac{[1\,2]^3}{[2\,3][3\,1]}. \tag{46}$$

Little group scaling also fixes the possible form of the all-minus and all-plus three-point amplitudes: $A(1^-, 2^-, 3^-) \sim \langle 12\rangle\langle 23\rangle\langle 31\rangle$ and $A(1^+, 2^+, 3^+) \sim [12][23][31]$, but in Yang–Mills theory the proportionality constant is zero. These amplitudes can be generated in a theory

[4] The factor of i comes from the Dyson expansion of the S-matrix, and in our conventions, scattering amplitudes are the elements of the matrix iT where $S = \mathbb{1} + iT$.

[5] Flipping the helicity sends $\lambda_\alpha \to \tilde{\lambda}_{\dot\alpha}$, and a minus sign arises from the different convention in defining the angle and square brackets as in (12).

with a higher-dimensional, non-renormalisable interaction of the form $\mathrm{Tr}\,F^3$, where F is the field strength [37–39].

Conceptually it is very important that we can determine three-point amplitudes just from symmetry considerations. These amplitudes will be the seeds of the BCFW recursion relation, discussed in section 5.

4.2. From Feynman diagrams

As a useful exercise in spinor gymnastics, we will now derive (45) from QCD Feynman rules. Using the colour-ordered three-point vertex in (36) we find (with all momenta taken as outgoing)

$$A(1^-2^-3^+) = i\frac{g}{\sqrt{2}}\Big[(p_1-p_2)\cdot\epsilon_3^{(+)}\epsilon_1^{(-)}\cdot\epsilon_2^{(-)} + (p_2-p_3)\cdot\epsilon_1^{(-)}\epsilon_2^{(-)}\cdot\epsilon_3^{(+)} + (p_3-p_1)\cdot\epsilon_2^{(-)}\epsilon_3^{(+)}\cdot\epsilon_1^{(-)}\Big], \tag{47}$$

where the polarisation vectors are given in (18). Choosing the same reference spinor for the two negative-helicity gluons we can set $\epsilon_1^{(-)}\cdot\epsilon_2^{(-)}=0$, and using momentum conservation and the transversality condition $p_i\cdot\epsilon_i=0$ we can write this as

$$A(1^-2^-3^+) = ig\sqrt{2}\Big[p_2\cdot\epsilon_1^{(-)}\,\epsilon_2^{(-)}\cdot\epsilon_3^{(+)} - p_1\cdot\epsilon_2^{(-)}\,\epsilon_3^{(+)}\cdot\epsilon_1^{(-)}\Big]. \tag{48}$$

One can easily work out the various dot products

$$\begin{aligned}
\epsilon_2^{(-)}\cdot\epsilon_3^{(+)} &= -\frac{\langle 2\xi\rangle[3\xi]}{[2\xi]\langle 3\xi\rangle}, & \epsilon_1^{(-)}\cdot\epsilon_3^{(+)} &= -\frac{\langle 1\xi\rangle[3\xi]}{[1\xi]\langle 3\xi\rangle},\\
p_2\cdot\epsilon_1^{(-)} &= \frac{1}{\sqrt{2}}\frac{\langle 12\rangle[2\xi]}{[1\xi]}, & p_1\cdot\epsilon_2^{(-)} &= -\frac{1}{\sqrt{2}}\frac{\langle 12\rangle[1\xi]}{[2\xi]},
\end{aligned} \tag{49}$$

and therefore,

$$\begin{aligned}
A(1^-2^-3^+) &= -ig\langle 12\rangle\frac{[3\xi]}{\langle 3\xi\rangle}\left(\frac{\langle 2\xi\rangle}{[1\xi]}+\frac{\langle 1\xi\rangle}{[2\xi]}\right) = ig\langle 12\rangle\frac{[3\xi]}{\langle 3\xi\rangle}\frac{\langle\xi|p_1+p_2|\xi]}{[1\xi][2\xi]}\\
&= ig\frac{\langle 12\rangle[3\xi]^2}{[1\xi][2\xi]}.
\end{aligned} \tag{50}$$

Finally we use three-point momentum conservation to simplify

$$\frac{[3\xi]}{[1\xi]} = \frac{\langle 23\rangle[3\xi]}{\langle 23\rangle[1\xi]} = \frac{\langle 12\rangle}{\langle 23\rangle}, \qquad \frac{[3\xi]}{[2\xi]} = \frac{\langle 13\rangle[3\xi]}{\langle 13\rangle[2\xi]} = \frac{\langle 12\rangle}{\langle 31\rangle}, \tag{51}$$

thus arriving at the result (45). One could repeat this calculation for the scattering of three gravitons, this time using the three-point vertex of [40], arriving at a result proportional to $\big[A(1^-,2^-,3^+)\big]^2$. The expression for the vertex in that paper contains at least 171 terms, which gives no hints of such a remarkable squaring relation[6]!

[6] The reader is not encouraged to try.

5. BCFW recursion relation

5.1. Derivation of the recursion

It was long believed that amplitudes may be determined from their analytic properties. The route followed in [41] was to complexify Mandelstam invariants and study amplitudes as a function of these. Unfortunately, complex analysis in many variables is complex! The Britto–Cachazo–Feng–Witten (BCFW) recursion relation [42, 43] avoids this problem by mapping the singularities of tree-level amplitudes into poles in a *single* complex variable z. To see this at work, consider a tree-level n-gluon amplitude $A_n(p_1,\dots,p_n)$, and introduce the following deformation of the spinors of two adjacent particles 1 and n, often indicated as $[n1\rangle$:

$$\begin{aligned} &\lambda_1 \to \hat{\lambda}_1(z) = \lambda_1 - z\lambda_n, \qquad && \tilde{\lambda}_1 \to \tilde{\lambda}_1, \\ &\lambda_n \to \lambda_n, && \tilde{\lambda}_n \to \hat{\tilde{\lambda}}_n(z) = \tilde{\lambda}_n + z\tilde{\lambda}_1, \end{aligned} \tag{52}$$

with $z \in \mathbb{C}$. We denote the shifted, z-dependent quantities by a hat. The corresponding deformation of the momenta,

$$p_1^{\dot\alpha\alpha} \to \hat{p}_1^{\dot\alpha\alpha}(z) = \tilde{\lambda}_1^{\dot\alpha}\,(\lambda_1 - z\lambda_n)^{\alpha}, \qquad p_n^{\dot\alpha\alpha} \to \hat{p}_n^{\dot\alpha\alpha}(z) = (\tilde{\lambda}_n + z\tilde{\lambda}_1)^{\dot\alpha}\,\lambda_n^{\alpha}, \tag{53}$$

preserves both overall momentum conservation and the on-shell conditions,

$$\hat{p}_1(z) + \hat{p}_n(z) = p_1 + p_n, \qquad \hat{p}_1^2(z) = 0, \qquad \hat{p}_n^2(z) = 0, \tag{54}$$

so that $A_n(z) = A_n(\hat{p}_1(z), p_2, \dots, p_{n-1}, \hat{p}_n(z))$ is a one-parameter family of amplitudes. Note that $\hat{p}_1$ and $\hat{p}_2$ in (53) are now complex—we are now working in complexified Minkowski space. This makes the three-point amplitudes of section 4 non-vanishing, which will then become the seeds of the recursion.

What are the analytic properties of $A_n(z)$? It is well known that tree amplitudes have simple poles in multi-particle channels. This can be seen from the Feynman diagrammatic expansion: pick all diagrams which have a propagator i/P^2, where P is a sum of momenta (which will be adjacent for colour-ordered amplitudes, or generic in gravity). As P goes on shell, the singular diagrams in this class combine into the product of an amplitude to the left and one to the right of this propagator. This implies that the deformed amplitude $A_n(z)$ has precisely $n-3$ *simple* poles in z: with $P_i := \sum_{j=1}^{i-1} p_j$, these have the form

$$\frac{i}{\hat{P}_i^2(z)} := \frac{i}{P_i^2 - z\langle n|P_i|1]} = -\frac{1}{\langle n|P_i|1]}\frac{i}{z - z_{P_i}}, \tag{55}$$

where $\hat{P}_i(z) = \hat{p}_1(z) + p_2 + \cdots p_{i-1}$, and

$$z_{P_i} = \frac{P_i^2}{\langle n|P_i|1]}, \quad \forall\ i \in [3, n-1]. \tag{56}$$

It follows that, as $z \to z_{P_i}$, the amplitude $A_n(z)$ factorises as

$$\begin{aligned} A_n(z) \xrightarrow{z\to z_{P_i}} \frac{i}{\hat{P}_i^2(z)} \sum_{h=\pm} & A_{\rm L}(\hat{1}(z_{P_i}), 2, \dots, i-1, -\hat{P}^{-h}(z_{P_i})) \\ & \times A_{\rm R}(\hat{P}^{h}(z_{P_i}), i, \dots, n-1, \hat{n}(z_{P_i})), \end{aligned} \tag{57}$$

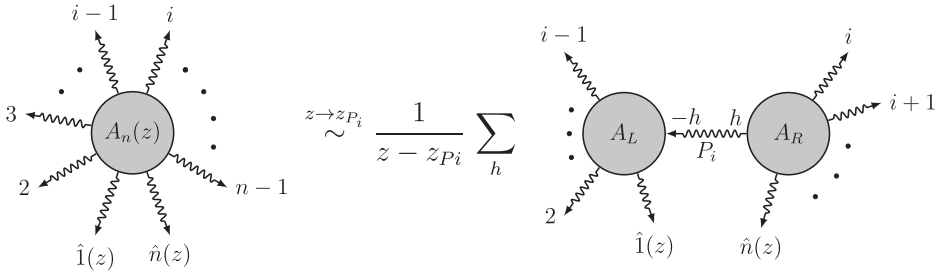

Figure 3. Factorisation of the z-deformed amplitude $\mathcal{A}_n(z)$.

see figure 3. The sum over s in (57) runs over all possible states propagating between A^{L} and A^{R}, and is theory dependent. For gluons it is a sum over $h = \{+, -\}$.

We are only interested in the original amplitude, i.e. $A_n(z = 0)$, and we can use complex analysis to construct it from the knowledge of the residues of $A_n(z)$:

$$\begin{aligned} A_n = A_n(z=0) &= \frac{1}{2\pi i}\oint_{C_0}\frac{\mathrm{d}z}{z}A_n(z) \\ &= \sum_{i=2}^{n-1}\sum_{h=\pm} A_{\mathrm{L}}^{-h}(z_{P_i})\frac{i}{P_i^2}A_{\mathrm{R}}^{h}(z_{P_i}) + \mathrm{Res}(z=\infty). \end{aligned} \tag{58}$$

Here C_0 is a small circle around $z = 0$ that only contains the pole around the origin. To obtain (58) we have deformed this into a large circle at infinity, now encircling all the poles z_{P_i} in the complex plane but with an opposite orientation. If $A_n(z) \to 0$ as $z \to \infty$ we can drop the boundary term $\mathrm{Res}(z = \infty)$. As we shall argue in a moment, this is the case for gauge theories under certain conditions. With this assumption, we arrive at the celebrated BCFW recursion relation [43]:

$$\begin{aligned} A_n = \sum_{i=3}^{n-1}\sum_{h=\pm} & A_i\Big(\hat{1}(z_{P_i}), 2, \ldots, -\hat{P}_i^{-h}(z_{P_i})\Big) \\ & \times \frac{i}{P_i^2}A_{n+2-i}\big(\hat{P}_i^{h}(z_{P_i}), i, \ldots, n-1, \hat{n}(z_{P_i})\big), \end{aligned} \tag{59}$$

with z_{P_i} defined in (56) and $P_i = p_1 + p_2 + \cdots + p_{i-1}$. This relation is constructive: the amplitudes appearing on the right-hand side have lower multiplicity than A_n. Hence, with the seed three-gluon amplitudes (45) and (46), we can use this relation to construct *all* n-gluon trees without using Feynman diagrams! In this derivation we chose to shift two neighbouring legs $\hat{1}$ and $\hat{n}$. In fact, one can also shift non-neighbouring legs or even more than two legs to obtain alternative recursion relations [44, 45].

An open issue is the vanishing of the boundary term in (58). For this we need that

$$\frac{1}{2\pi i}\oint_{\infty}\frac{\mathrm{d}z}{z}A_n(z) = 0, \tag{60}$$

which in turns requires a large-z falloff of the amplitude as $A_n(z) \sim z^{-1}$. In fact, the large-z behaviour depends on the helicities of the shifted legs, and one can show that

$$A(\hat{1}^+, \hat{n}^-) \overset{z\to\infty}{\sim} \frac{1}{z}, \qquad A(\hat{1}^+, \hat{n}^+) \overset{z\to\infty}{\sim} \frac{1}{z}, \qquad A(\hat{1}^-, \hat{n}^-) \overset{z\to\infty}{\sim} \frac{1}{z}, \tag{61}$$

yet $A(\hat{1}^-, \hat{n}^+) \overset{z\to\infty}{\sim} z^3$, which is then a forbidden $[n1\rangle$shift. It is straightforward to show the first relation by analysing the colour-ordered Feynman rules; the other scalings are more technical to derive [46], see [47] for a pedagogical discussion.

5.2. Gravity and other theories

Can we generalise the BCFW recursion to other *massless* quantum field theories? If we recap its derivation, only two ingredients were needed to establish it:

(a) Tree-level amplitudes factorise on simple poles, when the square of the sum of a subset of external momenta vanishes. Note that for colour-ordered amplitudes we only needed to consider adjacent channels but this was not essential, factorisation is a completely general property of unitary theories!

(b) The deformed amplitude $A_n(z)$ falls off as $1/z$ at infinity. This depends on the theory and is related to its ultraviolet behaviour.

So in order to reconstruct tree amplitudes we need to consider all multi-particle channels

$$P_I^\mu := \sum_{i\in I} p_i^\mu, \quad \text{with} \quad I \in \{\text{any subset of the momenta } p_1, \ldots, p_n\}. \tag{62}$$

Whenever $P_I^2 = 0$ we have a pole, and if a two-particle BCFW shift is used the set I must contain only one of the shifted momenta so that P_I^2 becomes z-dependent. Concretely, the BCFW recursion for a shift of legs 1 and n as in (52) in gravity takes the form [48, 49]

$$\begin{aligned} M_n = \sum_Q \sum_{h=\pm\pm} & M_{\rm L}\Big(\hat{1}(z_{P_Q}), Q, -\hat{P}_Q^{-h}(z_{P_Q})\Big) \\ & \times \frac{i}{P_Q^2} M_{\rm R}\big(\hat{P}_Q^h(z_{P_Q}), \bar{Q}, \hat{n}(z_{P_Q})\big), \end{aligned} \tag{63}$$

where Q denotes *all* subsets of momenta in $\{p_2, \ldots, p_{n-1}\}$, $\bar{Q}$ its complement and $P_Q = p_1 + \sum_{i\in Q} P_i$. Finally, we note that the BCFW recursion can be generalised to massive theories [50, 51], to rational parts of one-loop amplitudes in QCD and gravity [52–56], form factors [57, 58], non-linear sigma models and effective field theories [59–62]. Supersymmetric recursion relations [63, 64] are reviewed in section 8. In the maximally supersymmetric case, that is in $\mathcal{N} = 4$ SYM theory, a generalisation of the BCFW recursion to loop-level planar amplitudes was achieved using the formalism of on-shell diagrams and positive Grassmannians of [65]. These important developments connecting to the Amplituhedron approach are reviewed in chapter 7 of this review [66]. Criteria to construct recursion relations in general field theories were studied in [67], also making use of multi-line shifts [44, 68].

5.3. The MHV amplitude from the BCFW recursion relation

As an application, we now derive by induction the Parke–Taylor formula (1). We already know from section 4 that it is true for $n = 3$. Therefore we only need to prove recursively that the formula is correct. We will focus on the case where particles n and 1 have negative helicity, and

choose our $[n1\rangle$shifts of (52). The MHV amplitude has no multi-particle factorisation. In fact, only one BCFW diagram contributes, where A_L in figure 3 is a three-point $\overline{\text{MHV}}$ amplitude (46) and A_R is an $(n-1)$-point MHV amplitude. From (56), the position of the pole is $z_P = \frac{(p_1+p_2)^2}{\langle n|P|1]} = \frac{\langle 12][21]}{\langle n2][21]} = \frac{\langle 12\rangle}{\langle n2\rangle}$. The amplitudes A_L and A_R are then

$$\begin{aligned} A_{\rm L} &= A_3^{\overline{\rm MHV}}(\hat{1}^-, 2^+, -\hat{P}^+) = -ig\frac{[2(-\hat{P})]^3}{[12][(-\hat{P})1]}, \\ A_{\rm R} &= A_{n-1}^{\rm MHV}(\hat{P}^-, 3^+, 4^+, \dots (n-1)^+, \hat{n}^-) = ig^{n-3}\frac{\langle \hat{n}\hat{P}\rangle^3}{\langle \hat{P}3\rangle\langle 34\rangle\dots\langle (n-1)\hat{n}\rangle}. \end{aligned} \tag{64}$$

Using (17), the fact that λ_n and $\tilde{\lambda}_1$ are not shifted in our $[n1\rangle$shift of (52), as well as

$$\langle \hat{n}\hat{P}\rangle[\hat{P}2] = \langle n\hat{1}\rangle\,[12] = \langle n1\rangle\,[12], \qquad \langle 3\hat{P}\rangle\,[\hat{P}1] = \langle 32\rangle\,[21], \tag{65}$$

we find

$$\begin{aligned} \hat{A}_{\rm L}\frac{i}{(p_1+p_2)^2}\hat{A}_{\rm R} &= -ig^{n-2}\frac{\langle n1\rangle^3\,[12]^3}{[12][21]\langle 32\rangle[21]\,\langle 12\rangle\langle 34\rangle\dots\langle (n-1)\,n\rangle} \\ &= ig^{n-2}\frac{\langle n1\rangle^4}{\langle 12\rangle\dots\langle n1\rangle}, \end{aligned} \tag{66}$$

in agreement with (1) for the chosen helicities. MHV amplitudes with different helicity assignments can easily be obtained using the same strategy as above.

5.4. What's special about Yang–Mills MHV amplitudes?

The MHV amplitude (1) derived in the last section is special in many ways. First, it does not have any multi-particle poles—a fact that follows from the vanishing of the amplitudes[7] $A_n(1^\pm, 2^+, \dots, n^+)$. Second, it is a holomorphic function of the spinor variables λ. As anticipated in the introduction, Witten was able to relate this to the property that MHV amplitudes have support on a complex line in twistor space [4]. This is easy to show: reintroducing the momentum conservation delta function $(2\pi)^4\delta^{(4)}(p) = \int \mathrm{d}^4x \mathrm{e}^{\mathrm{i}p\cdot x}$, the amplitude in twistor space is obtained by performing a half-Fourier transform from spinor variables $(\lambda, \tilde{\lambda})$ to twistor variables $(\lambda,\ \mu)$:

$$\begin{aligned} &\int\prod_{i=1}^n \frac{\mathrm{d}^2\tilde{\lambda}_i}{(2\pi)^2}\,\mathrm{e}^{\mathrm{i}[\mu_i\tilde{\lambda}_i]}A_n^{\rm MHV}\ (2\pi)^4\delta^{(4)}\Big(\sum\lambda_i\tilde{\lambda}_i\Big) \\ &\qquad = A_n^{\rm MHV}\int\mathrm{d}^4x\prod_{i=1}^n\delta^{(2)}(\mu_i^{\dot\alpha} + x^{\dot\alpha\alpha}\lambda_{i\alpha}). \end{aligned} \tag{67}$$

Hence the transformed amplitude vanishes unless the gluon twistor space coordinates $(\lambda_i,\ \mu_i)$ satisfy $\mu^{\dot\alpha} + x^{\dot\alpha\alpha}\lambda_\alpha = 0$, $\dot\alpha = 1, 2$, which is the equation of a (complex) line in twistor space. As shown in [4], amplitudes with q negative-helicity gluons, which we call N^{q-2}MHV, are supported on algebraic curves in twistor space of degree $q-1+L$, where L is the number of loops. The case of disconnected curves leads to the so-called MHV diagram method [10], while connected prescriptions were developed in [7–9].

[7] A proof that $A_n(1^\pm, 2^+, \dots, n^+) = 0$ for $n > 3$ is provided in section 8.4.

6. Symmetries of scattering amplitudes

6.1. Poincaré and conformal symmetry

Let us now discuss the symmetry properties of scattering amplitudes. These can be obvious (Poincaré), less obvious (conformal) or hidden (dual conformal or Yangian), as we will discuss in the following[8]. In relativistic quantum field theory, amplitudes are Poincaré invariant by construction. To see this, we seek a representation of the Poincaré symmetry generators—translation and Lorentz generators—in spinor-helicity variables [4]. Translations $p^{\alpha\dot\alpha}$ are realised as a multiplicative operator

$$p^{\alpha\dot\alpha} = \sum_{i=1}^{n} \lambda_i^{\alpha}\, \tilde\lambda_i^{\dot\alpha}, \tag{68}$$

and the corresponding invariance $p^{\alpha\dot\alpha}\, \mathcal{A}_n(\lambda_i, \tilde\lambda_i) = p^{\alpha\dot\alpha}\, \delta^{(4)}(p^{\alpha\dot\alpha})\, A_n(\lambda_i, \tilde\lambda_i) = 0$ is manifest by virtue of the total momentum conservation delta function. The Lorentz generators are symmetric bi-spinors, $m_{\alpha\beta}$ and $\overline{m}_{\dot\alpha\dot\beta}$, realised as first-order differential operators,

$$m_{\alpha\beta} = \sum_{i=1}^{n} \lambda_{i\,(\alpha}\, \partial_{i\,\beta)}, \qquad \overline{m}_{\dot\alpha\dot\beta} = \sum_{i=1}^{n} \tilde\lambda_{i\,(\dot\alpha}\, \partial_{i\,\dot\beta)}, \tag{69}$$

with $\partial_{i\alpha} \coloneqq \frac{\partial}{\partial\lambda_i^{\alpha}}$, $\partial_{i\dot\alpha} \coloneqq \frac{\partial}{\partial\tilde\lambda_i^{\dot\alpha}}$ and $r_{(\alpha\beta)} \coloneqq \frac{1}{2}\,(r_{\alpha\beta} + r_{\beta\alpha})$ denotes symmetrisation. Lorentz invariance of $\mathcal{A}_n(\lambda_i, \tilde\lambda_i)$, that is $m_{\alpha\beta}\, \mathcal{A}_n(\lambda_i, \tilde\lambda_i) = \overline{m}_{\dot\alpha\dot\beta}\, \mathcal{A}_n(\lambda_i, \tilde\lambda_i) = 0$ is manifest, as the spinor brackets $\langle ij\rangle$ and $[ij]$ are invariant under $m_{\alpha\beta}$ and $\overline{m}_{\dot\alpha\dot\beta}$, e.g.

$$m_{\alpha\beta}\, \langle jk\rangle = \sum_{i=1}^{n} \lambda_{i\,(\alpha}\, \partial_{i\,\beta)}\, \lambda_j^{\gamma} \lambda_{k\,\gamma} = \lambda_{j\,\alpha}\lambda_{k\,\beta} - \lambda_{j\,\beta}\lambda_{k\,\alpha} + (\alpha \leftrightarrow \beta) = 0. \tag{70}$$

Classical Yang–Mills theory is invariant under an additional, less obvious symmetry: conformal symmetry. It originates from the fact that pure Yang–Mills theory and massless QCD do not carry any dimensionful parameter and are thus invariant under scale transformations (or dilatations) $x^{\mu} \to \kappa^{-1} x^{\mu}$, or, in momentum space $p^{\mu} \to \kappa p^{\mu}$. The dilatation generator in spinor-helicity variables acting on n-point amplitudes reads [4]

$$d = \sum_{i=1}^{n} \left(\frac{1}{2} \lambda_i^{\alpha}\, \partial_{i\,\alpha} + \frac{1}{2} \tilde\lambda_i^{\dot\alpha}\, \partial_{i\,\dot\alpha} + 1 \right), \tag{71}$$

reflecting the mass dimensions $1/2$ of the spinors, i.e. $[d, \lambda_i] = \frac{1}{2}\,\lambda_i$ and $[d, \tilde\lambda_i] = \frac{1}{2}\,\tilde\lambda_i$.

6.2. Example: the MHV amplitude

As an example, we now wish to check the invariance of the MHV amplitudes $\mathcal{A}_n^{\text{MHV}} = \delta^{(4)}(\sum_i p_i) A_n^{\text{MHV}}$ with A_n^{MHV} given in (1). The dilatation operator d in (71) simply measures the mass dimension of the object it acts on. We note the mass dimensions $[\delta^{(4)}(p)] = -4$, $[\langle ij\rangle^4] = 4$ and $[(\langle 12\rangle \ldots \langle n1\rangle)^{-1}] = -n$, hence

$$\mathrm{d}\, \mathcal{A}_n^{\text{MHV}} = (-4 + 4 - n + n)\, \mathcal{A}_n^{\text{MHV}} = 0, \tag{72}$$

[8] Hidden symmetries are not invariances of the action.

as required. Relativistic scale-invariant quantum field theories are conformal, i.e. the dilatation symmetry is accompanied by invariance under so-called special conformal transformations $k_{\alpha\dot\alpha}$. This symmetry generator is realised in terms of a second-order differential operator in spinor-helicity variables [4],

$$k_{\alpha\dot\alpha} = \sum_{i=1}^{n} \partial_{i\,\alpha}\,\partial_{i\,\dot\alpha}. \tag{73}$$

Checking this symmetry for MHV amplitudes is instructive yet requires a little bit of algebra [4], see [47] for a pedagogical exposition.

In summary, together with the Poincaré and dilatation generators, the set of operators $\{p_{\alpha\dot\alpha}, k_{\alpha\dot\alpha}, m_{\alpha\beta}, \overline{m}_{\dot\alpha\dot\beta}, d\}$ generate the four-dimensional conformal group $SO(2,4)$ which leave tree-level pure Yang–Mills and massless QCD amplitudes invariant.

7. Collinear and soft limits in gauge theory and gravity

7.1. Yang–Mills theory

7.1.1. Collinear limits. Scattering amplitudes in Yang–Mills theories have a universal behaviour when two (or more) particle momenta become collinear, which in turn can be used to constrain their form, or check the correctness of a calculation. In the following we discuss the case of two gluons with momenta p_1 and p_2 becoming collinear. This is described by setting $p_1 = zP$ and $p_2 = (1-z)P$, where $P := p_1 + p_2$ and $P^2 \to 0$ in the collinear limit. The universal behaviour of tree-level amplitudes can then be described as

$$A_n(1,\ldots,n) \xrightarrow{p_1 \| p_2} \sum_{h=\pm} \mathrm{Split}_{-h}(1,2)\,A_{n-1}(P^h,3,\ldots,n). \tag{74}$$

The *splitting amplitudes* $\mathrm{Split}_{-\lambda}(1,2)$ diverge in the collinear limit, and are given by

$$\begin{aligned} &\mathrm{Split}_-(1^-,2^-) = 0, && \mathrm{Split}_-(1^+,2^+) = \frac{1}{\sqrt{z(1-z)}}\frac{1}{\langle 12\rangle},\\ &\mathrm{Split}_+(1^+,2^-) = \frac{(1-z)^2}{\sqrt{z(1-z)}}\frac{1}{\langle 12\rangle}, && \mathrm{Split}_-(1^+,2^-) = -\frac{z^2}{\sqrt{z(1-z)}}\frac{1}{[12]}. \end{aligned} \tag{75}$$

An elegant way to derive this universal behaviour at tree level is based on the MHV diagram method[9] [10], later extended to to loop amplitudes in [69, 70]. While we will not review it here (see e.g. [71] for details), the basic rules are very easy to explain: MHV amplitudes are continued off shell and used as vertices; to an internal leg whose momentum P is a sum of several external momenta, we associate the spinor

$$\lambda_{\hat P}^{\alpha} \to P^{\dot\alpha\alpha}\tilde\xi_{\dot\alpha}, \tag{76}$$

where $|\xi]$ is a reference spinor (this is often called an *off-shell continuation* of the spinor); and MHV vertices are joined using scalar propagators i/P^2. Finally, by counting negative helicities, one can immediately see that MHV diagrams contributing to an N^kMHV amplitude must

[9] MHV diagrams can also be understood as multi-line BCFW recursion relations, where one shifts the $\tilde\lambda$ spinors of *all* the negative-helicity gluons [44].

contain $k+1$ MHV vertices. To make contact with section 5.4, note that this corresponds to a disconnected curve of degree $k+1$ in twistor space—the union of $k+1$ complex lines.

MHV diagrams treat positive and negative helicities on different footing, hence we need to distinguish two types of collinear limits: those where the number of negative helicities is unchanged, that is $++\to+$ and $+-\to-$; and those where this number is reduced by one, that is $--\to-$ and $+-\to+$. In both cases, the MHV diagrams that contribute in the limit have the two legs that become collinear attached to the same MHV vertex [10]. In the first case, corresponding to the second and third splitting amplitudes in (75), the collinear behaviour descends directly from the single MHV vertex containing the two momenta that are becoming collinear; while in the second, it arises from an MHV diagram where the two particles going collinear belong to a three-point MHV vertex, connected to another MHV vertex with the usual scalar propagator of the MHV diagrammatic approach. As an example we now derive collinear factorisation in the case $+-\to+$. The relevant MHV diagram is shown in figure 4, and gives

$$i\frac{\langle 2\ -\hat{P}\rangle^3}{\langle -\hat{P}\,1\rangle\langle 12\rangle}\frac{i}{\langle 12\rangle[21]}A_{n-1}(\hat{P}^+,\ldots). \tag{77}$$

Following (76), the spinor $\lambda_{\hat{P}}$ is given by $\lambda_{\hat{P}}=(p_1+p_2)|\xi]/[\hat{P}\xi]$, where $|\xi]$ is the reference spinor. Using this and (17), we get

$$\langle 2\ -\hat{P}\rangle = i\frac{\langle 21\rangle[1\xi]}{[\hat{P}\xi]}, \qquad \langle 1\ -\hat{P}\rangle = i\frac{\langle 12\rangle[2\xi]}{[\hat{P}\xi]}, \tag{78}$$

and hence

$$A_n \xrightarrow{p_1\| p_2} -\frac{1}{[12]}\frac{[1\xi]^3}{[\hat{P}\xi]^2[2\xi]}A_{n-1}(\hat{P}^+,\ldots). \tag{79}$$

Replacing $\tilde{\lambda}_1\to\sqrt{z}\tilde{\lambda}_{\hat{P}}$, $\tilde{\lambda}_2\to\sqrt{1-z}\tilde{\lambda}_{\hat{P}}$, we arrive at

$$A_n \xrightarrow{p_1\| p_2} -\frac{z^2}{\sqrt{z(1-z)}}\frac{1}{[12]}A_{n-1}(P^+,\ldots), \tag{80}$$

where $P=p_1+p_2$, thus reproducing the last splitting amplitude in (75).

We conclude by mentioning that collinear behaviour at one loop [72, 73] can also be studied [70] using quantum MHV diagrams [69, 74–76].

7.1.2. Soft limits. Amplitudes have a universal behaviour also in soft limits, where the momentum of a particle becomes small[10]. At tree level,

$$A_n(1,\ldots,a,s,b,\ldots,n) \xrightarrow{p_s\to 0} \mathcal{S}^{(0)}(a,s,b)\,A_{n-1}(1,\ldots,a,b,\ldots,n), \tag{81}$$

where $\mathcal{S}^{(0)}(a,s,b)$ is a tree-level soft (or eikonal) factor,

$$\mathcal{S}^{(0)}(a,s^+,b) = \frac{\langle a\,b\rangle}{\langle a\,s\rangle\,\langle s\,b\rangle}, \qquad \mathcal{S}^{(0)}(a,s^-,b) = -\frac{[a\,b]}{[a\,s]\,[s\,b]}. \tag{82}$$

Note the dependence on the helicity of the soft particle (but not on the helicities of the particles adjacent to it in colour space). The derivation from MHV diagrams is straightforward for the

[10] An extensive discussion of soft limits can be found in chapter 11 of this review [77].

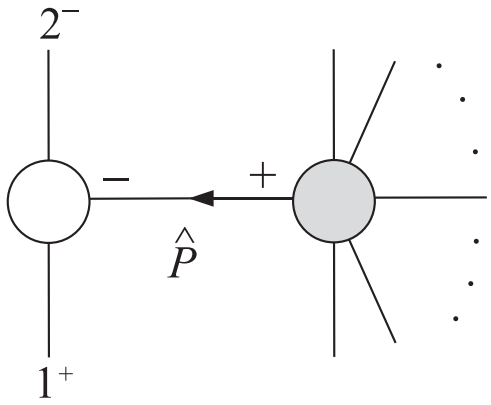

Figure 4. The MHV diagram contributing to the collinear limit $--\to -$. The grey (white) amplitudes is (anti)MHV.

first case. The second case, where the gluon becoming soft has negative helicity, is special since MHV vertices have precisely two negative helicities and a generic MHV vertex would simply vanish in the limit. Two diagrams have to be considered in this case, shown in figure 5: in the first one, an MHV three-point vertex with external gluons a and s (s is the leg whose momentum is becoming soft) is joined to an MHV vertex to which the leg b belongs, maintaining the colour ordering a, s, b; in the second, s and b belong to a three-point MHV vertex, which is then linked to a second MHV vertex containing the gluon a. Focusing on the case where particles a and b have positive helicities as an example, the first diagram gives

$$\begin{aligned} i\frac{\langle s\ -\hat{P}_A\rangle^3}{\langle -\hat{P}_A a\rangle\langle as\rangle}\frac{i}{\langle sa\rangle[as]}A_{n-1}(\hat{P}_A,b,\ldots) &= \frac{[a\xi]^3}{[s\xi][sa]}\frac{1}{[\hat{P}_A\xi]^2}A_{n-1}(\hat{P}_A,b,\ldots) \\ &\to \frac{1}{[s\xi]}\frac{[a\xi]}{[sa]}A_{n-1}(\hat{P}_A,b,\ldots), \end{aligned} \tag{83}$$

while the second evaluates to

$$\begin{aligned} & i\frac{\langle -\hat{P}_B s\rangle^3}{\langle sb\rangle\langle b\ -\hat{P}_B\rangle}\frac{i}{\langle sb\rangle[bs]}A_{n-1}(\hat{P}_B,b,\ldots) \\ &\quad = -\frac{[b\xi]^3}{[s\xi][sb]}\frac{1}{[\hat{P}_B\xi]^2}A_{n-1}(a^+,\hat{P}_B,\ldots) \\ &\quad \to -\frac{1}{[s\xi]}\frac{[b\xi]}{[sb]}A_{n-1}(a^+,\hat{P}_B,\ldots), \end{aligned} \tag{84}$$

where $|\xi]$ is the usual MHV-diagram reference spinor, and

$$|\hat{P}_A\rangle = \frac{(p_a+p_s)|\xi]}{[\hat{P}_A\xi]}, \qquad |\hat{P}_B\rangle = \frac{(p_b+p_s)|\xi]}{[\hat{P}_B\xi]}. \tag{85}$$

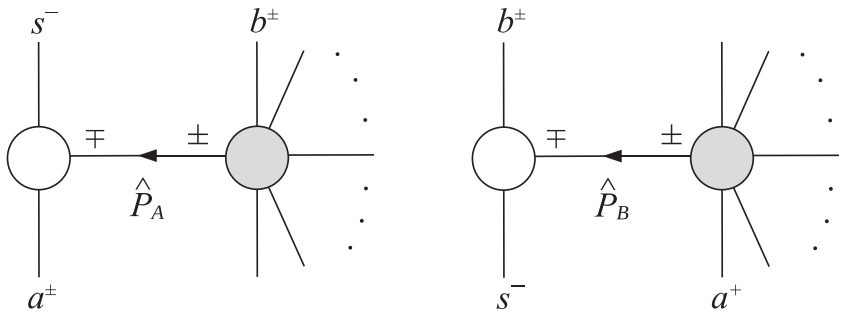

Figure 5. The two MHV diagrams contributing to the soft limit $p_s \to 0$ for the helicities (a^+, s^-, b^+).

We also used (17), and

$$\langle s\hat{P}_A\rangle = \frac{\langle sa\rangle[a\xi]}{[\hat{P}_A\xi]}, \qquad \langle a\hat{P}_A\rangle = \frac{\langle as\rangle[s\xi]}{[\hat{P}_A\xi]}, \qquad \langle s\hat{P}_B\rangle = \frac{\langle sb\rangle[b\xi]}{[\hat{P}_B\xi]},$$
$$\langle b\hat{P}_B\rangle = \frac{\langle bs\rangle[s\xi]}{[\hat{P}_B\xi]}. \tag{86}$$

Summing the contributions in (83) and (84), and taking the soft limit (with $\hat{P}_A \to p_a$, $\hat{P}_B \to p_b$) we obtain

$$A_n(a, s^-, b, \ldots) \xrightarrow{p_s\to 0} -\frac{[ab]}{[as][sb]} A_{n-1}(a, b, \ldots), \tag{87}$$

in agreement with $\mathcal{S}^{(0)}(a, s^-, b)$ in (82). Similar derivations can be carried out for the other possible helicities of particles a and b.

7.1.3. Soft limits from recursion relations. There is an alternative, powerful way to derive soft theorems from the BCFW recursion relation. It was originally proposed in [78], where it was found that not only the leading but also the subleading soft behaviour of graviton amplitudes is universal. A similar approach was devised in Yang–Mills theory in [79], as we now briefly review. Choosing to shift the momenta of particles s and b, a single diagram contributes in the soft limit, which is identical to that on the left-hand side of figure 5 now to be interpreted as a BCFW diagram. For concreteness we carry out the computation for the case that legs a and s carry helicity $+1$, however the result is independent of the helicity of particle a, hence we will drop its helicity label. With the shifts $\hat{\lambda}_s = \lambda_s + z\lambda_b$, $\hat{\tilde{\lambda}}_b = \tilde{\lambda}_b - z\tilde{\lambda}_s$, the recursive diagram evaluates to

$$A_n(a, s^+, b, \ldots) \to -i\frac{[as]^3}{[-\hat{P}_A a][s - \hat{P}_A]} \frac{i}{(p_a + p_s)^2} A_{n-1}(z^*), \tag{88}$$

and $z^* = -\langle as\rangle/\langle ab\rangle$ is the position of the pole for this BCFW diagram. The internal momentum evaluated at this pole can be written as $\hat{P}_A = \lambda_a\left[\tilde{\lambda}_a + \tilde{\lambda}_s(\langle sb\rangle/\langle ab\rangle)\right]$ (after using the Schouten identity), and using this one quickly arrives at

$$A_n(a^+, s^+, b, \ldots) \xrightarrow{p_s\to 0} \frac{\langle ab\rangle}{\langle as\rangle\langle sb\rangle} A_{n-1}(z^*), \tag{89}$$

where $A_{n-1}(z^*) = A_{n-1}(\{\lambda_a, \tilde{\lambda}_a + \frac{\langle sb\rangle}{\langle ab\rangle}\tilde{\lambda}_s\}, \{\lambda_b, \tilde{\lambda}_b + \frac{\langle as\rangle}{\langle ab\rangle}\tilde{\lambda}_s\}, \ldots)$. To leading order in the soft limit, one simply replaces $A_{n-1}(z^*) \to A_{n-1}(a, b, \ldots)$ thus reproducing the soft factor in (82). One can also be more ambitious and keep subleading terms in the limit. Rescaling the soft momentum as $p_s \to \delta p_s$ to keep track of terms, one finds that

$$A_n(a, s^+, b, \ldots) \xrightarrow{p_s \to 0} \left(\frac{1}{\delta^2}\mathcal{S}^{(0)} + \frac{1}{\delta}\mathcal{S}^{(1)}\right) A_{n-1}(a, b, \ldots) + \mathcal{O}(\delta), \tag{90}$$

where the subleading soft factor $\mathcal{S}^{(1)}$ is

$$\mathcal{S}^{(1)} = \frac{1}{\langle as\rangle}\tilde{\lambda}_s\frac{\partial}{\partial\tilde{\lambda}_a} + \frac{1}{\langle sb\rangle}\tilde{\lambda}_s\frac{\partial}{\partial\tilde{\lambda}_b}. \tag{91}$$

7.2. Gravity

7.2.1. Collinear limits. Unlike Yang–Mills amplitudes, gravity amplitudes in real Minkowski space are non-singular in collinear limits, more precisely they only have phase singularities, which become simple poles in complex Minkowski space. Concretely [80], if we send $p_i \to zP$ and $p_j \to (1-z)P$ as $P^2 = (p_i + p_j)^2 \to 0$, we have

$$\mathcal{M}_n(i^{h_i}, j^{h_j}, \ldots) \xrightarrow{p_i \| p_j} \sum_{h=\pm\pm} \text{Split}^{\text{GR}}_{-h}(i^{h_i}, j^{h_j})\mathcal{M}_{n-1}(P^h, \ldots) + R_n, \tag{92}$$

where h and σ denote the helicities of the gravitons. The remainder R_n is free of phase singularities/poles and the splitting amplitudes are given by

$$\begin{aligned} &\text{Split}^{\text{GR}}_{--}(i^{++}, j^{++}) = -\frac{1}{z(1-z)}\frac{[i\,j]}{\langle i\,j\rangle}, \qquad \text{Split}^{\text{GR}}_{++}(i^{--}, j^{++}) = -\frac{z^3}{(1-z)}\frac{[i\,j]}{\langle i\,j\rangle}, \\ &\text{Split}^{\text{GR}}_{++}(i^{++}, j^{++}) = 0, \end{aligned} \tag{93}$$

where the missing cases can be obtained from parity, or simply vanish. The ratio of spinor brackets appearing in the splitting amplitudes is manifestly a phase in real Minkowski space, but in complex Minkowski space the brackets are independent and if the collinear limit is taken as $\langle ij\rangle \to 0$, the ratio becomes singular.

The gravity splitting amplitudes can be derived easily using the fact that the three-graviton amplitudes are simply squares of the corresponding three-gluon amplitudes leading to a simple relation between graviton and gluon splitting amplitudes [80]

$$\text{Split}^{\text{GR}}_{\pm\pm}(i^{2h_i}, j^{2h_j}) = s_{ij}\left[\text{Split}_{\pm}(i^{h_i}, j^{h_j})\right]^2, \tag{94}$$

where the Yang–Mills splitting amplitudes are given in (75).

7.2.2. Soft limits. As already mentioned in section 7.1.3, the leading [81], subleading and sub-subleading [78] soft limits of gravity amplitudes are universal[11]. These can be obtained using the four-dimensional BCFW recursion relation [78], with the result

$$\mathcal{M}_n \xrightarrow{p_s \to 0} \left(\frac{1}{\delta}\mathcal{S}^{(0)}_{\text{grav}}(q) + \mathcal{S}^{(1)}_{\text{grav}}(q) + \delta\,\mathcal{S}^{(2)}_{\text{grav}}(q)\right)\mathcal{M}_{n-1} + \mathcal{O}(\delta^2), \tag{95}$$

[11] The sub-subleading soft factor quoted here is for Einstein–Hilbert theory. In general it can receive additional, theory-dependent corrections [82].

where, for a positive-helicity soft graviton s^+,

$$\begin{aligned}
\mathcal{S}^{(0)}_{\text{grav}}(s^+) &= \sum_a \frac{[sa]}{\langle sa\rangle}\frac{\langle xa\rangle}{\langle xs\rangle}\frac{\langle ya\rangle}{\langle ys\rangle},\\
\mathcal{S}^{(1)}_{\text{grav}}(s^+) &= \frac{1}{2}\sum_a \frac{[sa]}{\langle sa\rangle}\left(\frac{\langle xa\rangle}{\langle xs\rangle}+\frac{\langle ya\rangle}{\langle ys\rangle}\right)\tilde{\lambda}_s^{\dot\alpha}\frac{\partial}{\partial\tilde{\lambda}_a^{\dot\alpha}}.\\
\mathcal{S}^{(2)}_{\text{grav}}(s^+) &= \frac{1}{2}\sum_a \frac{[sa]}{\langle sa\rangle}\tilde{\lambda}_s^{\dot\alpha}\tilde{\lambda}_s^{\dot\beta}\frac{\partial^2}{\partial\tilde{\lambda}_a^{\dot\alpha}\partial\tilde{\lambda}_a^{\dot\beta}}.
\end{aligned} \tag{96}$$

The sum over a is over the remaining $n-1$ particles, and $|x\rangle$ and $|y\rangle$ are reference spinors. The soft factors for the case where s has negative helicity can be found by conjugation. $\mathcal{S}^{(0)}$ is the famous Weinberg soft factor [81], and we also quote below expressions for the soft factors valid in any dimension in terms of polarisation tensors:

$$\begin{aligned}
\mathcal{S}^{(0)} &= \sum_a \frac{k_a^\mu \epsilon_{\mu\nu}(s)k_a^\nu}{k_a\cdot p_s}, \qquad & \mathcal{S}^{(1)} &= -i\sum_a \frac{k_a^\mu \epsilon_{\mu\nu}(s)J_a^{\nu\rho}k_{s\rho}}{k_a\cdot p_s},\\
\mathcal{S}^{(2)} &= -\frac{1}{2}\sum_a \frac{\epsilon_{\mu\nu}(s)k_{s\rho}J_a^{\mu\rho}k_{s\sigma}J_s^{\nu\sigma}}{k_a\cdot p_s},
\end{aligned} \tag{97}$$

where $J_a^{\mu\nu} = L_a^{\mu\nu}+\Sigma_a^{\mu\nu}$, and $L_a^{\mu\nu} = i\left(k_a^\mu\frac{\partial}{\partial k_{a\nu}} - k_a^\nu\frac{\partial}{\partial k_{a\mu}}\right)$, $\Sigma_a^{\mu\nu} = i\left(\epsilon_a^\mu\frac{\partial}{\partial\epsilon_{a\nu}} - \epsilon_a^\nu\frac{\partial}{\partial\epsilon_{a\mu}}\right)$. We also mention that soft theorems beyond leading order can be elegantly derived from gauge invariance [83, 84]. Finally, it is interesting to note that double soft limits are also universal, and corresponding theorems can be established, with the simultaneous and consecutive limits leading to different types of universal behaviour [85, 86].

8. Supersymmetric amplitudes

8.1. Generalities

The spectrum of maximally supersymmetric $\mathcal{N}=4$ SYM theory contains the following states[12]:

- Two gluons $G^\pm(p)$ with helicities $1,-1$,
- Four Weyl fermions ψ_A with helicity $+1/2$, transforming in the fundamental of the R-symmetry group $SU(4)_R$, and four Weyl fermions $\bar\psi^A$ with helicity $-1/2$ in the anti-fundamental representation, with $A=1,\ldots,4$, and
- Six real scalar fields (corresponding to particles of zero helicity) $\phi_{[AB]}$ in the antisymmetric tensor representation of the R-symmetry group ($A,B=1,\ldots,4$).

One can then combine the states into an on-shell superfield [88]

$$\begin{aligned}
\Phi(\eta,p) \coloneqq\ & G^+(p) + \eta^A\psi_A(p) + \frac{\eta^A\eta^B}{2!}\phi_{[AB]}(p) + \epsilon_{ABCD}\frac{\eta^A\eta^B\eta^C}{3!}\bar\psi^D(p)\\
&+\eta^1\eta^2\eta^3\eta^4 G^-(p),
\end{aligned} \tag{98}$$

[12] See e.g. [87] for a review.

where the η^A are four auxiliary Graßmann variables. For each particle, the coordinates $(\lambda, \tilde{\lambda}, \eta)$ parameterise an on-shell superspace [89]. The supersymmetry generators q^A and $\bar{q}_A$ satisfy the algebra $\{q^A_\alpha, \bar{q}_{B\dot{\alpha}}\} = \lambda_\alpha \tilde{\lambda}_{\dot{\alpha}}\, \delta^A_B$, and have a natural realisation on this superspace as $q^A_\alpha = \lambda_\alpha \eta^A$, $\bar{q}_{A\dot{\alpha}} = \tilde{\lambda}_{\dot{\alpha}} \frac{\partial}{\partial \eta^A}$, or, for n particles,

$$q^A_\alpha \;=\; \sum_{i=1}^{n} \lambda_{i\alpha} \eta_i^A, \qquad \bar{q}_{A\dot{\alpha}} \;=\; \sum_{i=1}^{n} \tilde{\lambda}_{i\dot{\alpha}} \frac{\partial}{\partial \eta_i^A}. \tag{99}$$

The next step is to combine all amplitudes with a given number of particles n and fixed total helicity into a *superamplitude*[13] $\mathcal{A}$. This superamplitude can then be expanded in powers of the η_i^As, with each coefficient of the expansion being a component amplitude. A term containing k_i powers of η_i corresponds to an amplitude where the ith particle has helicity $h_i = 1 - k_i/2$, with the total helicity being $\sum_{i=1}^n h_i$. In other words, to get an amplitude with helicity h_i for particle i we need to pick the term containing $2 - 2h_i$ powers of η_i in the superamplitude.

Superamplitudes are invariant under the q and $\bar{q}$ supersymmetries, in addition to being invariant under translations. The latter symmetry is implemented by pulling out a δ-function of total momentum conservation $\delta^{(4)}(p)$, with $p := \sum_{i=1}^n \lambda_i \tilde{\lambda}_i$, and similarly we can realise the q-supersymmetry manifestly via a δ-function of supermomentum conservation[14]. Summarising, we will set

$$\mathcal{A}_n := \delta^{(4)}(p) \delta^{(8)}(q)\; A_n, \tag{100}$$

where $q = \sum_{i=1}^n \eta_i \lambda_i$ is the total supermomentum. It is then easily checked that invariance under $\bar{q}$ supersymmetry implies that $\bar{q} A_n = 0$ on the support of the two δ-functions.

8.2. MHV and NMHV superamplitudes

Our first example is the MHV superamplitude. Its elegant expression was given in [88]:

$$\mathcal{A}_n^{\text{MHV}}(1, \ldots, n) \;=\; i\, g^{n-2} \frac{\delta^{(4)}(p)\, \delta^{(8)}(q)}{\langle 12\rangle \langle 23\rangle \ldots \langle n1\rangle}. \tag{101}$$

From this it is easy to extract component amplitudes as outlined in the previous section. For instance, the MHV amplitude with negative helicity gluons i^- and j^- can be extracted as the coefficient of $\eta_i^4 \eta_j^4$ in the expansion of (101), leading to[15]

$$A_n^{\text{MHV}}(1^+, \ldots, i^-, \ldots, j^-, \ldots, n^+) = i g^{n-2} \frac{\langle ij\rangle^4}{\langle 12\rangle \langle 23\rangle \cdots \langle n1\rangle}.$$

Recall that we derived this for neighboring $\{i, j\} = \{n, 1\}$ in section 5.3.

Next we consider the NMHV superamplitudes. These have the form [90, 91]

$$\mathcal{A}_n^{\text{NMHV}} = \mathcal{A}_n^{\text{MHV}} \sum_{u,v=i+2}^{i+n-1} R_{iuv}, \tag{102}$$

[13] Not to be confused with the complete amplitudes of section 3, traditionally denoted in the same way.

[14] The three-point case is special and will be discussed in (104).

[15] A useful formula is $\delta^{(8)}(\lambda_1 \eta_1 + \lambda_2 \eta_2 + \cdots) = \langle 12\rangle^4 \prod_{A=1}^4 \eta_1^A \eta_2^A + \cdots$.

where the functions R_{rst} are defined as

$R_{rst} :=$ 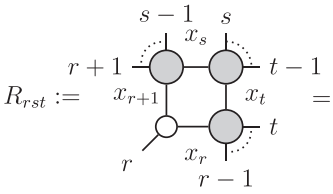

$$= \frac{\langle s-1\, s\rangle\langle t-1\, t\rangle\, \delta^{(4)}\big(\Xi_{rst}\big)}{x_{st}^2\langle r|x_{rt}x_{ts}|s-1\rangle\langle r|x_{rt}x_{ts}|s\rangle\langle r|x_{rs}x_{st}|t-1\rangle\langle r|x_{rs}x_{st}|t\rangle} \tag{103}$$

and $\Xi_{rst} := \langle r|x_{rs}x_{st}|\theta_{tr}\rangle + \langle r|x_{rt}x_{ts}|\theta_{sr}\rangle$. Here we have introduced the so-called dual, or region (super)momenta[16] x_i and θ_i, defined $\lambda_i\tilde{\lambda}_i := x_i - x_{i+1}$, $\lambda_i\eta_i := \theta_i - \theta_{i+1}$, so that $x_{ij} = \sum_{k=i}^{j-1}\lambda_k\tilde{\lambda}_k$, $\theta_{ij} = \sum_{k=1}^{j-1}\lambda_k\eta_k$, with $x_{n+1} = x_1$, $\theta_{n+1} = \theta_1$. We also showed a convenient diagrammatic notation for the invariants introduced in [92]. In section 9.3 we will prove that the NMHV is dual superconformal covariant.

8.3. Supersymmetric BCFW recursion relation

We now discuss how to supersymmetrise the BCFW recursion relation of section 5.1 [63, 64]. As in the non-supersymmetric case, we construct amplitudes recursively starting from two three-point superamplitudes: the first one has the total MHV helicity, and is given by (101) for $n = 3$, while the three-point $\overline{\text{MHV}}$ superamplitude is [63, 64]

$$\mathcal{A}_3^{\overline{\text{MHV}}} \;=\; -i\,g\,\delta^{(4)}(p_1+p_2+p_3)\,\frac{\delta^{(4)}(\eta_1[23]\,+\,\eta_2[31]\,+\,\eta_3[12])}{[12]\,[23]\,[31]}. \tag{104}$$

It was shown in [63] that, despite its slightly unusual supersymmetric delta function, the $\overline{\text{MHV}}$ superamplitude is invariant under supersymmetry, as well as covariant under the dual superconformal symmetry of [90].

Similarly to the discussion of section 4.1, three-point superamplitudes can be determined from symmetry considerations alone up to an overall normalisation. For instance, the form of the three-point MHV superamplitude can be fixed by requiring that it depends only on the holomorphic spinors $\lambda_1, \lambda_2, \lambda_3$ and satisfies the relations $\hat{h}_i\,\mathcal{A}_3^{\text{MHV}} = \mathcal{A}_3^{\text{MHV}}$, $i = 1, 2, 3$, where

$$\hat{h}_i := \frac{1}{2}\left(-\lambda_i^\alpha\frac{\partial}{\partial\lambda_i^\alpha} + \tilde{\lambda}_i^{\dot\alpha}\frac{\partial}{\partial\tilde{\lambda}_i^{\dot\alpha}} + \eta_i^A\frac{\partial}{\partial\eta_i^A}\right), \tag{105}$$

which express the fact that the on-shell superfield (98) has helicity $+1$.

8.3.1. Derivation. We now derive the supersymmetric recursion relation. We begin by observing that in order to maintain supersymmetry we must accompany the momentum shifts by a supermomentum shift. The following (super)shifts

$$\hat{\tilde{\lambda}}_1(z) := \tilde{\lambda}_1 + z\tilde{\lambda}_2, \qquad \hat{\lambda}_2(z) = \lambda_2 - z\lambda_1, \qquad \hat{\eta}_1(z) = \eta_1 + z\eta_2, \tag{106}$$

manifestly preserve (super)momentum conservations and the on-shell conditions. As in the non-supersymmetric case, we define a one-parameter family of superamplitudes,

$$\mathcal{A}_n(z) := \mathcal{A}_n(\{\lambda_1, \hat{\tilde{\lambda}}_1, \hat{\eta}_1\}, \{\hat{\lambda}_2, \tilde{\lambda}_2, \eta_2\}, \ldots), \tag{107}$$

[16] See section 9.2 for a discussion of such quantities in the context of dual superconformal invariance.

where the dots denote the unshifted (super)momenta of the remaining $n-2$ particles. The derivation of the recursion relation parallels that of its non-supersymmetric cousin, with the result [63, 64]

$$\mathcal{A}_n \;=\; \sum_P \int \mathrm{d}^4\eta_{\hat{P}}\; \mathcal{A}_{\rm L}(z_P)\frac{i}{P^2}\mathcal{A}_{\rm R}(z_P), \tag{108}$$

where $\eta_{\hat{P}}$ is the Graßmann coordinate associated to the internal particle with momentum $\hat{P}$. The sum is over all diagrams where such that the shifted momenta belong to different superamplitudes. The two superamplitudes in (108) are computed on the solution z_P of $\hat{P}^2(z)=0$, with $\hat{P}(z) := P + z\lambda_1\tilde{\lambda}_2$. Note that in (108) the total helicities of $\mathcal{A}_{\rm L}$ and $\mathcal{A}_{\rm R}$ must sum to the total helicity of $\mathcal{A}$.

The derivation of (108) rests on the important fact that $\mathcal{A}_n(z)\to 0$ as $z\to\infty$ [63, 64]. Specifically, we will now show that

$$\mathcal{A}_n^{\mathcal{N}=4}(z) \overset{z\to\infty}{\sim} \frac{1}{z}, \qquad \mathcal{A}_n^{\mathcal{N}=8}(z) \overset{z\to\infty}{\sim} \frac{1}{z^2}. \tag{109}$$

To do so, we note that in the maximally supersymmetric $\mathcal{N}=4$ SYM or $\mathcal{N}=8$ supergravity theories, we have enough supersymmetry transformations to set to zero *two* of the η^A variables in the superamplitude $\mathcal{A}_n(\lambda_1,\tilde{\lambda}_1,\eta_1;\lambda_2,\tilde{\lambda}_2,\eta_2;\ldots;\lambda_n,\tilde{\lambda}_n,\eta_n)$, for instance η_1 and η_2. We can then determine the $2\mathcal{N}$ parameters $\zeta_B^{\dot{\alpha}}$ in a generic $\bar{q}$ supersymmetry transformation $\bar{q}_\zeta := \zeta_B^{\dot{\alpha}}\bar{q}_{\dot{\alpha}}^B$, with $B=1,\ldots,\mathcal{N}$, in such a way that $e^{\bar{q}_\zeta}\eta_1^A = e^{\bar{q}_\zeta}\eta_2^A = 0$, that is $\bar{q}_\zeta\eta_{1,2}^A = -\eta_{1,2}^A$. The solution is

$$\zeta_{\dot{\alpha}}^A \;=\; \frac{1}{[12]}\Big(-\tilde{\lambda}_{1\dot{\alpha}}\eta_2^A + \tilde{\lambda}_{2\dot{\alpha}}\eta_1^A\Big), \tag{110}$$

and the action on the remaining $n-2$ Graßmann variables η_i is

$$e^{\bar{q}_\zeta}\eta_i \;:=\; \eta_i' \;=\; \eta_i - \eta_1\frac{[i\,2]}{[1\,2]} + \eta_2\frac{[i\,1]}{[1\,2]}. \tag{111}$$

As we have seen in section 8.1, supersymmetry invariance of a superamplitude implies that $\delta^{(4)}(p)\delta^{(2\mathcal{N})}(q)\,[\bar{q}_{\dot{\beta}}^B A_n] = 0$, hence $e^{\bar{q}_\zeta}A_n = A_n$ on the support of the delta functions. Acting with the $\bar{q}$ operator explicitly, we get

$$\mathcal{A}_n(\lambda_1,\tilde{\lambda}_1,0;\lambda_2,\tilde{\lambda}_2,0;\lambda_3,\tilde{\lambda}_3,\eta_3';\ldots) = \mathcal{A}_n(\lambda_1,\tilde{\lambda}_1,\eta_1;\lambda_2,\tilde{\lambda}_2,\eta_2;\lambda_3,\tilde{\lambda}_3,\eta_3;\ldots), \tag{112}$$

with η_i' defined as in (111) (for all $i=3,\ldots,n$). We can now use (112) to prove that our superamplitudes $\mathcal{A}_n(z)$ defined in (107) have the large-z behaviour advertised in (109). The key observation is that the supersymmetry transformation that sets $\eta_1(z)$ and η_2 to zero is z-independent: indeed, using (106) and (110) we see that

$$\zeta_{\dot{\alpha}}^A = \frac{-\hat{\tilde{\lambda}}_{1\dot{\alpha}}\eta_2^A + \tilde{\lambda}_{2\dot{\alpha}}\hat{\eta}_1^A}{[12]} \;=\; \frac{-\tilde{\lambda}_{1\dot{\alpha}}\eta_2^A + \tilde{\lambda}_{2\dot{\alpha}}\eta_1^A}{[12]}. \tag{113}$$

As a result $\mathcal{A}_n(z) = \mathcal{A}_n(\lambda_1,\hat{\tilde{\lambda}}_1,0;\hat{\lambda}_2,\tilde{\lambda}_2,0;\ldots;\lambda_i,\tilde{\lambda}_i,\eta_i';\ldots;\lambda_n,\tilde{\lambda}_n,\eta_n')$, where crucially none of the η_i' contain z: the only z-dependence occurs through $\hat{\tilde{\lambda}}_1$ and $\hat{\lambda}_2$. The large-z behaviour of $\mathcal{A}_n(z)$ is then identical to that of a gluon (or graviton) amplitude where particles 1 and 2 have positive helicity. Such amplitudes fall off as $1/z$ at large z for Yang–Mills theory [43], or $1/z^2$ in gravity [46], thus proving (109).

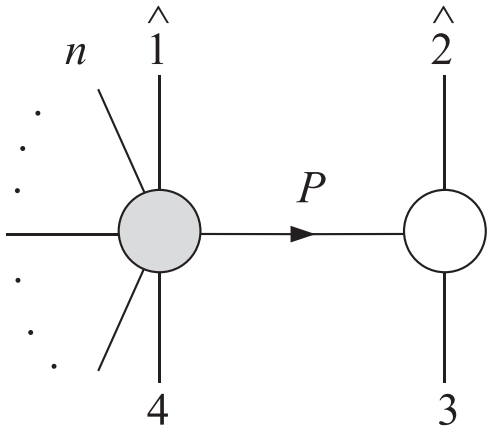

Figure 6. BCFW diagram for the n-point MHV recursion. In the derivation we use a $[12\rangle$ shift.

8.3.2. Application to MHV superamplitudes. We now use the supersymmetric recursion relation of [63, 64] to derive the MHV superamplitude (101). With the supershifts in (106), there is a single recursive diagram to consider, shown in figure 6. The right-hand side is always a three-point $\overline{\text{MHV}}$ superamplitude, whereas that on the left-hand side is an $(n-1)$-point MHV superamplitude. We will assume that the latter has the form given in (101), and then derive it for n points using the recursion. Starting from $n=4$ this gives of course a derivation of the superamplitude at any n. The building blocks in the supersymmetric recursion (108) are then

$$\mathcal{A}_{\rm L} = ig^{n-3}\,\delta^{(4)}\left(\sum_{i=4}^{n} p_i + \hat{p}_1 + \hat{P}\right)\frac{\delta^{(8)}\big(\sum_{i=4}^{n} q_i + \lambda_1\hat{\eta}_1 + \eta_{\hat{P}}\lambda_{\hat{P}}\big)}{\langle 1\hat{P}\rangle\langle\hat{P}4\rangle\ldots\langle n1\rangle}, \tag{114}$$

$$\mathcal{A}_{\rm R} = -ig\,\frac{\delta^{(4)}(\hat{p}_2 + p_3 - \hat{P})\,\delta^{(4)}(\eta_{-\hat{P}}[23] + \eta_2[3\,{-}\hat{P}] + \eta_3[{-}\hat{P}\,2])}{[{-}\hat{P}\,2][23][3\,{-}\hat{P}]}.$$

Using the identity

$$\delta^{(8)}\left(\hat{\eta}_1\lambda_1 + \sum_{i=4}^{n}\eta_i\lambda_i + \eta_{\hat{P}}\lambda_{\hat{P}}\right)\delta^{(4)}(\eta_{-\hat{P}}[23] + \eta_2[3\,{-}\hat{P}] + \eta_3[{-}\hat{P}\,2])$$
$$= \delta^{(8)}\left(\sum_{i\in L,R}\hat{\eta}_i\hat{\lambda}_i\right)\delta^{(4)}(\eta_{-\hat{P}}[23] + \eta_2[3\,{-}\hat{P}] + \eta_3[{-}\hat{P}\,2]), \tag{115}$$

and (super)momentum conservation $\sum_i \hat{\eta}_i\hat{\lambda}_i = \sum_i \eta_i\lambda_i$, $\sum_i \hat{p}_i = \sum_i p_i$, we arrive at the result $\mathcal{A}_n = \delta^{(4)}\big(\sum_{i\in L,R} p_i\big)\,\delta^{(8)}\big(\sum_{i\in L,R}\eta_i\lambda_i\big)\,A_n$, where

$$A_n = \frac{ig^{n-2}}{P_{23}^2}\,\frac{1}{\langle 45\rangle\ldots\langle n1\rangle[23]\,\langle 1\hat{P}\rangle\langle\hat{P}4\rangle[{-}\hat{P}2][3\,{-}\hat{P}]}$$
$$\times\int \mathrm{d}^4\eta_{\hat{P}}\,\delta^{(4)}(\eta_{-\hat{P}}[23] + \eta_2[3\hat{P}] + \eta_3[\hat{P}2]). \tag{116}$$

It is straightforward to see that $\langle 1\hat{P}\rangle\langle\hat{P}4\rangle[-\hat{P}2][3\ -\hat{P}] = -\langle 1|2|3]\langle 4|3|2] = -\langle 12\rangle\langle 34\rangle[23]^2$, finally obtaining

$$A_n \ = \ \frac{ig^{n-2}}{\langle 12\rangle\langle 23\rangle\ldots\langle n1\rangle}. \tag{117}$$

We also note that the supersymmetric recursion relation was solved in closed form in [93].

8.4. Vanishing Yang–Mills amplitudes

n-gluon amplitudes with $n > 3$ where all or all but one of the gluons have the same helicity are zero at tree level in any theory[17]. Intriguingly, one can derive this fact using supersymmetry: at tree level $\mathcal{N} = 4$ SYM has the same gluon amplitudes of pure Yang–Mills; because of the $\delta^{(8)}$ of supermomentum conservation, the first non-vanishing amplitudes must have at least two negative-helicity gluons (providing each four powers of η), except for the three-point case (104) which is quartic in η. Pleasingly, supersymmetry can be used to make powerful statements on non-supersymmetric amplitudes!

9. Superconformal, dual superconformal and Yangian symmetries

As mentioned in the introduction, scattering amplitudes in $\mathcal{N} = 4$ SYM are remarkably simple. Thanks to the finiteness of the theory [95] they are ultraviolet finite, and furthermore they are constrained by several symmetries. Some of these are symmetries of the Lagrangian—the standard superconformal symmetry group—but in addition there are symmetries which are visible only in the S-matrix of the theory: the dual superconformal and Yangian symmetries. In the next sections we present a snapshot of these symmetries, and describe some of their consequences on the S-matrix of $\mathcal{N} = 4$ SYM.

9.1. Superconformal symmetry

We introduced the supersymmetry generators q^A_α and $\bar{q}_{A\dot{\alpha}}$ of $\mathcal{N} = 4$ SYM in (99), where we saw that they leave the superamplitude invariant by virtue of the supermomentum conserving delta function $\delta^{(8)}(q)$ of (100). In the presence of conformal symmetry, the commutator of a special conformal and the supersymmetry generators introduces a set of new Graßmann-odd generators known as superconformal generators, s and $\bar{s}$:

$$\begin{aligned} [k_{\alpha\dot{\alpha}}, q^{\beta\,A}] &= \delta^\beta_\alpha\, \bar{s}^A_{\dot{\alpha}}, \qquad & \bar{s}^A_{\dot{\alpha}} &= \eta^A\, \tilde{\partial}_{\dot{\alpha}}, \\ [k_{\alpha\dot{\alpha}}, \bar{q}^{\dot{\beta}}_A] &= \delta^{\dot{\beta}}_{\dot{\alpha}}\, s_{\alpha\,A}, \qquad & s_{\alpha\,A} &= \partial_\alpha\, \partial_A. \end{aligned} \tag{118}$$

The complete $\mathcal{N} = 4$ superconformal symmetry algebra finally takes the form

$$\begin{aligned} &\{q^{\alpha\,A}, \bar{q}^{\dot{\alpha}}_B\} = \delta^A_B\, p^{\alpha\dot{\alpha}}, \qquad && \{s_{\alpha\,A}, \bar{s}^B_{\dot{\alpha}}\} = \delta^A_B\, k_{\alpha\dot{\alpha}} \\ &\{q^{\alpha\,A}, s_{\beta\,B}\} = m^\alpha{}_\beta\, \delta^A_B + \delta^\alpha_\beta\, r^A{}_B + \frac{1}{2}\,\delta^\alpha_\beta\,\delta^A_B\,(d+c) \\ &\{\bar{q}^{\dot{\alpha}}_A, \bar{s}^B_{\dot{\beta}}\} = \overline{m}^{\dot{\alpha}}{}_{\dot{\beta}}\, \delta^A_B - \delta^{\dot{\alpha}}_{\dot{\beta}}\, r^B{}_A + \frac{1}{2}\,\delta^{\dot{\alpha}}_{\dot{\beta}}\,\delta^B_A\,(d-c) \\ &[p^{\alpha\dot{\alpha}}, s_{\beta\,A}] = \delta^\alpha_\beta\, \bar{q}^{\dot{\alpha}}_A, \qquad && [p^{\alpha\dot{\alpha}}, \bar{s}^A_{\dot{\beta}}] = \delta^{\dot{\alpha}}_{\dot{\beta}}\, q^{\alpha A}, \end{aligned} \tag{119}$$

[17] And to all loops in the presence of supersymmetry, see e.g. [94] for a proof.

with the central charge $c = 1 + \frac{1}{2}(\lambda^\alpha \partial_\alpha - \tilde{\lambda}^{\dot\alpha}\partial_{\dot\alpha} - \eta^A \partial_A) = 1 - h$ as well as an additional global $\mathfrak{su}(4)$ R-symmetry generator $r^A{}_B$

$$r^A{}_B = \eta^A\,\partial_B - \frac{1}{4}\delta^A_B\,\eta^C\,\partial_C, \qquad \partial_A := \frac{\partial}{\partial \eta^A}, \tag{120}$$

which acts as an internal rotation in η^A-space. This superalgebra is known as $\mathfrak{psu}(2,2|4)$.

9.2. Dual superconformal symmetry

Remarkably, the $\mathcal{N} = 4$ SYM theory enjoys an additional hidden invariance known as dual superconformal symmetry. To make this symmetry manifest, one has to parameterise the momenta and supermomenta of the scattered particles in terms of dual momenta x_i and supermomenta θ_i. These are defined as

$$p_{i\alpha\dot\alpha} = \lambda_{i\alpha}\tilde{\lambda}_{i\dot\alpha} = (x_i - x_{i+1})_{\alpha\dot\alpha}, \qquad \eta_i^A \lambda_{i\alpha} = \theta^A_{i\alpha} - \theta^A_{i+1\alpha}, \tag{121}$$

and we require that $x_{n+1} = x_1$ and $\theta_{n+1} = \theta_1$. Note that one can make consistent assignments for the region momenta only for planar diagrams. An advantage of this parameterisation is that momentum conservation is automatic: the only constraint on the x_is is the on-shell conditions $(x_i - x_{i+1})^2 = 0$, while the fermionic variables θ_i must also satisfy the on-shell condition $(\theta_i - \theta_{i+1})\lambda_i = 0$. Momentum and supermomentum conservation are then implemented with the delta functions $\delta^{(4)}(x_1 - x_{n+1})\delta^{(8)}(\theta_1 - \theta_{n+1})$.

Without spoiling momentum and supermomentum conservation, we can then act with inversions on the dual momenta and supermomenta [90]:

$$x_{\alpha\dot\beta} \to\ I[x_{\alpha\dot\beta}] = \frac{x_{\beta\dot\alpha}}{x^2} := x^{-1}_{\beta\dot\alpha}, \qquad \theta^{A\alpha} \to\ I[\theta^{A\alpha}] = (x^{-1})^{\dot\alpha\beta}\theta^A_\beta. \tag{122}$$

This transformation makes sense since dual momenta, unlike the momenta, are unconstrained. It is also important that dual conformal inversions do not change the lightlike nature of a momentum—this is indeed one of the claims to fame of the conformal group: $(\frac{x^\mu}{x^2} - \frac{y^\mu}{y^2})^2 = 0$ if $(x - y)^2 = 0$. Note that (122) implies that

$$I[(x_{ij})_{\alpha\dot\beta}] = -(x_j^{-1}x_{ij}x_i^{-1})_{\beta\dot\alpha}, \tag{123}$$

with $x_{ij} := x_i - x_j$, and in particular $I[x_{ii+1}] = -x^{-1}_{i+1}x_{ii+1}x_i^{-1}$. In order to determine what is $I[\lambda^\alpha]$, we note that we want to preserve the constraint $\lambda^\beta(x_{ii+1})_{\beta\dot\alpha} = 0$. It then follows that $(x^{-1}_{i+1}x_{ii+1}x_i^{-1})_{\alpha\dot\beta}\, I[\lambda^\beta] = 0$, which can be solved by choosing

$$\lambda_i^\beta \to I[\lambda_i^\beta] = (x_i^{-1})^{\dot\beta\alpha}\lambda_{i\alpha}. \tag{124}$$

This also implies that

$$\langle i\, i+1\rangle \to \frac{\langle i\, i+1\rangle}{x_i^2}, \tag{125}$$

as it can be seen after using $x_{ii+1}|i\rangle = 0$. The transformation of $\tilde{\lambda}_i$ under an inversion can be found by noticing that from $\lambda_i\tilde{\lambda}_i = x_{ii+1}$ it follows that $\tilde{\lambda}_i^{\dot\alpha} = x^{\dot\alpha\beta}_{ii+1}\lambda_{i+1\beta}/\langle ii+1\rangle$. Using then (123)–(125) one quickly arrives at

$$\tilde{\lambda}_i^{\dot\alpha} \to I[\tilde{\lambda}_i^{\dot\alpha}] = \tilde{\lambda}_{i\dot\beta}(x^{-1}_{i+1})^{\dot\beta\alpha}. \tag{126}$$

Special conformal transformations are then obtained by performing an inversion followed by a translation and another inversion. Combined with supersymmetry, this covers all superconformal transformations.

The dual supersymmetries are either manifest or related to ordinary special superconformal symmetry [90], which is an invariance of the $\mathcal{N} = 4$ theory. Hence the invariance of the S-matrix under the full dual superconformal symmetry only requires that we prove invariance under dual inversions. This was achieved in [63], by constructing the supersymmetric BCFW recursion relation reviewed in section 8.3. In a nutshell, the proof relies on the fact that the building blocks of each recursive diagram respect dual superconformal symmetry, hence guaranteeing the covariance of the final answer.

Finally, we mention that the first strong hint of dual conformal symmetry was observed at loop level rather than at tree level [96], as we now outline. It is well known that all one-loop amplitudes in the maximally supersymmetric theory can be written in terms of box integrals [97], such as the one shown in figure 7. A box integral can be defined as

$$I(x_1, \ldots, x_4) \;=\; \int \frac{\mathrm{d}^4 x_5}{(2\pi)^4} \frac{1}{x_{51}^2 x_{52}^2 x_{53}^2 x_{54}^2}, \tag{127}$$

where we have introduced dual momenta as $p_1 := x_1 - x_2, \ldots, p_4 := x_4 - x_1$, and the momenta of the internal legs are $x_{51}, \ldots, x_{54}$. The advantage of this expression is that the loop measure is simply $\mathrm{d}^4 x_5$, and there is no need to pick a particular internal leg as the integration variable. Note that we have written the integration measure in four dimensions; this is allowed only when the integral does not require (infrared) regularisation, which is the case when all the p_i are massive[18], otherwise we can simply replace $\mathrm{d}^4 x_5 \to \mathrm{d}^D x_5$ with $D = 4 - 2\epsilon$, and choose $\epsilon < 0$. Leaving momentarily this fact aside, let us study the transformation properties of (127) under dual conformal symmetry. Under the inversion (122), we simply have

$$x_{ij}^2 \to \frac{x_{ij}^2}{x_i^2 x_j^2}, \tag{128}$$

so that introducing $x_5' = (x_5)^{-1}$, and using $x_{5'i'}^2 = \frac{x_{5i}^2}{x_5^2 x_i^2}$ as well as $d^4 x_5' = \frac{d^4 x_5}{(x_5^2)^4}$, we find that

$$I(x_1', \ldots, x_4') = (x_1^2 \ldots x_4^2) I(x_1, \ldots, x_4). \tag{129}$$

Hence the box integrals are covariant under inversions, and since integrals are invariant under translations of the dual momenta, it follows that all box integrals, if evaluated strictly in four dimensions, are dual conformal covariant [96].

Usually one encounters box integrals where at least one of the external momenta is massless, in which case they are infrared divergent and have an anomaly (computed in [102]); these integrals are usually called 'pseudo-conformal'. Dual conformal symmetry is then anomalous at loop level [90, 103], and the anomaly of the amplitudes turns out to be closely related to that of the polygonal lightlike Wilson loop [104, 105] dual to the amplitude [106–108]. Using this anomaly one can find useful constraints on supercoefficients in the expansion of superamplitudes in an integral basis [102, 109]. We also mention that pseudo-conformality of the integrals has been used to write the four-point MHV amplitude up to five [110], six and seven loops [111], following the remarkable direct calculations at three [112] and four loops [113, 114]. We will come back to loop amplitudes in section 10.

[18] The corresponding so-called 'four-mass' box has been evaluated in [98], see also [99–101] for more recent calculations of the same quantity.

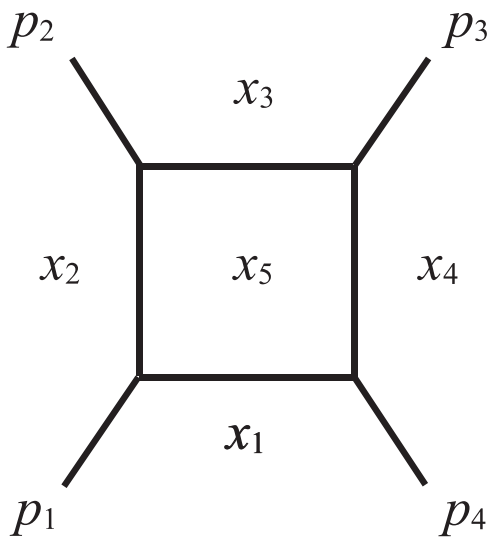

Figure 7. A one-loop box function. Here $p_1 \coloneqq x_1 - x_2, \ldots, p_4 \coloneqq x_4 - x_1$.

9.3. Dual superconformal covariance of the MHV and NMHV superamplitudes

We begin by showing that the tree-level MHV superamplitude (101) is covariant under dual conformal symmetry [91]. As explained earlier, it is sufficient to consider dual inversions. Using (125), we see that $\prod_{i=1}^{n}\langle ii+1\rangle \to \prod_{i=1}^{n} x_i^2\langle ii+1\rangle$. One then observes that the combination of delta functions $\delta^{(4)}(x_i - x_{n+1})\delta^{(8)}(\theta_1 - \theta_{n+1})$ is invariant under inversions. Hence the MHV superamplitude transforms covariantly under inversions:

$$\mathcal{A}_n^{\text{MHV}}(1,2,\ldots,n) \to \mathcal{A}_n^{\text{MHV}}(1,2,\ldots,n)\prod_{k=1}^{n} x_k^2. \tag{130}$$

Next we discuss the NMHV superamplitudes, whose explicit expression is shown in (102). To prove that they transform covariantly, we need to show that the R-functions in (103) are dual superconformal invariant. It is convenient to define the four-bracket

$$\langle i, j-1, j, k\rangle \coloneqq \langle i|x_{ij}x_{jk}|k-1\rangle\langle j-1j\rangle, \tag{131}$$

whose usefulness arises from the fact that it is a dual conformal invariant. An elegant way to see this is to introduce momentum twistors [115, 116]

$$Z_i^{\hat{A}} = \begin{pmatrix}\lambda_i^{\alpha}\\ \mu_i^{\dot{\alpha}}\end{pmatrix}, \qquad \mu_i^{\dot{\alpha}} = x_i^{\dot{\alpha}\alpha}\lambda_{i\alpha}, \tag{132}$$

on which conformal transformations act linearly—they are realised as $SL(4)$ transformations on the index $\hat{A}$. The four-bracket (131) can then be recast as

$$\langle i, j-1, j, k\rangle = \epsilon_{\hat{A}\hat{B}\hat{C}\hat{D}} Z_i^{\hat{A}} Z_{j-1}^{\hat{B}} Z_j^{\hat{C}} Z_k^{\hat{D}}, \tag{133}$$

which is manifestly invariant under $SL(4)$ transformations. To address dual superconformal transformations, it is then convenient to introduce supertwistor variables

$$\mathcal{Z}_i^M = \begin{pmatrix} Z_i^{\hat{A}} \\ \chi_i^A \end{pmatrix}, \qquad \chi_i^A = \theta_i^{A\,\alpha}\lambda_{i\alpha}. \tag{134}$$

These transform in the fundamental representation of the supergroup $SL(4|4)$, whose projective real section $PSU(2,2|4)$ is precisely the (dual) superconformal group of $\mathcal{N}=4$ SYM. Given five arbitrary superstwistors $\mathcal{Z}_a,\ldots,\mathcal{Z}_e$, it is straightforward to show that

$$[a,b,c,d,e] = \frac{\delta^{(4)}(\langle a,b,c,\mathrm{d}\rangle\chi_e + \text{cyclic})}{\langle a,b,c,\mathrm{d}\rangle\langle b,c,d,e\rangle\langle c,d,e,a\rangle\langle d,e,a,b\rangle\langle e,a,b,c\rangle} \tag{135}$$

is an $SL(4|4)$ invariant[19]. This is useful since one can prove that $R_{rst} = [s-1,s,t-1,t,r]$ [116], from which dual superconformal invariance of the R-functions follows.

9.4. Yangian symmetry

The generators of the dual superconformal symmetry algebra $\{P,K,S,\bar{S},Q,\bar{Q}\}$ are most naturally written in an extended superspace given by the set of variables $\{\lambda^\alpha,\tilde{\lambda}^{\dot\alpha},\eta^A,x^{\alpha\dot\alpha},\theta^{\alpha A}\}$ that are subject to the constraints of (121). Explicitly, the dual superconformal generators K and S take the form

$$\begin{aligned} K^{\alpha\dot\alpha} &= \sum_{i=1}^n \left[x_i^{\alpha\dot\beta} x_i^{\dot\alpha\beta}\frac{\partial}{\partial x_i^{\beta\dot\beta}} + x_i^{\dot\alpha\beta}\theta_i^{\alpha B}\frac{\partial}{\partial\theta_i^{\beta B}} + x_i^{\dot\alpha\beta}\lambda_i^\alpha\frac{\partial}{\partial\lambda_i^\beta} + x_{i+1}^{\alpha\dot\beta}\tilde{\lambda}_i^{\dot\alpha}\frac{\partial}{\partial\tilde{\lambda}_i^{\dot\beta}} + \tilde{\lambda}_i^{\dot\alpha}\theta_{i+1}^{\alpha B}\frac{\partial}{\partial\eta_i^B}\right], \\ S_\alpha^A &= \sum_{i=1}^n \left[-\theta_{i\alpha}^B\theta_i^{\beta A}\frac{\partial}{\partial\theta_i^{\beta B}} + x_{i\alpha}{}^{\dot\beta}\theta_i^{\beta A}\frac{\partial}{\partial x_i^{\beta\dot\beta}} + \lambda_{i\alpha}\theta_i^{\gamma A}\frac{\partial}{\partial\lambda_i^\gamma} + x_{i+1\,\alpha}{}^{\dot\beta}\eta_i^A\frac{\partial}{\partial\tilde{\lambda}_i^{\dot\beta}} - \theta_{i+1\,\alpha}^B\eta_i^A\frac{\partial}{\partial\eta_i^B}\right], \end{aligned} \tag{136}$$

and can be shown to commute with the constraints (121). An interesting question is what algebraic structure emerges if one commutes the superconformal and dual superconformal generators with one another, i.e. studies the closure of the two algebras. It turns out that this induces an infinite-dimensional symmetry algebra known as the Yangian $Y[\mathfrak{psu}(2,2|4)]$ [117]. A Yangian algebra $Y(\mathfrak{g})$ built upon a simple Lie algebra $\mathfrak{g}$ is a deformation of the loop algebra realised by generators $J_a^{(n)}$ with levels $n\in\mathbb{N}$ [118, 119]. The level-zero and level-one generators obey the commutation relations

$$[J_a^{(0)},J_b^{(0)}\} = f_{ab}^c J_c^{(0)}, \qquad [J_a^{(0)},J_b^{(1)}\} = f_{ab}^c J_c^{(1)}, \tag{137}$$

where $[.,.\}$ denotes a graded commutator. The higher-level generators follow from commutators of the level-one generators. In addition, there are Serre relations [118, 119] which generalise the usual Jacobi identities. The co-products of the level-zero and level-one Yangian generators express the action on two-particle states, and read

$$\begin{aligned} \Delta(J_a^{(0)}) &= J_a^{(0)}\otimes\mathbb{1} + \mathbb{1}\otimes J_a^{(0)}, \\ \Delta(J_a^{(1)}) &= J_a^{(1)}\otimes\mathbb{1} + \mathbb{1}\otimes J_a^{(1)} + f_a{}^{bc}J_b^{(0)}\otimes J_c^{(0)}. \end{aligned} \tag{138}$$

[19] Note that (135) is invariant under $\mathcal{Z}_i^M\to\zeta_i\mathcal{Z}_i^M$, in other words these are projective coordinates in super twistor space. This transformation is related to little group scaling of the spinor-helicity variables.

In the last term above, the adjoint indices of the structure constant are raised and lowered with the group metric $\mathrm{Tr}(J^{(0)}_{R\,a}\,J^{(0)}_{R\,b})$ with $J^{(0)}_{R,a}$ in the defining representation of $\mathfrak{g}$. The level-one generators are then given by

$$J^{(1)}_a = \sum_{i=1}^{n} J^{(1)}_{ia} + f_a{}^{cb} \sum_{i\leqslant 1<j\leqslant n} J^{(0)}_{ib}\, J^{(0)}_{jc}. \tag{139}$$

In the problem at hand, the level-zero generators $J^{(0)}_a$ coincide with the generators of the superconformal algebra $\mathfrak{psu}(2,2|4)$ of (119). Interestingly, the dual superconformal generators K and S of (136) can be identified with the level-one Yangian generators of $Y[\mathfrak{psu}(2,2|4)]$. In order to see this one solves the constraints (121) via

$$x_i^{\alpha\dot\alpha} = x_1^{\alpha\dot\alpha} - \sum_{j<i} \lambda_j^{\alpha}\tilde\lambda_j^{\dot\alpha}, \qquad \theta_i^{\alpha A} = \theta_1^{\alpha A} - \sum_{j<i}\lambda_j^{\alpha}\eta_j^{A} \qquad \text{for } 2\leqslant i\leqslant n+1, \tag{140}$$

eliminating $x_i^{\alpha\dot\alpha}$ and $\theta_i^{\alpha A}$, and expresses the dual superconformal generators in the original superspace variables $\{\lambda_i^{\alpha}, \tilde\lambda_i^{\dot\alpha}, \eta_i^{A}\}$ to discover that some of the generators become trivial, namely P and Q, while others overlap with the original superconformal ones, namely $\bar S$ and $\bar Q$. The non-trivial generators turn out to be K and S. One can show that S is explicitly given, up to a term ΔS that trivially annihilates the amplitudes, by

$$S^A_\alpha + \Delta S^A_\alpha = -\frac{1}{2}\sum_{i<j}\left[m^{\gamma}_{i\alpha} q^A_{j\gamma} - \frac{1}{2}(d_i + c_i) q^A_{j\alpha} + p^{\dot\beta}_{i\alpha}\bar s^A_{j\beta} + q^B_{i\alpha} r^A_{jB} - (i\leftrightarrow j)\right], \tag{141}$$

and indeed takes the form (139), with the 'densities' $J^{(0)}_{ia}$ appearing quadratically along with a trivial evaluation representation $J^{(1)}_{ia} = 0$. A similar structure emerges for K [117].

The Yangian is a hidden symmetry of tree-level superamplitudes, that is for any generator $J \in Y(\mathfrak{psu}(2,2|4))$ one finds $J\,\mathcal{A} = 0$ up to contact terms related to collinear kinematic configurations [120]. In fact the Yangian symmetry also constrains the structure of planar loop integrands, however infrared divergences break the symmetry at the integrated level [121–123]. Being an infinite-dimensional symmetry algebra, the Yangian points to a hidden integrability of planar $\mathcal{N} = 4$ SYM, see [124] for a review.

Finally, the Yangian generators have a particularly simple form when re-expressed in the supertwistor variables of (134):

$$\begin{aligned} J^{(0)M}{}_N &= \sum_i \mathcal{Z}_i^M \frac{\partial}{\partial \mathcal{Z}_i^N}, \\ J^{(1)M}{}_N &= \sum_{i>j}\left[\mathcal{Z}_i^M \mathcal{Z}_j^O \frac{\partial}{\partial \mathcal{Z}_i^O}\frac{\partial}{\partial \mathcal{Z}_j^N} - (i\leftrightarrow j)\right]. \end{aligned} \tag{142}$$

Written in these variables the Yangian symmetry of the scattering amplitudes can be made most manifest.

10. Loops from unitarity cuts

10.1. Basic ideas

The fundamental tenet of the modern amplitudes programme [97, 125–127] is to use gauge-invariant quantities such as amplitudes or form factors as input in computations, avoiding the

use of Feynman diagrams. In previous sections we have shown how this can be achieved at tree level, and the next question is how to extend this approach to loop amplitudes. As we will now review, we can efficiently recycle tree-level amplitudes to obtain loops from trees[20].

If we are tasked to stay away from Feynman rules we have to go back to more fundamental principles of QFT—the relevant ones for us are locality and unitarity. These tell us that at tree level the only allowed singularities are simple poles arising from propagator factors $\frac{i}{p^2-m^2+i\varepsilon}$, and the residue at such poles is the product of smaller scattering amplitudes. These facts underpin tree-level factorisation theorems discussed in section 5.1, which in turn lead to the BCFW recursion relations.

Unitarity is the statement of conservation of probability, it means that if we scatter something the probability that something happens is one:

$$S^\dagger S = 1. \tag{143}$$

Now writing the S-matrix as a trivial (forward) piece plus a part that describes the non-trivial scattering as $S = 1 + \mathrm{i}T$ we find

$$T^\dagger T = -i(T - T^\dagger). \tag{144}$$

The formal matrix product on the left-hand side implies a summation over all possible intermediate (helicity) states and an on-shell phase-space integration $\int \mathrm{d}^4 p_i\, \delta(p_i^2 - m_i^2)$ for each intermediate particle. Taking matrix element of (144) between external states, one obtains a product of amplitudes that equals the imaginary part (or discontinuity) of the full amplitude, from which one can in principle obtain the amplitude from a dispersion integral of the form $\int \mathrm{d}s' \frac{\mathrm{Im}A(s')}{s-s'}$ where s is some Mandelstam variable. This is conceptually deep and beautiful, but unfortunately not of much practical use in particular if we consider a process with more than four particles[21].

10.2. General structure of one-loop amplitudes

From now on we will focus on planar one-loop amplitudes in gauge theories. At one-loop, using (30), these can be written in terms of a single primitive amplitude $A^{(1)}_{n;1}$ (and for brevity we will henceforth call it $A^{(1)}_n$). It is well known [97] that also the non-planar contributions can be expressed as linear combinations of the $A^{(1)}_n$, giving a further reason to focus on the computation of the planar parts.

Of utmost importance is the fact that one-loop amplitudes can be decomposed in terms of scalar Feynman integrals which contain transcendental functions such as logarithms and dilogarithms, i.e. functions that contain discontinuities, and rational parts. In general the answer will contain ultraviolet (UV) and infrared (IR) divergences which we regulate using dimensional regularisation. From now on we consider massless gauge theories, which implies that tadpoles are absent. In this case one can write the following ansatz for a general one-loop amplitude:

$$A^{(1)}_n = \sum_i a_i I_{4,i} + \sum_j b_j I_{3,j} + \sum_k c_k I_{2,k} + R_n, \tag{145}$$

[20] A different incarnation of this can be recognised in the Feynman tree theorem [128, 129], see [70] for a discussion and comparison of this theorem to the unitarity approach.

[21] We also mention important applications of unitarity to the study of black hole scattering in general relativity [130–144], and in theories of modified gravity with higher-derivative interactions [145–149]. See chapters 13 and 14 of this review [150, 151] for more details.

where we have introduced the scalar Feynman integrals

$$I_{n,i} = \int \frac{\mathrm{d}^D \ell}{(2\pi)^D} \frac{1}{\ell^2 (\ell - K_{i,1})^2 \dots (\ell - K_{i,n-1})^2}, \tag{146}$$

where the $K_{i,j}$ correspond to appropriate sums of subsets of external momenta p_i. In the presence of colour ordering, only adjacent momentum labels appear in the set. The $I_{4,i}$ and $I_{3,i}$ are called boxes and triangles, which are UV finite but contain IR divergences, and the $I_{2,i}$ are UV-divergent bubble integrals. We can motivate the ansatz (145) as follows. Had we started from a gedanken Feynman integral computation of a one-loop n-gluon amplitude, we would have found many more and much more complicated integrals, the most complicated one being an n-gon

$$\int \frac{\mathrm{d}^D \ell}{(2\pi)^D} \frac{P_n(\ell)}{\ell^2 (\ell - p_1)^2 (\ell - p_1 - p_2)^2 \dots (\ell + p_n)^2}, \tag{147}$$

where $P_n(\ell)$ is a polynomial of degree n in the loop momenta, coming from the n momentum-dependent three-gluon vertices. Such an integral is usually called a tensor integral. Thanks to a theorem by Passarino and Veltman (PV) [152], all such higher-point and tensor integrals can be PV-reduced to only scalar bubbles, triangles and boxes. Since all these integrals have been evaluated and are tabulated, the remaining non-trivial task is to find the coefficients a_i, b_j and c_k.

Before moving to concrete examples, we now discuss how one can put unitarity to work to determine these coefficients algebraically without ever performing any integrals, following the groundbreaking work of [97, 125].

10.3. Unitarity at one loop: two-particle cuts

The main idea is to compute the discontinuities (or imaginary parts) of the left-hand side and the right-hand side of (145):

$$\begin{aligned} \mathrm{Disc}(s_{i\dots j}) A_n^{(1)} = &\sum_i a_i \mathrm{Disc}(s_{i\dots j}) I_{4,i} + \sum_j b_j \mathrm{Disc}(s_{i\dots j}) I_{3,j} \\ &+ \sum_k c_k \mathrm{Disc}(s_{i\dots j}) I_{2,k}, \end{aligned} \tag{148}$$

in all (two- or multi-particle) kinematic channels, with $s_{i\dots j} = (p_i + p_{i+1} + \dots + p_j)^2$. The left-hand side of (144) is then evaluated as a product of two tree amplitudes convoluted with a two-particle phase-space integral corresponding to two internal on-shell states, and we have to sum over all internal helicities. This procedure is usually called a *two-particle cut* because two off-shell propagators are put on shell:

$$\frac{i}{\ell_{1,2}^2 + i\varepsilon} \to 2\pi \delta(\ell_{1,2}^2), \tag{149}$$

and the discontinuity of the one-loop amplitude in the channel $s_{i\dots j}$ is then given by

$$\begin{aligned} \mathrm{Disc}(s_{i\dots j}) A_n^{(1)} = \sum_{h_1,h_2} \int \frac{\mathrm{d}^D \ell_1}{(2\pi)^{D-2}} \delta(\ell_1^2) \delta(\ell_2^2)\, A^{\mathrm{tree}}(-\ell_2^{-h_2}, i \dots j, \ell_1^{h_1}) \\ \times A^{\mathrm{tree}}(-\ell_1^{-h_1}, j+1, \dots, i-1, \ell_2^{h_2}), \end{aligned} \tag{150}$$

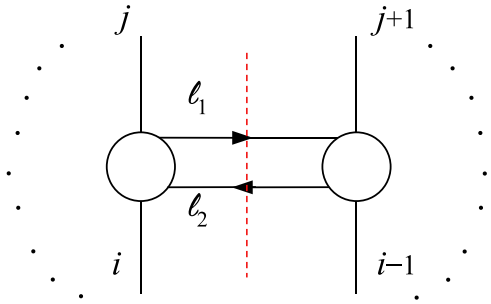

Figure 8. A cut diagram evaluating the discontinuity in the $s_{i\ldots j}$-channel.

with $\ell_2 = \ell_1 + p_i + p_{i+1} + \cdots + p_j$ (see figure 8). One could perform this phase-space integral to obtain the discontinuity of the amplitude in this channel, however a more useful approach, advocated in [125], is to observe that if we uplift this integral to a full Feynman integral by undoing (149), we obtain a Feynman integral

$$\sum_{h_1,h_2} \int \frac{\mathrm{d}^D \ell_1}{(2\pi)^D} \frac{i}{\ell_1^2} \frac{i}{(\ell_2^2)} A^{\text{tree}}(-\ell_2^{-h_2}, i \ldots j, \ell_1^{h_1}) \times A^{\text{tree}}(-\ell_1^{-h_1}, j+1, \ldots, i-1, \ell_2^{h_2}), \tag{151}$$

that has the correct discontinuity of the amplitude in this particular channel. Hence the *integrand* thus produced must be part of the complete answer, and by going through all kinematic channels we have enough constraints to fix the integrand for the amplitude. The key advantage is that we can simplify the cut integrand (150) as much as possible using on-shell conditions and powerful spinor-helicity techniques before lifting it back to a full Feynman loop integrand (151). Once we have combined the information from all cuts, we can PV-reduce the resulting integrand (which is an algebraic process) and read off the coefficients a_i, b_j and c_k.

A comment on the rational terms R_n in (145) is in order. In [97, 125] it was shown that such terms vanish at one loop in supersymmetric theories, and in computing unitarity cuts it is enough to use tree amplitudes valid strictly in four dimensions. This allows us to use powerful spinor-helicity techniques. However, if we work in pure Yang–Mills or QCD we obtain only part of the answer—the four-dimensional cut-constructible pieces, missing further rational terms. In order to get these we must perform unitarity cuts in $D = 4 - 2\epsilon$ dimensions [153, 154], which requires amplitudes where at least the cut legs are in D dimensions. External momenta can be kept in four dimensions if, as we do, we use the four-dimensional helicity scheme [155, 156]. We will return to this in section 10.7.

10.4. Example: four-gluon amplitude in N=4 SYM from two-particle cuts

We will now illustrate the previous discussion by computing the one-loop four-gluon amplitude $A^{(1)}(1^-2^-3^+4^+)$ from two-particle cuts. There are two channels to consider, namely the s-channel and the t-channel, corresponding to the Mandelstam invariants $s = (p_1 + p_2)^2$ and $t = (p_2 + p_3)^2$. In the s-channel, the internal states can only be gluons, and the amplitudes entering the cut are (see figure 9)[22]:

[22] In this section we drop powers of g, which can easily be reinstated at the end.

$$
\begin{aligned}
A((-\ell_2)^+, 1^-, 2^-, \ell_1^+) &= i\frac{\langle 12\rangle^4}{\langle -\ell_2 1\rangle\langle 12\rangle\langle 2\ell_1\rangle\langle \ell_1 - \ell_2\rangle},\\
A(-\ell_1^-, 3^+, 4^+, \ell_2^-) &= i\frac{\langle \ell_2 - \ell_1\rangle^4}{\langle -\ell_1 3\rangle\langle 34\rangle\langle 4\ell_2\rangle\langle \ell_2 - \ell_1\rangle}.
\end{aligned}
\tag{152}
$$

Multiplying the product of these two amplitudes with $\frac{i}{\ell_1^2}\frac{i}{\ell_2^2}$ we find the cut integrand

$$
\begin{aligned}
&\mathrm{Disc}(s)A^{(1)}(1^-2^-3^+4^+)\\
&\quad = A_4^{\text{tree}} \times \int \frac{\mathrm{d}^D\ell_1}{(2\pi)^D}\frac{i}{\ell_1^2\ell_2^2}\frac{\langle 23\rangle\langle 41\rangle\langle \ell_1\ell_2\rangle^2}{\langle \ell_2 1\rangle\langle 2\ell_1\rangle\langle \ell_1 3\rangle\langle 4\ell_2\rangle}\Big|_{s-\text{cut}},
\end{aligned}
\tag{153}
$$

where we have pulled out the tree amplitude $i\frac{\langle 12\rangle^4}{\langle 12\rangle\langle 23\rangle\langle 34\rangle\langle 41\rangle}$ and used our convention $\lambda_{-p} = \mathrm{i}\lambda_p$. By rationalising two of the denominator factors using $\langle 2\ell_1\rangle[\ell_1 2] = (\ell_1 + p_2)^2$ and $\langle \ell_1 3\rangle[3\ell_1] = -(\ell_1 - p_3)^2$ we can further massage the integrand to find

$$
\begin{aligned}
&A_4^{\text{tree}} \times \frac{i}{\ell_1^2\ell_2^2(\ell_1+p_2)^2(\ell_1-p_3)^2}\frac{\langle 23\rangle\langle 41\rangle\langle \ell_2 \overbrace{\ell_1\rangle[\ell_1}^{=\ell_2-p_1-p_2} 2][3 \overbrace{\ell_1]\langle \ell_1}^{=\ell_2+p_3+p_4} \ell_2\rangle}{\langle \ell_2 1\rangle\langle 4\ell_2\rangle}\\
&\quad = A_4^{\text{tree}} \times \frac{i}{\ell_1^2\ell_2^2(\ell_1+p_2)^2(\ell_1-p_3)^2}(-\langle 23\rangle\langle 41\rangle[12][34])\\
&\quad = istA_4^{\text{tree}} \times \frac{1}{\ell_1^2\ell_2^2(\ell_1+p_2)^2(\ell_1-p_3)^2},
\end{aligned}
\tag{154}
$$

from which we see that $istA_4^{\text{tree}}$ is the coefficient of the zero-mass box function [157]

$$
\begin{aligned}
I_4^{0\text{m}}(s,t) &= \int \frac{\mathrm{d}^D\ell}{(2\pi)^D}\frac{1}{\ell^2(\ell+p_1+p_2)^2(\ell+p_2)^2(\ell-p_3)^2}\\
&= -i\frac{2c_\Gamma}{st}\left\{-\frac{1}{\epsilon^2}\left[(-s)^{-\epsilon}+(-t)^{-\epsilon}\right]+\frac{1}{2}\log^2\left(\frac{s}{t}\right)+\frac{\pi^2}{2}\right\},
\end{aligned}
\tag{155}
$$

with

$$
c_\Gamma = \frac{\Gamma(1+\epsilon)\Gamma(1-\epsilon)^2}{(4\pi)^{2-\epsilon}\Gamma(1-2\epsilon)}.
\tag{156}
$$

Since we have only considered the s-channel cut, we know that $istA_4^{\text{tree}}I_{0\text{m}}(s,t)$ must be part of the full answer but we can only trust terms that have discontinuities in s. To complete the computation we need to consider also the t-channel, also shown in figure 9. Initially, this looks more complicated because on both sides of the cuts the external legs are one positive and one negative helicity gluon and this allows all possible states of $\mathcal{N} = 4$ SYM to appear as internal states: $h = -1, -1/2, 0, 1/2, 1$, with multiplicities $1, 4, 6, 4, 1$.

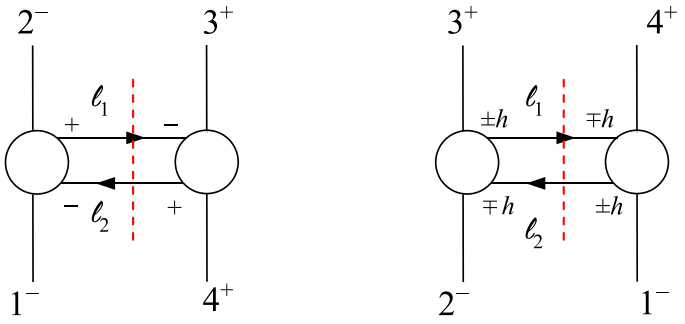

Figure 9. The *s*- and *t*-channel cut diagrams contributing to the one-loop MHV amplitude in $\mathcal{N}=4$ SYM.

The corresponding tree amplitudes entering the cut are

$$\begin{aligned} A((-\ell_2)^{-h},2^-,3^+,\ell_1^h) &= i\frac{\langle -\ell_2 2\rangle^{2+2h}\langle \ell_1 2\rangle^{2-2h}}{\langle -\ell_2 2\rangle\langle 23\rangle\langle 3\ell_1\rangle\langle \ell_1\ -\ell_2\rangle}, \\ A(-\ell_1^{-h},4^+,1^-,\ell_2^h) &= i\frac{\langle -\ell_1 1\rangle^{2+2h}\langle \ell_2 1\rangle^{2-2h}}{\langle -\ell_1 4\rangle\langle 41\rangle\langle 1\ell_2\rangle\langle \ell_2\ -\ell_1\rangle}, \end{aligned} \tag{157}$$

and the *t*-channel cut is given by the product of these amplitudes and summing over h. Focusing on the product of numerators, the sum with the correct multiplicities gives

$$\begin{aligned} &\sum_h \binom{4}{2+2h} \langle -\ell_2 2\rangle^{2+2h}\langle \ell_1 2\rangle^{2-2h}\langle -\ell_1 1\rangle^{2+2h}\langle \ell_2 1\rangle^{2-2h} \\ &\qquad = \big(\langle \ell_1 2\rangle\langle \ell_2 1\rangle - \langle \ell_1 1\rangle\langle \ell_2 2\rangle\big)^4 = \langle 12\rangle^4\langle \ell_1\ell_2\rangle^4. \end{aligned} \tag{158}$$

The numerator is then the same as in the *s*-channel and denominator factors are obtained from a cyclic relabelling of the external legs. Thus from the *t*-channel cut we get

$$ist A_4^{\text{tree}} \times \frac{1}{\ell_1^2\ell_2^2(\ell_1+p_3)^2(\ell_1-p_4)^2}, \tag{159}$$

which is proportional to the integrand of the box function $I_4^{0\text{m}}(s,t)$ up to a trivial shift of the loop momentum. Summarising, the unique answer consistent with both cuts is

$$A_4^{(1)}(1^-,2^-,3^+,4^+) = ist\, A_4^{\text{tree}}(1^-,2^-,3^+,4^+)\, I_4^{0\text{m}}(s,t). \tag{160}$$

One remarkable outcome of this computation is that it does not lead to any bubble or triangle integrals, and is consistent with the general fact that one-loop amplitudes in $\mathcal{N}=4$ SYM only contain boxes [97, 125]. This can be linked to the improved power-counting behaviour of this theory, and in fact is a property of all one-loop amplitudes in the theory. It can also be related to dual (pseudo)conformal symmetry of the box functions [96], as anticipated in section 9.2. Also note that $\mathcal{N}=4$ SYM is UV-finite to all orders, and hence bubble integrals must be absent.

In the expression of one-loop amplitudes involving massless particles one encounters IR divergences which are known to be universal. For colour-ordered one-loop amplitudes, these

take the form [158, 159]

$$-A_n^{\text{tree}} \times c_\Gamma \sum_{i=1}^{n} \frac{(-s_{i,i+1})^{-\epsilon}}{\epsilon^2}. \tag{161}$$

One can see this in our four-point example by noticing that a factor of st in the coefficient cancels the $1/(st)$ factor in $I_{0\text{m}}$ of (155). It is also known [160–162] that IR divergences are governed by Sudakov form factors, we will return to this in section 11.2.

10.5. Generalised unitarity

A key observation in our discussion so far is that any one-loop amplitude of massless particles can be expressed in terms of a linear combination of a complete basis of scalar integrals functions: bubbles, triangles and boxes. Performing a two-particle unitarity cut as above amounts to picking two internal propagators with momenta ℓ_1 and ℓ_2 and putting them on-shell. In this factorisation limit we obtained a product of two tree amplitudes providing the cut integrand, while at the level of the ansatz in terms of integral functions this selects a particular set of integral functions that have these two propagators in common. This picks a unique bubble, which only has two propagators, but allows in general a number of triangles and boxes. Considering all possible two-particle cuts gives us sufficient constraints to fix all the coefficients of the integral functions, but the information is entangled between the various cut constraints.

A natural question is then if we can find a procedure, or rather projection, that directly selects a particular integral function and allows us to tackle individual integral coefficients directly. The loop momentum ℓ_1^μ has four independent components and the two-particle cut only constrains two via $\delta(\ell_1^2) = \delta(\ell_2^2) = 0$; in principle we can impose up to two additional constraints $\delta(\ell_3^2) = 0$ and/or $\delta(\ell_4^2) = 0$. Such *generalised cuts* [126, 127] are called triple cuts and quadruple cuts, respectively, where the latter is also known as a maximal cut or leading singularity.

In the case of a triple cut, the integrand is a product of three tree amplitudes [126],

$$\begin{aligned}\sum_{h_{\ell_1},h_{\ell_2},h_{\ell_3}} & A(-\ell_1, i, \ldots, j-1, \ell_2) \times A(-\ell_2, j, \ldots, k-1, \ell_3) \\ & \times A(-\ell_3, k, \ldots i-1, \ell_1),\end{aligned} \tag{162}$$

with $\ell_2 = \ell_1 - p_i - \ldots - p_{j-1}$ and $\ell_3 = \ell_1 + p_k + \ldots + p_{i-1}$ and $\ell_{1,2,3}^2 = 0$, where a sum over internal helicity states is implied. Such a cut will select a unique triangle and a number of boxes that share the same three propagators. Notice that this cut does not detect contributions from bubbles, since they have only two propagators. Furthermore, there is a one-dimensional phase-space integration left.

We now consider a quadruple, or maximal cut, shown in figure 10. Cutting four momenta collapses the loop integration to a sum over a set of solutions that in general is two dimensional. Indeed the cut conditions $\ell_{1,2,3,4}^2 = 0$, with $\ell_2 = \ell_1 - p_i - \ldots - p_{j-1}$, $\ell_3 = \ell_2 - p_j - \ldots - p_{k-1}$ and $\ell_4 = \ell_1 + p_l + \ldots + p_{i-1}$, are equivalent to

$$\ell_1^2 = 0, \qquad \ell_2^2 - \ell_1^2 = 0, \qquad \ell_3^2 - \ell_1^2 = 0, \qquad \ell_4^2 - \ell_1^2 = 0. \tag{163}$$

This is one quadratic equation and three linear ones, hence there are two solutions.

Consider now our ansatz (145). The quadruple cut of the left-hand side is a product of four tree amplitudes, shown in figure 10. As for the right-hand side, the quadruple cut picks a unique box function, times its coefficient. After integration, the quadruple cut of a scalar box, with all

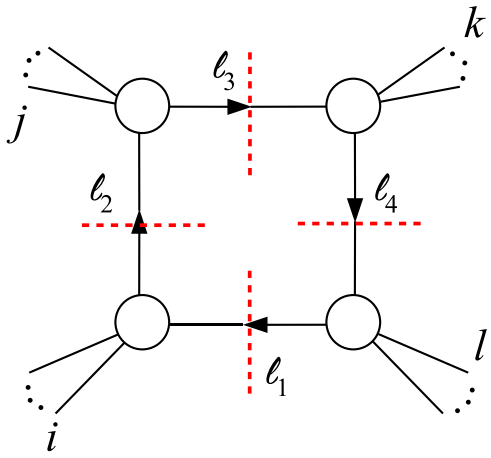

Figure 10. Generic quadruple cut of a one-loop amplitude.

four propagators replaced by delta functions, simply gives 1 times a Jacobian. However this Jacobian appears on both sides and can then be dropped. Thus we arrive at the important result that the box coefficient is equal to [127]

$$a_{i,j,k,l} = \frac{1}{2}\sum A(-\ell_1, i, \ldots, j-1, \ell_2) \times A(-\ell_2, j, \ldots, k-1, \ell_3) \\ \times A(-\ell_3, k, \ldots, l-1, \ell_4) \times A(-\ell_4, l, \ldots, i-1, \ell_1), \tag{164}$$

where the sum is over the solution set of (163) and the helicities of the four cut legs, and the factor of $1/2$ is due to the averaging over the two solutions. As mentioned in section 10.4, bubble and triangle integrals are absent in $\mathcal{N}=4$ SYM, hence one-loop amplitudes in this theory are completely determined by quadruple cuts.

10.6. Example: one-loop MHV superamplitude in N=4 SYM from quadruple cuts

The simplest application of generalised unitarity is to the computation of the one-loop MHV amplitude in $\mathcal{N}=4$ SYM, which we will now perform using superamplitudes [91]. It is easy to see that the only non-vanishing quadruple cut has the 'two-mass easy' configuration shown in figure 11, where two massless legs sit on opposite three-point $\overline{\text{MHV}}$ superamplitudes, while the remaining two are MHV. The two solutions to the cut equations can be found e.g. in the appendix of [163]. The first one is

$$\ell_1 = \frac{|1\rangle\langle s|Q}{\langle 1s\rangle}, \qquad \ell_2 = \frac{|1\rangle\langle s|P}{\langle s1\rangle}, \qquad \ell_3 = \frac{|s\rangle\langle 1|P}{\langle s1\rangle}, \qquad \ell_4 = \frac{|s\rangle\langle 1|Q}{\langle 1s\rangle}, \tag{165}$$

while the second can be obtained by exchanging $|\bullet\rangle \leftrightarrow |\bullet]$. Note that in (165) one has

$$\lambda_{\ell_1} \sim \lambda_{\ell_2} \sim \lambda_1, \qquad \lambda_{\ell_3} \sim \lambda_{\ell_4} \sim \lambda_s. \tag{166}$$

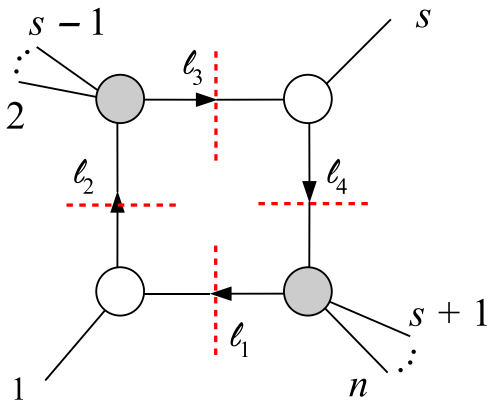

Figure 11. Quadruple cut diagram contributing to a one-loop MHV amplitude. The white amplitudes are $\overline{\text{MHV}}$ while the grey ones MHV.

In the case at hand only the first solution contributes since the two three-point amplitudes are $\overline{\text{MHV}}$, and hence vanish when evaluated on the second solution, which has $\tilde{\lambda}_{\ell_1} \sim \tilde{\lambda}_{\ell_2} \sim \tilde{\lambda}_1$ and $\tilde{\lambda}_{\ell_3} \sim \tilde{\lambda}_{\ell_4} \sim \tilde{\lambda}_s$.

The supercoefficient corresponding to the quadruple cut in figure 11 is then

$$\begin{aligned}\mathcal{C}(1,P,s,Q) = \frac{1}{2}\int \prod_{i=1}^{4} \mathrm{d}^4\eta_{\ell_i} \\ \mathcal{A}_3^{\overline{\text{MHV}}}(-\ell_1,1,\ell_2)\mathcal{A}^{\text{MHV}}(-\ell_2,2,\ldots,s-1,\ell_3)\mathcal{A}_3^{\overline{\text{MHV}}}(-\ell_3,s,\ell_4) \\ \times \mathcal{A}^{\text{MHV}}(-\ell_4,s+1,\ldots,n,\ell_1),\end{aligned} \tag{167}$$

where the spinors are evaluated on the solutions in (165), and the integral over the four internal Graßmann variables elegantly takes care of the state sums. We also set $P := \sum_{i=2}^{s-1} p_i$ and $Q := \sum_{i=s+1}^{n} p_i$. The relevant amplitudes are:

$$\begin{aligned}\mathcal{A}_3^{\overline{\text{MHV}}}(-\ell_1,1,\ell_2) &= -i\frac{\delta^{(4)}(\eta_{-\ell_1}[1\,\ell_2] + \eta_1[\ell_2\,-\ell_1] + \eta_{\ell_2}[-\ell_1\,1])}{[1\,\ell_2][l_2\,-\ell_1][-\ell_1\,1]}, \\ \mathcal{A}_3^{\overline{\text{MHV}}}(-\ell_3,s,\ell_4) &= -i\frac{\delta^{(4)}(\eta_{-\ell_3}[s\,\ell_4] + \eta_s[\ell_4\,-\ell_3] + \eta_{\ell_4}[-\ell_3\,s])}{[s\,\ell_4][\ell_4\,-\ell_3][-\ell_3\,s]}, \\ \mathcal{A}^{\text{MHV}}(-\ell_2,2,\ldots,s-1,\ell_3) &= i\frac{\delta^{(8)}\left(\lambda_{\ell_3}\eta_{\ell_3} - \lambda_{\ell_2}\eta_{\ell_2} + \sum_{i=2}^{s-1}\lambda_i\eta_i\right)}{\langle -\ell_2\,2\rangle\ldots\langle s-1\,\ell_3\rangle\langle\ell_3\,-\ell_2\rangle}, \\ \mathcal{A}^{\text{MHV}}(-\ell_4,s+1,\ldots,n,\ell_1) &= i\frac{\delta^{(8)}\left(-\lambda_{\ell_4}\eta_{\ell_4} + \lambda_{\ell_1}\eta_{\ell_1} + \sum_{i=s+1}^{n}\lambda_i\eta_i\right)}{\langle -\ell_4\,s+1\rangle\ldots\langle n\,\ell_1\rangle\langle\ell_1\,-\ell_4\rangle}.\end{aligned} \tag{168}$$

Next we perform the Graßmann integrations. This task is simplified by noticing that by supermomentum conservation, we expect to find a result proportional to $\delta^{(8)}(\sum_{i=1}^{n}\lambda_i\eta_i)$; we can then simply replace, for instance, the $\delta^{(8)}$ in the last amplitude in (168) by this overall supermomentum conservation delta function. Then the integration over η_{ℓ_1} and η_{ℓ_4} must be done using the $\delta^{(4)}$ in the two $\overline{\text{MHV}}$ superamplitudes, giving a factor of $[1\ell_2]^4[\ell_3 s]^4$; integrating over η_{ℓ_2} and η_{ℓ_3} using the remaining $\delta^{(8)}$ gives a factor of $\langle\ell_2\ell_3\rangle^4$.

The quadruple-cut integrand can then be simplified by using momentum conservation and (166). Factoring out $\mathcal{A}_{\rm MHV}(1,\ldots,n)$, one easily arrives at the result

$$\mathcal{C}(1,P,s,Q) = -\frac{1}{2}\mathcal{A}_n^{\rm MHV}\ [s\ell_3]\langle\ell_3\ell_2\rangle[\ell_2 1]\langle 1s\rangle = -\frac{1}{2}\mathcal{A}_n^{\rm MHV}\ {\rm Tr}_+(s\ell_3\ell_2 1). \tag{169}$$

The evaluation of the last trace can be carried out using (165). One finds

$${\rm Tr}_+(s\ell_3\ell_2 1) = \langle s|P|1]\,\langle 1|P|s] = P^2Q^2 - (P+p_1)^2(Q+p_s)^2, \tag{170}$$

so that in conclusion

$$\mathcal{C}(1,P,s,Q) = \frac{1}{2}\mathcal{A}_n^{\rm MHV}\ \left[(P+p_1)^2(Q+p_s)^2 - P^2Q^2\right]. \tag{171}$$

This is the coefficient of the two-mass easy box function[23]

$$\begin{aligned} &I^{\rm 2me}(p,q,P,Q) \\ &\quad = \int \frac{{\rm d}^D\,\ell}{(2\pi)^D}\frac{1}{\ell^2(\ell-p)^2(\ell-p-P)^2(\ell+Q)^2} \\ &\quad = -i\frac{2c_\Gamma}{st-P^2Q^2}\left\{-\frac{1}{\epsilon^2}\left[(-s)^{-\epsilon}+(-t)^{-\epsilon}-(-P^2)^{-\epsilon}-(-Q^2)^{-\epsilon}\right]\right. \\ &\qquad + {\rm Li}_2\left(1-\frac{P^2}{s}\right)+{\rm Li}_2\left(1-\frac{P^2}{t}\right){\rm Li}_2\left(1-\frac{Q^2}{s}\right)+{\rm Li}_2\left(1-\frac{Q^2}{t}\right) \\ &\qquad \left.- {\rm Li}_2\left(1-\frac{P^2Q^2}{st}\right)+\frac{1}{2}\log^2\left(\frac{s}{t}\right)\right\}, \end{aligned} \tag{172}$$

where for generality we relabeled $p_1 \to p$, $p_s \to q$ and set $s = (P+p)^2$ and $t = (P+q)^2$. Note that the last factor in (171) cancels a corresponding one in the expression for $I^{\rm 2me}$.

10.7. Supersymmetric decomposition and rational terms

As discussed earlier, one-loop amplitudes in supersymmetric theories are special in that the only rational terms that appear are tied to terms which have discontinuities in four dimensions, allowing for the use of spinor-helicity methods.

In non-supersymmetric theories, amplitudes can still be reconstructed from their cuts, but this requires us to work in $4-2\epsilon$ dimensions, with $\epsilon \neq 0$ [153, 154]. While this is important conceptually, it also implies that we have to work with gluon amplitudes in away from four dimensions and the elegance of the spinor-helicity formalism.

A crucial simplification comes from the following observation, known as the supersymmetric decomposition of one-loop gluon amplitudes in pure Yang–Mills: a one-loop amplitude $\mathcal{A}_{\rm g}$ with gluons running in the loop can be re-written as [97, 125]

$$A_{\rm g}^{(1)} = \underbrace{(A_{\rm g}^{(1)} + 4A_{\rm f}^{(1)} + 3A_{\rm s}^{(1)})}_{A^{(1)}_{\mathcal{N}=4}} - \underbrace{4(A_{\rm f}^{(1)} + A_{\rm s}^{(1)})}_{A^{(1)}_{\mathcal{N}=1}} + A_{\rm s}^{(1)}, \tag{173}$$

[23] We mention that there is an alternative expression for this function containing only four polylogarithms [69], related to this one by an application of Mantel's nine-dilogarithm identity [164].

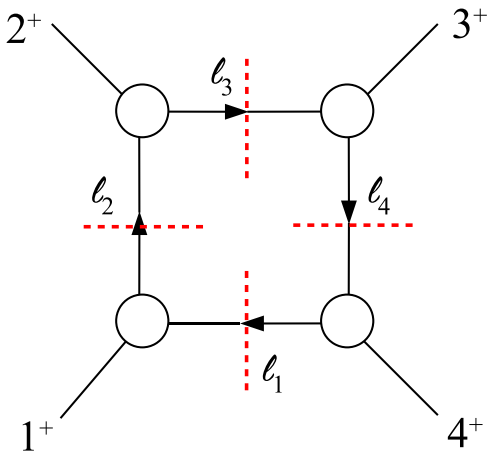

Figure 12. Quadruple cut diagram contributing to the all-plus one-loop amplitude. The internal loop is a real scalar field.

where $A_{\rm f}^{(1)}$ ($A_{\rm s}^{(1)}$) is an amplitude with the same external particles as before but with a Weyl fermion (complex scalar) in the adjoint of the gauge group circulating in the loop. This decomposition is powerful since we recognise that the first two terms on the right-hand side of (173) come from an $\mathcal{N}=4$ multiplet and (minus four times) a chiral $\mathcal{N}=1$ multiplet, respectively; therefore, they are four-dimensional cut-constructible—an observation that simplifies their calculation considerably. The last term in (173), $A_{\rm s}^{(1)}$, is the contribution due to a complex scalar in the loop, which in D dimensions is much easier to compute than having a gluon in the loop.

An instructive example is all-plus four-point amplitude in pure Yang–Mills $A^{(1)}(1^+2^+3^+4^+)$ produced by gluons running in the loop. Using (173) we can immediately relate this to the situation where a scalar is running in the loop since the first two contributions in (173) vanish for this helicity configuration in any supersymmetric theory. Thus, the entire contribution comes from the last term in (173) (figure 12).

In order to compute it, we can perform a D-dimensional quadruple cut [165], by gluing four three-point amplitudes involving two scalars of mass μ^2 and one gluon. Such amplitudes have the form

$$A(\ell_1, p_1^+, \ell_2) = A(\ell_1, p_1^+, \ell_2) = \frac{\langle \xi|\ell_1|p_1]}{\langle \xi p_1\rangle}, \tag{174}$$

where $\ell_1+\ell_2+p_1=0$ and $|\xi\rangle$ is an arbitrary reference spinor. The D-dimensional quadruple cut integrand is then given by

$$\frac{\langle \xi_1|\ell_1|1]}{\langle \xi_1 1\rangle}\,\frac{\langle \xi_2|\ell_2|2]}{\langle \xi_2 2\rangle}\,\frac{\langle \xi_3|\ell_3|3]}{\langle \xi_3 3\rangle}\,\frac{\langle \xi_4|\ell_4|4]}{\langle \xi_4 4\rangle}, \tag{175}$$

which, using the D-dimensional on-shell condition $(\ell_i^{(D)})^2=0=(\ell_i^{(4)})^2-\mu^2$ and momentum conservation, evaluates to $\mu^4\,\frac{[12][34]}{\langle 12\rangle\langle 34\rangle}$. We also have used here the standard trick that a massless scalar in D dimensions can be viewed as a massive scalar in $D=4$ with mass μ^2 coming from the loop momentum components in the extra (-2ϵ) dimensions, which we have to integrate over.

Finally, it can also be seen [165] that two-particle and three-particle cuts do not give any new contributions, and hence we arrive at the result (after replacing the four delta functions by propagators):

$$A^{(1)}(1^+2^+3^+4^+) = 2\frac{[12][34]}{\langle 12\rangle\langle 34\rangle} I_4^{0\mathrm{m}}[\mu^4], \tag{176}$$

where $I_4^{0\mathrm{m}}[\mu^4] = -\frac{i}{(4\pi)^2}\frac{1}{6} + \mathcal{O}(\epsilon)$ is the scalar box integral with an insertion of μ^4 [154], and the factor of two comes from the two real scalars running in the loop.

10.8. Beyond unitarity and higher loops

In the discussion above we only gave a flavour of the power of unitarity methods at one loop. In recent years these methods have been extended in many fruitful directions, in particular generalised unitarity has been adapted to the computation of higher-loop amplitudes in essentially any theory as long as all internal propagators are massless. These include analytic approaches, and several numerical implementations for amplitudes in QCD up to two loops. In parallel, tremendous progress has been made in the evaluation of the required two- and higher-loop Feynman integrals, and some of this progress is reviewed in detail in chapters 3 [166] and 4 [167] of this review.

Furthermore, for highly symmetric theories such as $\mathcal{N} = 4$ supersymmetric Yang–Mills, even more advanced methods have been developed. These employ bootstrap ideas that completely avoid the (separate) determination of coefficients of the basis of integral functions and the problem of evaluating the integrals themselves. These are reviewed in chapter 5 [168] of this review, and are based on a vastly improved understanding of the mathematical properties of complete amplitudes and the relevant function spaces, and include: transcendental functions and their associated symbols, the relation between singularities of amplitudes and cluster algebras, and the Steinmann relations. Recently, these developments have been exploited in [169] for an unprecedented eight-loop computation of form factors (see section 11 for more on form factors). Readers interested in these exciting topics are invited to consult chapter 5 of this review [168].

11. BPS and non-BPS form factors. Applications to Higgs amplitudes

11.1. General properties

Form factors appear in several important contexts in gauge theory. The form factor of (gauge-invariant) $\mathcal{O}(x)$ between the vacuum and an n-particle state is defined as

$$\begin{aligned} F_{\mathcal{O}}(1,\ldots,n;q) &:= \int \mathrm{d}^4 x\, e^{-iq\cdot x}\langle 1\ldots n|\mathcal{O}(x)|0\rangle \\ &= (2\pi)^4\ \delta^{(4)}\left(q - \sum_{i=1}^{n} p_i\right)\langle 1\ldots n|\mathcal{O}(0)|0\rangle, \end{aligned} \tag{177}$$

where the momentum conserving δ-function follows from translation invariance. All legs are on shell except that corresponding to the operator, since in general $q^2 \neq 0$, hence form factors fall in between correlators (fully off shell) and amplitudes (fully on shell).

In addition to conceptual reasons, form factors are important because of their role in several contexts. Notable examples include the form factor of the electromagnetic current, which

computes the electron $g-2$, and that of the hadronic electromagnetic current with an external hadronic state, which appears in the study of deep inelastic scattering and $e^+e^- \to$ hadrons.

Form factors also play a prominent role in the study of scattering processes in QCD involving the Higgs boson and many gluons. At one loop, the coupling of the Higgs to the gluons is induced by a quark loop, with the top giving the most important contribution. These gluon-fusion processes can be described using an effective field theory approach, with the quark loop traded for a set of local interactions of increasing dimension. The leading interaction in the limit $m_{\rm H} \ll m_{\rm t}$, where $m_{\rm H}$ and $m_{\rm t}$ are the masses of the Higgs and the top quark, is the dimension-5 operator $\mathcal{L}_5 \sim H\ {\rm Tr}(F^2)$, where H denotes the Higgs boson and F the gluon field strength [170–172]. It follows that the amplitude of a Higgs and a n gluons in the limit of infinite top mass is the form factor $\langle g_1 \dots g_n|{\rm Tr}(F^2)|0\rangle$ of the operator ${\rm Tr}(F^2)$.

Form factors share some of the beautiful properties of amplitudes, including their simplicity. For instance, at tree level one has [38]

$$\langle 1^+, \dots, i^-, \dots, j^-, \dots n^+|\ {\rm Tr}(F^2_{\rm SD})\,|0\rangle \sim \frac{\langle ij\rangle^4}{\langle 12\rangle\langle 23\rangle \dots \langle n1\rangle}, \tag{178}$$

with $q = p_1 + \cdots p_n$, and where $F_{\rm SD}$ denotes the self-dual part of the field strength. It follows from the discussion above that this is the leading Higgs plus multi-gluon MHV amplitude at tree level. A systematic study of form factors was initiated in [57], and quickly extended to supersymmetric form factors [58]. Among the various results, they satisfy BCFW recursion relations [57], also at loop level [173], can be computed using (generalised) unitarity, and are invariant under a form of dual conformal symmetry [174], which is broken at loop level. Analytic non-supersymmetric form factors were recently computed at one loop [175] using dimensional reconstruction [176–179].

A recent line of research has investigated supersymmetric form factors and possible patterns or similarities with non-supersymmetric, phenomenologically relevant ones. While supersymmetrising the state is straightforward, some thoughts have to be devoted to which operators it may be worthwhile to consider. In this respect, one can observe that the operator ${\rm Tr}(F^2_{\rm SD})$ discussed earlier is the first term in the on-shell Lagrangian of $\mathcal{N}=4$ SYM, which has the schematic form

$$\mathcal{L}_{\rm on-shell} \sim Tr(F^2_{\rm SD}) + g\ {\rm Tr}(\psi\psi\phi) + g^2\ {\rm Tr}([\phi,\phi]^2). \tag{179}$$

It is a descendant of the half-BPS operator ${\rm Tr}(X^2)$, with X being any of the (complex) scalars in $\mathcal{N}=4$ SYM, and is obtained by acting on it with four supersymmetry charges. Both ${\rm Tr}(X^2)$ and $\mathcal{L}_{\rm on-shell}$ belong to the chiral part of the stress-tensor multiplet $\mathcal{T}_2$ [180] and, because they are protected, their form factors are free of UV divergences. Such form factors were studied vigorously in several works [58, 181–185]. This study was later extended to non-protected operators [186–189] such as the Konishi multiplet.

Form factors are a source of many surprises, and we would like to list some of the most unexpected ones. To begin with, it was found at two loops [181] and later confirmed at higher loops [169, 184, 185], that the form factor of the stress–tensor multiplet in $\mathcal{N}=4$ SYM with three external particles is maximally transcendental, similarly to amplitudes[24]. Even more surprisingly, it was found in [181] that the two-loop remainder is identical to the maximally transcendental part of that of the form factor $\langle g^+g^+g^\pm|\ {\rm Tr}\ F^2_{\rm SD}|0\rangle$ [190] in QCD—the first occurrence of the principle of maximal transcendentality [191] in a kinematic-dependent quantity. These

[24] The precise statement is for certain finite remainders [112] of the form factors obtained by subtracting universal infrared-divergent terms.

connections do not stop at protected operators: the maximally transcendental part of the remainder of the minimal form factor of the operator $\mathrm{Tr}(X[Y,Z])$, that is $\langle \bar{X}\bar{Y}\bar{Z}|\,\mathrm{Tr}(X[Y,Z])|0\rangle$ is identical to that of $\langle \bar{X}\bar{X}\bar{X}|\,\mathrm{Tr}(X^3)|0\rangle$ [186]; and finally, this equality extends to the form factor of the operator $\mathrm{Tr}\,(F^3_{\mathrm{SD}})$ [187–189], which describes higher-derivative corrections to the Higgs effective theory [192–196]. In [197] a proof of the principle of maximal transcendentality for two-loop form factors involving $\mathrm{Tr}\,(F^2)$ and $\mathrm{Tr}\,(F^3)$ was presented. As a result, it seems that the maximally transcendental part of Higgs plus multi-gluon processes could be equivalently computed in $\mathcal{N}=4$ SYM!

We also mention the intriguing connections between the (infrared-finite) remainder functions of the three-point form factor $\langle \bar{X}\bar{X}\bar{X}|\,\mathrm{Tr}(X^3)|0\rangle$ and the remainder for the six-point MHV amplitude [169, 181, 184, 185], which recently have been explained by an antipodal duality that relates the discontinuities of the form factor to the derivatives of the amplitude. The remainder functions for these two quantities can be expressed in terms of three dimensionless variables, (u,v,w), representing ratios of Mandelstam variables satisfying $u+v+w=1$ in the former case, and unconstrained dual-conformal invariant cross-ratios in the latter. This remarkable duality then connects the form factor remainder function and the parity-even part of the amplitude remainder function on the surface $u+v+w=1$.

Finally, form factors found an application in [198, 199] to the study of the complete one-loop dilatation operator of $\mathcal{N}=4$ SYM [200–202], with the Yangian invariance of the latter [203] being a direct consequence [204] of that of the $\mathcal{N}=4$ SYM S-matrix [117]. We also mention recent applications in effective field theories of the standard model, e.g. in classifying marginal operators and studying the mixing problem [205–209].

11.2. Example: one-loop Sudakov form factor

To have a taste of form factors, we now compute that of the on-shell Lagrangian (179) with an external state of two positive-helicity gluons, known as the Sudakov form factor. Only the field-strength part of $\mathcal{L}_{\mathrm{on-shell}}$ contributes, and at tree level we can normalise the operator to have $F^{\mathrm{tree}}_{\mathrm{Tr}(F^2)}(1^+2^+)=[12]^2$. This form factor depends on a single kinematic invariant $s=(p_1+p_2)^2$, and at one loop we only have a cut in this channel. This gives

$$\begin{aligned} F^{(1)}_{\mathrm{Tr}(F^2)}(1^+2^+)|_{s-\mathrm{cut}} &= F^{\mathrm{tree}}_{\mathrm{Tr}(F^2)}(-\ell_1^+ - \ell_2^+)A_4^{(0)}(\ell_1^-,1^+,2^+,\ell_2^-) \\ &= 2[-\ell_1 - \ell_2]^2 \times i\frac{\langle \ell_2\ell_1\rangle^3}{\langle \ell_1 1\rangle\langle 12\rangle\langle 2\ell_2\rangle} = \frac{2i(\ell_1+\ell_2)^2\langle \ell_2\ell_1\rangle[\ell_2\ell_1]}{\langle 12\rangle\langle 2 \underbrace{\ell_2\rangle[\ell_2}_{\ell_2=-\ell_1-p_1-p_2} \ell_1]\langle \ell_1 1\rangle} \\ &= \frac{-2i(p_1+p_2)^3}{\langle 12\rangle^2(\ell_1+p_1)^2} = \frac{-2is[12]^2}{(\ell_1+p_1)^2}. \end{aligned} \tag{180}$$

In order to obtain the uplifted integrand, following the strategy described in section 10.4, we have to multiply this by $\frac{i}{\ell_1^2}\frac{i}{\ell_2^2}$, and further integrating we find $2is[12]^2\times I_3^{1\mathrm{m}}(s)$, where the one-mass triangle is given by

$$I_3^{1\mathrm{m}}(s) = \int \frac{\mathrm{d}^{4-2\epsilon}\ell}{(2\pi)^{4-2\epsilon}} \frac{1}{\ell^2(\ell+p_1)^2(\ell+p_1+p_2)^2} = -i\frac{c_\Gamma}{\epsilon^2}(-s)^{-1-\epsilon}. \tag{181}$$

In conclusion, we find that

$$F^{(1)}_{\mathrm{Tr}(F^2)}(1^+2^+)/F^{\mathrm{tree}}_{\mathrm{Tr}(F^2)}(1^+2^+) = -\frac{2c_\Gamma}{\epsilon^2}(-s)^{-\epsilon}. \tag{182}$$

Note that the Sudakov form factor is equal to twice the IR-divergent term of the contribution of a given two-particle invariant $s_{i,i+1}$ to the one-loop amplitude computed in (161). Interestingly this relation holds for general one-loop amplitudes (see for instance [210] for a unitarity-based proof), and also beyond one loop [161, 162].

Acknowledgments

It is a pleasure to thank James Bedford, Lorenzo Bianchi, Gang Chen, James Drummond, Ömer Gürdoğan, Johannes Henn, Paul Heslop, Edward Hughes, Dimitrios Korres, Martyna Kostacińska Jones, Simon McNamara, Robert Mooney, Rodolfo Panerai, Brenda Penante, Bill Spence, Congkao Wen, Gang Yang and Donovan Young for enjoyable collaborations on topics related to this article. Many thanks to Manuel Accettulli Huber, Stefano De Angelis and Shun-Qing Zhang for their careful reading of our article and for comments. This work was supported by the European Union's Horizon 2020 research and innovation programme under the Marie Skłodowska-Curie Grant Agreement No. 764850 '*SAGEX*'. We also acknowledge support from the Science and Technology Facilities Council (STFC) Consolidated Grant ST/T000686/1 '*Amplitudes, strings & duality*'.

Data availability statement

No new data were created or analysed in this study.

Appendix A. Conventions and Lorentz transformations of spinor variables

Conventions. Spinor indices are raised and lowered using the Levi-Civita tensor as

$$\begin{aligned} \lambda^\alpha &= \epsilon^{\alpha\beta}\lambda_\beta, \qquad & \lambda_\alpha &= \epsilon_{\alpha\beta}\lambda^\beta, \\ \tilde{\lambda}^{\dot\alpha} &= \epsilon^{\dot\alpha\dot\beta}\tilde{\lambda}_{\dot\beta}, \qquad & \tilde{\lambda}_{\dot\alpha} &= \epsilon_{\dot\alpha\dot\beta}\tilde{\lambda}^{\dot\beta}, \end{aligned} \tag{A.1}$$

with $\epsilon^{\alpha\gamma}\,\epsilon_{\gamma\beta} = \delta^\alpha_{\ \beta}$, and $\epsilon^{\dot\alpha\dot\gamma}\,\epsilon_{\dot\gamma\dot\beta} = \delta^{\dot\alpha}_{\ \dot\beta}$. We also define

$$\sigma_{\mu\alpha\dot\alpha} = (\mathbb{1}, \vec{\sigma}), \qquad \bar\sigma_\mu^{\dot\alpha\alpha} = (\mathbb{1}, -\vec{\sigma}), \tag{A.2}$$

where $\vec\sigma$ are the Pauli matrices. They are related as

$$\sigma_{\mu\,\alpha\dot\alpha} = \epsilon_{\alpha\beta}\,\epsilon_{\dot\alpha\dot\beta}\,\bar\sigma_\mu^{\dot\beta\beta}. \tag{A.3}$$

We also note the completeness relations

$$\sigma_{\mu\,\alpha\dot\alpha}\,\sigma^\mu_{\beta\dot\beta} = 2\,\epsilon_{\alpha\beta}\,\epsilon_{\dot\alpha\dot\beta}, \qquad \bar\sigma_\mu^{\dot\alpha\alpha}\,\bar\sigma^{\mu\dot\beta\beta} = 2\,\epsilon^{\alpha\beta}\,\epsilon^{\dot\alpha\dot\beta}, \tag{A.4}$$

and the normalisation condition

$$\mathrm{Tr}\,(\bar{\sigma}^{\mu}\sigma^{\nu}) = 2\,\eta^{\mu\nu}, \tag{A.5}$$

with $\eta^{\mu\nu} = (1,-1,-1,-1)$.

Transformations under the Lorentz group. The complexified four-dimensional Lorentz group $SO(3,1)$ is locally isomorphic to $SL(2,\mathbb{C}) \times SL(2,\mathbb{C})$, with the isomorphism being realised as in (7). Its representations are then labeled as (m,n), where $m,n \in \frac{1}{2}\mathbb{Z}$. In real Minkowski space, the second $SL(2,\mathbb{C})$ has to be identified with the complex conjugate of the first[25]. Our helicity spinors λ and $\tilde{\lambda}$ then transform in the $(1/2,0)$ and $(0,1/2)$ representations, respectively, that is

$$\lambda_{\alpha} \to M_{\alpha}{}^{\beta}\,\lambda_{\beta}, \qquad \tilde{\lambda}_{\dot{\alpha}} \to (M^{*})_{\dot{\alpha}}{}^{\dot{\beta}}\,\tilde{\lambda}_{\dot{\beta}} = \tilde{\lambda}_{\dot{\beta}}\,(M^{\dagger})^{\dot{\beta}}{}_{\dot{\alpha}}, \tag{A.6}$$

and the momentum $p_{\alpha\dot{\alpha}}$ in the $(1/2,1/2)$, i.e.

$$p_{\alpha\dot{\alpha}} \to M_{\alpha}{}^{\beta}\,p_{\beta\dot{\beta}}\,(M^{*})_{\dot{\alpha}}{}^{\dot{\beta}} = (MpM^{\dagger})_{\alpha\dot{\alpha}}. \tag{A.7}$$

Here $M \in SL(2,\mathbb{C})$, so that $\det M = 1$. The Levi-Civita symbols $\epsilon_{\alpha\beta}$ and $\epsilon_{\dot{\alpha}\dot{\beta}}$ are invariant tensors: for instance, $\epsilon_{\alpha\beta} \to M_{\alpha}{}^{\alpha'}M_{\beta}{}^{\beta'}\epsilon_{\alpha'\beta'} = \det M\,\epsilon_{\alpha\beta} = \epsilon_{\alpha\beta}$. We can write this transformation in matrix form as $M\epsilon M^{\mathrm{T}} = \epsilon$, with a similar relation $M^{*}\epsilon M^{\dagger} = \epsilon$ for $\epsilon_{\dot{\alpha}\dot{\beta}}$. It is also important to work out the transformations of $\lambda^{\alpha} := \epsilon^{\alpha\beta}\lambda_{\beta}$ and $\tilde{\lambda}^{\dot{\alpha}} := \epsilon^{\dot{\alpha}\dot{\beta}}\tilde{\lambda}_{\dot{\beta}}$. Calling ϵ and $\tilde{\epsilon}$ the matrices whose elements are $\epsilon_{\alpha\beta}$ and $\epsilon^{\alpha\beta}$,

$$\lambda^{\alpha} \to \epsilon^{\alpha\beta}M_{\beta}{}^{\gamma}\epsilon_{\gamma\delta}\lambda^{\delta} = (\tilde{\epsilon}M\epsilon\lambda)^{\alpha} = \left(\tilde{\epsilon}\epsilon(M^{\mathrm{T}})^{-1}\lambda\right)^{\alpha} = \lambda^{\beta}(M^{-1})_{\beta}{}^{\alpha}, \tag{A.8}$$

where we used $M\epsilon = \epsilon(M^{\mathrm{T}})^{-1}$. Similarly $\tilde{\lambda}^{\dot{\alpha}} := \epsilon^{\dot{\alpha}\dot{\beta}}\tilde{\lambda}_{\dot{\beta}}$ transforms as

$$\tilde{\lambda}^{\dot{\alpha}} \to \epsilon^{\dot{\alpha}\dot{\beta}}(M^{*})_{\dot{\beta}}{}^{\dot{\gamma}}\,\epsilon_{\dot{\gamma}\dot{\rho}}\,\tilde{\lambda}^{\dot{\rho}} = (\tilde{\epsilon}\epsilon(M^{\dagger})^{-1}\tilde{\lambda})^{\dot{\alpha}} = ((M^{\dagger})^{-1})^{\dot{\alpha}}{}_{\dot{\beta}}\,\tilde{\lambda}^{\dot{\beta}}, \tag{A.9}$$

where we used $M^{*}\epsilon(M^{*})^{\mathrm{T}} = \epsilon$, from which it follows that $M^{*}\epsilon = \epsilon(M^{\dagger})^{-1}$, and we also called ϵ and $\tilde{\epsilon}$ the matrices with elements $\epsilon_{\dot{\alpha}\dot{\beta}}$ and $\epsilon^{\dot{\alpha}\dot{\beta}}$. Summarising, we have that

$$\begin{aligned} &\lambda_{\alpha} \to M_{\alpha}{}^{\beta}\,\lambda_{\beta}, && \tilde{\lambda}_{\dot{\alpha}} \to \tilde{\lambda}_{\dot{\beta}}\,(M^{\dagger})^{\dot{\beta}}{}_{\dot{\alpha}}, \\ &\lambda^{\alpha} \to \lambda^{\beta}(M^{-1})_{\beta}{}^{\alpha}, && \tilde{\lambda}^{\dot{\alpha}} \to ((M^{\dagger})^{-1})^{\dot{\alpha}}{}_{\dot{\beta}}\,\tilde{\lambda}^{\dot{\beta}}. \end{aligned} \tag{A.10}$$

As a result, the brackets $\langle i\,j\rangle := \lambda_{i}^{\alpha}\lambda_{j\alpha}$ and $[i\,j] := \tilde{\lambda}_{i\dot{\alpha}}\tilde{\lambda}^{j\dot{\alpha}}$ are manifestly Lorentz invariant.

ORCID iDs

Andreas Brandhuber https://orcid.org/0000-0002-4203-8811
Gabriele Travaglini https://orcid.org/0000-0002-6699-3960

[25] Recall from section 2.2 that in real Minkowski space $(\lambda^{\alpha})^{*} = \pm\tilde{\lambda}^{\dot{\alpha}}$. For completeness we also note that in $(++--)$ signature the Lorentz group $SO(2,2)$ is locally isomorphic to $SL(2,\mathbb{R}) \times SL(2,\mathbb{R})$, with the two $SL(2,\mathbb{R})$ factors being independent; in this case the spinor representations are real.

References

[1] Mangano M L and Parke S J 1991 *Phys. Rep.* **200** 301–67
[2] Parke S J and Taylor T R 1986 *Phys. Rev. Lett.* **56** 2459
[3] Mangano M, Parke S and Xu Z 1988 *Nucl. Phys.* B **298** 653–72
[4] Witten E 2004 *Commun. Math. Phys.* **252** 189–258
[5] Penrose R 1967 *J. Math. Phys.* **8** 345
[6] Penrose R and MacCallum M A H 1972 *Phys. Rep.* **6** 241–316
[7] Roiban R, Spradlin M and Volovich A 2004 *J. High Energy Phys.* JHEP04(2004)012
[8] Berkovits N 2004 *Phys. Rev. Lett.* **93** 011601
[9] Roiban R, Spradlin M and Volovich A 2004 *Phys. Rev.* D **70** 026009
[10] Cachazo F, Svrcek P and Witten E 2004 *J. High Energy Phys.* JHEP09(2004)006
[11] Dixon L J 1991 Future challenges for (N)NLO accuracy in QCD (https://indico.cern.ch/event/93790/contributions/1281096/attachments/1103796/1574776/LDTrentoFuture.pdf)
[12] Xu Z, Zhang D-H and Chang L 1987 *Nucl. Phys.* B **291** 392–428
[13] Gunion J F and Kunszt Z 1985 *Phys. Lett.* B **161** 333
[14] Kleiss R and Stirling W J 1985 *Nucl. Phys.* B **262** 235–62
[15] Bjorken J D and Chen M C 1966 *Phys. Rev.* **154** 1335–7
[16] Henry G R 1967 *Phys. Rev.* **154** 1534–6
[17] De Causmaecker P, Gastmans R, Troost W and Tai Tsun Wu T T 1981 *Phys. Lett.* B **105** 215
[18] De Causmaecker P, Gastmans R, Troost W and Wu T T 1982 *Nucl. Phys.* B **206** 53–60
[19] Berends F A, Kleiss R, De Causmaecker P, Gastmans R, Troost W and Wu T T 1982 *Nucl. Phys.* B **206** 61–89
[20] Berends F A, De Causmaecker P, Gastmans R, Kleiss R, Troost W and Wu T T 1984 *Nucl. Phys.* B **239** 382–94
[21] Berends F A, De Causmaeceker P, Gastmans R, Kleiss R, Troost W and Wu T T 1984 *Nucl. Phys.* B **239** 395–409
[22] Berends F A, De Causmaecker P, Gastmans R, Kleiss R, Troost W and Wu T T 1986 *Nucl. Phys.* B **264** 243
[23] Berends F A, De Causmaecker P, Gastmans R, Kleiss R, Troost W and Wu T T 1986 *Nucl. Phys.* B **264** 265–76
[24] Wigner E 1939 *Ann. Math.* **40** 149–204
[25] Bargmann V and Wigner E P 1948 *Proc. Natl Acad. Sci. USA* **34** 211
[26] Arkani-Hamed N, Huang T C and Huang Y t 2021 *J. High Energy Phys.* JHEP11(2021)070
[27] Ita H and Ozeren K 2012 *J. High Energy Phys.* JHEP02(2012)118
[28] Reuschle C and Weinzierl S 2013 *Phys. Rev.* D **88** 105020
[29] Bern Z and Kosower D A 1991 *Nucl. Phys.* B **362** 389–448
[30] Del Duca V, Dixon L and Maltoni F 2000 *Nucl. Phys.* B **571** 51–70
[31] Kleiss R and Kuijf H 1989 *Nucl. Phys.* B **312** 616–44
[32] Bern Z, Carrasco J J M and Johansson H 2008 *Phys. Rev.* D **78** 085011
[33] Bern Z, Carrasco J J M and Johansson H 2010 *Phys. Rev. Lett.* **105** 061602
[34] Bern Z, Carrasco J J, Chiodaroli M, Johansson H and Roiban R 2022 arXiv:2203.13013
[35] Johansson H and Ochirov A 2016 *J. High Energy Phys.* JHEP01(2016)170
[36] Melia T 2015 *J. High Energy Phys.* JHEP12(2015)107
[37] Dixon L J and Shadmi Y 1994 *Nucl. Phys.* B **423** 3–32
Dixon L J and Shadmi Y 1995 *Nucl. Phys.* B **452** 724 (erratum)
[38] Dixon L J, Glover E W N and Khoze V V 2004 *J. High Energy Phys.* JHEP12(2004)015
[39] Broedel J and Dixon L J 2012 *J. High Energy Phys.* JHEP10(2012)091
[40] DeWitt B S 1967 *Phys. Rev.* **162** 1239–56
[41] Eden R J, Landshoff P V, Olive D I and Polkinghorne J C 1966 *The Analytic S-Matrix* (Cambridge: Cambridge University Press)
[42] Britto R, Cachazo F and Feng B 2005 *Nucl. Phys.* B **715** 499–522
[43] Britto R, Cachazo F, Feng B and Witten E 2005 *Phys. Rev. Lett.* **94** 181602
[44] Risager K 2005 *J. High Energy Phys.* JHEP12(2005)003
[45] Elvang H, Freedman D Z and Kiermaier M 2009 *J. High Energy Phys.* JHEP06(2009)068
[46] Arkani-Hamed N and Kaplan J 2008 *J. High Energy Phys.* JHEP04(2008)076
[47] Henn J M and Plefka J C 2014 *Scattering Amplitudes in Gauge Theories* vol 883 (Berlin: Springer)

[48] Bedford J, Brandhuber A, Spence B and Travaglini G 2005 *Nucl. Phys.* B **721** 98–110
[49] Cachazo F and Svrcek P 2005 arXiv:hep-th/0502160
[50] Badger S D, Glover E W N, Khoze V V and Svrcek P 2005 *J. High Energy Phys.* JHEP07(2005)025
[51] Badger S D, Glover E W N and Khoze V V 2006 *J. High Energy Phys.* JHEP01(2006)066
[52] Bern Z, Dixon L J and Kosower D A 2005 *Phys. Rev.* D **71** 105013
[53] Bern Z, Dixon L J and Kosower D A 2005 *Phys. Rev.* D **72** 125003
[54] Brandhuber A, McNamara S, Spence B and Travaglini G 2007 *J. High Energy Phys.* JHEP03(2007)029
[55] Dunbar D C, Ettle J H and Perkins W B 2010 *J. High Energy Phys.* JHEP06(2010)027
[56] Alston S D, Dunbar D C and Perkins W B 2015 *Phys. Rev.* D **92** 065024
[57] Brandhuber A, Spence B, Travaglini G and Yang G 2011 *J. High Energy Phys.* JHEP01(2011)134
[58] Brandhuber A, Gurdogan O, Mooney R, Travaglini G and Yang G 2011 *J. High Energy Phys.* JHEP10(2011)046
[59] Kampf K, Novotny J and Trnka J 2013 *Phys. Rev.* D **87** 081701
[60] Cheung C, Kampf K, Novotny J and Trnka J 2015 *Phys. Rev. Lett.* **114** 221602
[61] Cheung C, Kampf K, Novotny J, Shen C H and Trnka J 2016 *Phys. Rev. Lett.* **116** 041601
[62] Mojahed M A and Brauner T 2021 *Phys. Lett.* B **822** 136705
[63] Brandhuber A, Heslop P and Travaglini G 2008 *Phys. Rev.* D **78** 125005
[64] Arkani-Hamed N, Cachazo F and Kaplan J 2010 *J. High Energy Phys.* JHEP09(2010)016
[65] Arkani-Hamed N, Bourjaily J L, Cachazo F, Goncharov A B, Postnikov A and Trnka J 2016 *Grassmannian Geometry of Scattering Amplitudes* (Cambridge: Cambridge University Press)
[66] Herrmann E and Trnka J 2022 arXiv:2203.13018
[67] Cheung C, Shen C-H and Trnka J 2015 *J. High Energy Phys.* JHEP06(2015)118
[68] Cohen T, Elvang H and Kiermaier M 2011 *J. High Energy Phys.* JHEP04(2011)053
[69] Brandhuber A, Spence B and Travaglini G 2005 *Nucl. Phys.* B **706** 150–80
[70] Brandhuber A, Spence B and Travaglini G 2006 *J. High Energy Phys.* JHEP01(2006)142
[71] Brandhuber A, Spence B and Travaglini G 2011 *J. Phys. A: Math. Theor.* **44** 454002
[72] Kosower D A and Uwer P 1999 *Nucl. Phys.* B **563** 477–505
[73] Bern Z, Del Duca V, Kilgore W B and Schmidt C R 1999 *Phys. Rev.* D **60** 116001
[74] Bedford J, Brandhuber A, Spence B and Travaglini G 2005 *Nucl. Phys.* B **706** 100–26
[75] Bedford J, Brandhuber A, Spence B and Travaglini G 2005 *Nucl. Phys.* B **712** 59–85
[76] Quigley C and Rozali M 2005 *J. High Energy Phys.* JHEP01(2005)053
[77] McLoughlin T, Puhm A and Raclariu A M 2022 arXiv:2203.13022
[78] Cachazo F and Strominger A 2014 arXiv:1404.4091
[79] Casali E 2014 *J. High Energy Phys.* JHEP08(2014)077
[80] Bern Z, Dixon L, Perelstein M and Rozowsky J S 1999 *Nucl. Phys.* B **546** 423–79
[81] Weinberg S 1965 *Phys. Rev.* **140** B516–24
[82] Laddha A and Sen A 2017 *J. High Energy Phys.* JHEP10(2017)065
[83] Broedel J, de Leeuw M, Plefka J and Rosso M 2014 *Phys. Rev.* D **90** 065024
[84] Bern Z, Davies S, Di Vecchia P and Nohle J 2014 *Phys. Rev.* D **90** 084035
[85] Klose T, McLoughlin T, Nandan D, Plefka J and Travaglini G 2015 *J. High Energy Phys.* JHEP07(2015)135
[86] Volovich A, Wen C and Zlotnikov M 2015 *J. High Energy Phys.* JHEP07(2015)095
[87] D'Hoker E and Freedman D Z 2002 Supersymmetric gauge theories and the AdS/CFT correspondence *Theoretical Advanced Study Institute in Elementary Particle Physics (TASI 2001): Strings, Branes and Extra Dimensions* pp 3–158 arXiv:hep-th/0201253
[88] Nair V P 1988 *Phys. Lett.* B **214** 215–8
[89] Ferber A 1978 *Nucl. Phys.* B **132** 55–64
[90] Drummond J M, Henn J, Korchemsky G P and Sokatchev E 2010 *Nucl. Phys.* B **828** 317–74
[91] Drummond J M, Henn J, Korchemsky G P and Sokatchev E 2013 *Nucl. Phys.* B **869** 452–92
[92] Bern Z, Dixon L J and Kosower D A 2005 *Phys. Rev.* D **72** 045014
[93] Drummond J M and Henn J M 2009 *J. High Energy Phys.* JHEP04(2009)018
[94] Dixon L J 1996 Calculating scattering amplitudes efficiently *Theoretical Advanced Study Institute in Elementary Particle Physics (TASI 95): QCD and beyond* pp 539–84 arXiv:hep-ph/9601359
[95] Mandelstam S 1983 *Nucl. Phys.* B **213** 149–68
[96] Drummond J M, Henn J, Smirnov V A and Sokatchev E 2007 *J. High Energy Phys.* JHEP01(2007)064
[97] Bern Z, Dixon L, Dunbar D C and Kosower D A 1994 *Nucl. Phys.* B **425** 217–60

[98] 't Hooft G and Veltman M J G 1979 *Nucl. Phys.* B **153** 365–401
[99] Denner A, Nierste U and Scharf R 1991 *Nucl. Phys.* B **367** 637–56
[100] Bourjaily J L, Dulat F and Panzer E 2019 *Nucl. Phys.* B **942** 251–302
[101] Duhr C and Dulat F 2019 *J. High Energy Phys.* JHEP08(2019)135
[102] Brandhuber A, Heslop P and Travaglini G 2009 *J. High Energy Phys.* JHEP08(2009)095
[103] Brandhuber A, Heslop P and Travaglini G 2009 *J. High Energy Phys.* JHEP10(2009)063
[104] Drummond J M, Henn J, Korchemsky G P and Sokatchev E 2008 *Nucl. Phys.* B **795** 52–68
[105] Drummond J M, Henn J, Korchemsky G P and Sokatchev E 2010 *Nucl. Phys.* B **826** 337–64
[106] Alday L F and Maldacena J 2007 *J. High Energy Phys.* JHEP06(2007)064
[107] Drummond J M, Korchemsky G P and Sokatchev E 2008 *Nucl. Phys.* B **795** 385–408
[108] Brandhuber A, Heslop P and Travaglini G 2008 *Nucl. Phys.* B **794** 231–43
[109] Elvang H, Freedman D Z and Kiermaier M 2010 *J. High Energy Phys.* JHEP03(2010)075
[110] Bern Z, Carrasco J J M, Johansson H and Kosower D A 2007 *Phys. Rev.* D **76** 125020
[111] Bourjaily J L, DiRe A, Shaikh A, Spradlin M and Volovich A 2012 *J. High Energy Phys.* JHEP03(2012)032
[112] Bern Z, Dixon L J and Smirnov V A 2005 *Phys. Rev.* D **72** 085001
[113] Bern Z, Czakon M, Dixon L J, Kosower D A and Smirnov V A 2007 *Phys. Rev.* D **75** 085010
[114] Cachazo F, Spradlin M and Volovich A 2007 *Phys. Rev.* D **75** 105011
[115] Hodges A 2013 *J. High Energy Phys.* JHEP05(2013)135
[116] Mason L and Skinner D 2009 *J. High Energy Phys.* JHEP11(2009)045
[117] Drummond J, Henn J and Plefka J 2009 *J. High Energy Phys.* JHEP05(2009)046
[118] Drinfeld V G 1985 *Sov. Math. Dokl.* **32** 254–8
[119] Drinfeld V G 1986 *Zap. Nauchn. Semin.* **155** 18–49
[120] Bargheer T, Beisert N, Galleas W, Loebbert F and McLoughlin T 2009 *J. High Energy Phys.* JHEP11(2009)056
[121] Beisert N, Henn J, McLoughlin T and Plefka J 2010 *J. High Energy Phys.* JHEP04(2010)085
[122] Caron-Huot S and He S 2012 *J. High Energy Phys.* JHEP07(2012)174
[123] Bullimore M and Skinner D 2011 arXiv:1112.1056
[124] Beisert N *et al* 2012 *Lett. Math. Phys.* **99** 3–32
[125] Bern Z, Dixon L, Dunbar D C and Kosower D A 1995 *Nucl. Phys.* B **435** 59–101
[126] Bern Z, Dixon L and Kosower D A 2004 *J. High Energy Phys.* JHEP08(2004)012
[127] Britto R, Cachazo F and Feng B 2005 *Nucl. Phys.* B **725** 275–305
[128] Feynman R P 1963 *Acta Phys. Pol.* **24** 697–722
[129] Feynman R P 1972 Closed loop and tree diagrams *Magic without Magic* ed J R Klauder (San Francisco, CA: Freeman)
[130] Neill D and Rothstein I Z 2013 *Nucl. Phys.* B **877** 177–89
[131] Bjerrum-Bohr N E J, Donoghue J F and Vanhove P 2014 *J. High Energy Phys.* JHEP02(2014)111
[132] Bjerrum-Bohr N E J, Donoghue J F, Holstein B R, Plante L and Vanhove P 2015 *Phys. Rev. Lett.* **114** 061301
[133] Bjerrum-Bohr N E J, Donoghue J F, Holstein B R, Planté L and Vanhove P 2016 *J. High Energy Phys.* JHEP11(2016)117
[134] Bai D and Huang Y 2017 *Phys. Rev.* D **95** 064045
[135] Chi H-H 2019 *Phys. Rev.* D **99** 126008
[136] Bern Z, Cheung C, Roiban R, Shen C-H, Solon M P and Zeng M 2019 *Phys. Rev. Lett.* **122** 201603
[137] Bern Z, Cheung C, Roiban R, Shen C-H, Solon M P and Zeng M 2019 *J. High Energy Phys.* JHEP10(2019)206
[138] Parra-Martinez J, Ruf M S and Zeng M 2020 *J. High Energy Phys.* JHEP11(2020)023
[139] Di Vecchia P, Heissenberg C, Russo R and Veneziano G 2021 *J. High Energy Phys.* JHEP07(2021)169
[140] Bjerrum-Bohr N E J, Damgaard P H, Planté L and Vanhove P 2021 *J. High Energy Phys.* JHEP08(2021)172
[141] Brandhuber A, Chen G, Travaglini G and Wen C 2021 *J. High Energy Phys.* JHEP10(2021)118
[142] Herrmann E, Parra-Martinez J, Ruf M S and Zeng M 2021 *Phys. Rev. Lett.* **126** 201602
[143] Herrmann E, Parra-Martinez J, Ruf M S and Zeng M 2021 *J. High Energy Phys.* JHEP10(2021)148
[144] Bern Z, Parra-Martinez J, Roiban R, Ruf M S, Shen C-H, Solon M P and Zeng M 2021 *Phys. Rev. Lett.* **126** 171601
[145] Brandhuber A and Travaglini G 2020 *J. High Energy Phys.* JHEP01(2020)010
[146] Emond W T and Moynihan N 2019 *J. High Energy Phys.* JHEP12(2019)019

[147] Accettulli Huber M, Brandhuber A, De Angelis S and Travaglini G 2020 *Phys. Rev.* D **102** 046014
[148] Accettulli Huber M, Brandhuber A, De Angelis S and Travaglini G 2021 *Phys. Rev.* D **103** 045015
[149] Carrillo-González M, de Rham C and Tolley A J 2021 *J. High Energy Phys.* JHEP11(2021)087
[150] Bjerrum-Bohr N E J, Damgaard P H, Plante L and Vanhove P 2022 arXiv:2203.13024
[151] Kosower D A, Monteiro R and O'Connell D 2022 arXiv:2203.13025
[152] Passarino G and Veltman M 1979 *Nucl. Phys.* B **160** 151–207
[153] van Neerven W L 1986 *Nucl. Phys.* B **268** 453–88
[154] Bern Z and Morgan A G 1996 *Nucl. Phys.* B **467** 479–509
[155] Bern Z and Kosower D A 1992 *Nucl. Phys.* B **379** 451–561
[156] Bern Z, Freitas A D and Dixon L J 2002 *J. High Energy Phys.* JHEP03(2002)018
[157] Bern Z, Dixon L and Kosower D A 1994 *Nucl. Phys.* B **412** 751–816
[158] Giele W T and Glover E W N 1992 *Phys. Rev.* D **46** 1980–2010
[159] Kunszt Z, Signer A and Trócsányi Z 1994 *Nucl. Phys.* B **420** 550–64
[160] Mueller A H 1979 *Phys. Rev.* D **20** 2037
[161] Magnea L and Sterman G 1990 *Phys. Rev.* D **42** 4222–7
[162] Sterman G and Tejeda-Yeomans M E 2003 *Phys. Lett.* B **552** 48–56
[163] Risager Larsen K 2007 Unitarity and on-shell recursion methods for scattering amplitudes *PhD Thesis* Copenhagen University
[164] Mantel W 1898 *Nieuw Archief* **3** 292
[165] Brandhuber A, McNamara S, Spence B and Travaglini G 2005 *J. High Energy Phys.* JHEP10(2005)011
[166] Abreu S, Britto R and Duhr C 2022 arXiv:2203.13014
[167] Blümlein J and Schneider C 2022 arXiv:2203.13015
[168] Papathanasiou G 2022 arXiv:2203.13016
[169] Dixon L J, Gurdogan O, McLeod A J and Wilhelm M 2022 arXiv:2204.11901
[170] Wilczek F 1977 *Phys. Rev. Lett.* **39** 1304
[171] Shifman M A, Vainshtein A I, Voloshin M B and Zakharov V I 1979 *Sov. J. Nucl. Phys.* **30** 711–6
[172] Dawson S 1991 *Nucl. Phys.* B **359** 283–300
[173] Bianchi L, Brandhuber A, Panerai R and Travaglini G 2019 *J. High Energy Phys.* JHEP02(2019)182
[174] Bianchi L, Brandhuber A, Panerai R and Travaglini G 2019 *J. High Energy Phys.* JHEP02(2019)134
[175] Accettulli Huber M, Brandhuber A, De Angelis S and Travaglini G 2020 *Phys. Rev.* D **101** 026004
[176] Giele W T, Kunszt Z and Melnikov K 2008 *J. High Energy Phys.* JHEP04(2008)049
[177] Ellis R K, Giele W T, Kunszt Z and Melnikov K 2009 *Nucl. Phys.* B **822** 270–82
[178] Bern Z, Carrasco J J, Dennen T, Huang Y t and Ita H 2011 *Phys. Rev.* D **83** 085022
[179] Davies S 2011 *Phys. Rev.* D **84** 094016
[180] Eden B, Heslop P, Korchemsky G P and Sokatchev E 2013 *Nucl. Phys.* B **869** 329–77
[181] Brandhuber A, Travaglini G and Yang G 2012 *J. High Energy Phys.* JHEP05(2012)082
[182] Penante B, Spence B, Travaglini G and Wen C 2014 *J. High Energy Phys.* JHEP04(2014)083
[183] Brandhuber A, Penante B, Travaglini G and Wen C 2014 *J. High Energy Phys.* JHEP08(2014)100
[184] Dixon L J, McLeod A J and Wilhelm M 2021 *J. High Energy Phys.* JHEP04(2021)147
[185] Dixon L J, Gürdoğan Ö, McLeod A J and Wilhelm M 2022 *Phys. Rev. Lett.* **128** 111602
[186] Brandhuber A, Kostacinska M, Penante B, Travaglini G and Young D 2016 *J. High Energy Phys.* JHEP08(2016)134
[187] Brandhuber A, Kostacińska M, Penante B and Travaglini G 2017 *Phys. Rev. Lett.* **119** 161601
[188] Brandhuber A, Kostacinska M, Penante B and Travaglini G 2018 *J. High Energy Phys.* JHEP12(2018)076
[189] Brandhuber A, Kostacinska M, Penante B and Travaglini G 2018 *J. High Energy Phys.* JHEP12(2018)077
[190] Gehrmann T, Jaquier M, Glover E W N and Koukoutsakis A 2012 *J. High Energy Phys.* JHEP02(2012)056
[191] Kotikov A V, Lipatov L N, Onishchenko A I and Velizhanin V N 2004 *Phys. Lett.* B **595** 521–9
Kotikov A V, Lipatov L N, Onishchenko A I and Velizhanin V N 2006 *Phys. Lett.* B **632** 754–6 (erratum)
[192] Buchmüller W and Wyler D 1986 *Nucl. Phys.* B **268** 621–53
[193] Neill D 2009 arXiv:0908.1573
[194] Neill D 2009 arXiv:0911.2707

[195] Harlander R V and Neumann T 2013 *Phys. Rev.* D **88** 074015
[196] Dawson S, Lewis I M and Zeng M 2014 *Phys. Rev.* D **90** 093007
[197] Guo Y, Jin Q, Wang L and Yang G 2022 arXiv:2205.12969
[198] Zwiebel B I 2012 *J. Phys. A: Math. Theor.* **45** 115401
[199] Wilhelm M 2015 *J. High Energy Phys.* JHEP02(2015)149
[200] Beisert N, Kristjansen C and Staudacher M 2003 *Nucl. Phys.* B **664** 131–84
[201] Beisert N 2004 *Nucl. Phys.* B **676** 3–42
[202] Beisert N and Staudacher M 2003 *Nucl. Phys.* B **670** 439–63
[203] Dolan L, Nappi C R and Witten E 2003 *J. High Energy Phys.* JHEP10(2003)017
[204] Brandhuber A, Heslop P, Travaglini G and Young D 2015 *Phys. Rev. Lett.* **115** 141602
[205] Caron-Huot S and Wilhelm M 2016 *J. High Energy Phys.* JHEP12(2016)010
[206] Miró J E, Ingoldby J and Riembau M 2020 *J. High Energy Phys.* JHEP09(2020)163
[207] Baratella P, Fernandez C and Pomarol A 2020 *Nucl. Phys.* B **959** 115155
[208] Bern Z, Parra-Martinez J and Sawyer E 2020 *J. High Energy Phys.* JHEP10(2020)211
[209] Accettulli Huber M and De Angelis S 2021 *J. High Energy Phys.* JHEP11(2021)221
[210] Bena I, Bern Z, Kosower D A and Roiban R 2005 *Phys. Rev.* D **71** 106010